



Université des Sciences et Technologies de Lille

Ecole Doctorale de
Sciences de la Matière, du Rayonnement et l'Environnement

Thèse

Pour obtenir le grade de
Docteur de l'Université des Sciences et Technologies de Lille
Sciences de la Matière

Par

François BOUTON

Le 17 décembre 2010

**Influence of terpenes and terpenoids on the phase behavior
of micro- and macro-emulsions**

Devant le jury composé de :

Rapporteurs :

Dr. Conxita SOLANS, Université de Barcelone
Dr. Fabienne TESTARD, CEA

Examineurs :

Dr. Christel PIERLOT, ENSCL
Dr. Christian QUELLET, Société Givaudan

Directeurs :

Pr. Jean-Marie AUBRY, ENSCL
Pr. Véronique RATAJ, USTL

ACKNOWLEDGMENTS

This research project would not have been possible without the support of many people.

I wish to express my gratitude and my deep respect to Professor Jean-Marie Aubry for giving me the opportunity to make my research in his laboratory for being my mentor during this thesis. His ideas and suggestions had a major influence on this work. He was very tolerant with me and always showed me how to improve my scientific knowledge and how to write a scientific publication.

I would like to express my sincere gratitude to my advisor Professor Veronique Rataj, for her constant help and supportive actions during this thesis, for providing me helpful suggestions and for improving this manuscript thesis.

I would like to express my sincere gratitude and my deep respect to Dr. Conxita Solans and Dr Fabienne Testard for their kindnesses to judge this work. I am thankful that in the midst of all their activities, they accepted to be members of the thesis committee.

I owe my deepest gratitude to Dr. Christian Quellet who was abundantly helpful and offered invaluable assistance, support and guidance.

I would like to thank Dr. Christel Pierlot for providing me guidance, supportive work and agreed to carry an appreciation on this work. I had the opportunity to share his office during my stay at Lille and had great exchange of ideas with him.

I offer my regards and blessings to all of those who supported me in any respect during the completion of the project : Professor Azaroual, Valerie, Ying, Helene, Anne-Gaelle, Morgan, Sébastien, Aldo, Cédric...; my colleagues from Givaudan : Dr. Kumar Vedantam, Dr. Markus Gautschi, Dr. Andreas Goeke, Dr. Andras Borosy, Dr. Linda Li, Siron, Barry, Marie...

The author wishes to express his gratitude to his family: Helene, Robert, Nicolas, Carole and friends: Sylvie and Yakun; for their understanding and love, through the duration of his studies. I learned a lot during this occasion and I am convinced that this experience will undoubtedly help me in future.

The author would also like to convey thanks to Givaudan for providing the financial means and laboratory facilities during this work.

RESUME EN FRANCAIS

Comprendre les interactions du parfum avec les formulations de produits d'hygiène corporelle représente un défi permanent pour les parfumeurs. Prédire l'influence des matières premières constitutives des parfums sur le comportement de phase des microémulsions et des émulsions est, par conséquent, un besoin crucial pour les équipes de formulation. Dans ce contexte, notre travail a consisté, dans le premier chapitre de cette thèse, à présenter en détail les molécules de parfum étudiées : les terpènes et leurs dérivés, à expliciter les différents concepts appliqués et à passer en revue la littérature impliquant les systèmes à base de tensioactifs contenant du parfum.

Le deuxième chapitre est consacré à la détermination du comportement des phases, en utilisant le concept du HLD (Hydrophilic Lipophilic Deviation), de systèmes ternaires basés sur les alcools gras tétraéthoxylés purs (C_iE_4) et une série de mono- et sesquiterpènes comme huiles. Chaque système ternaire est étudié en localisant le point « X » (T^* , C^*) dans le diagramme dit « Fish » de Kahlweit et les terpènes ont été caractérisés par leur EACN (Equivalent Alkane Carbon Number) permettant une classification des différents parfums étudiés. L'évolution des valeurs d'EACN a été expliquée en considérant les changements structuraux des terpènes, tels que leur nombre de carbones, les isomérisations de chaînes, les cyclisations, la présence d'insaturations ou d'un noyau aromatique. Le cas du caryophyllène a été détaillé et comparé au n-hexane qui possède un EACN semblable bien qu'ils aient respectivement 15 et 6 carbones. Les températures de Fish (T^*) de 85 systèmes ternaires composés de trois tensioactifs C_iE_4 ($i = 6, 8, 10$), de 43 huiles d'hydrophobicités différentes et d'eau ont été déterminées et compilées. En tout, quatorze mono et sesquiterpènes plus 29 autres huiles modèles incluant des alcanes, les cyclohexènes, les cyclohexanes et les alkylbenzènes ont été étudiés afin d'établir un modèle QSPR (Quantitative Structure Properties Relationship) pour la prévision de T^* en fonction de la structure chimique des huiles. Seulement deux descripteurs moléculaires relatifs à l'isomérisation de chaîne (Kier A3) et à la polarisabilité (Average Negative Softness) de la molécule se sont avérés nécessaires pour modéliser les valeurs de T^* , et prédire la valeur d'EACN associés, pour des hydrocarbures insaturés et/ou cycliques et/ou branchés, s'étendant de la valeur -1.2 et à 28. Les résultats sont discutés en termes d'évolution du paramètre d'empilement « effectif » du tensioactif selon le degré de pénétration de l'huile dans le film interfacial et la température. La prévision de C^* pour le système C_6E_4 /terpènes/eau est également établie puis qualitativement discutée.

Dans le troisième et dernier chapitre, d'autres systèmes complexes à base de dérivés terpéniques sont décrits. Premièrement, des systèmes à l'équilibre tels que des microémulsions sont une fois de plus étudiés mais en employant cette fois une phase huileuse contenant un dérivé terpénique porteur d'une fonction polaire comme par exemple, un alcool terpénique. La présence de telles fonctions augmente, d'une part, la solubilité monomérique des alcools gras polyéthoxylés dans l'huile et confère à la molécule des propriétés cosurfactives lorsque l'huile est l'alcool amphiphile (alcool ou phénol). Au niveau de la création du parfum, les dérivés terpéniques sont plus intéressants que les terpènes parce qu'ils offrent un accès plus large à une gamme de notes olfactives plus plaisantes et plus diversifiées. Deuxièmement, l'influence des dérivés terpéniques sur des systèmes hors équilibre tels que des émulsions formulées avec des alcanes ou des silicones est étudiée.

La présence d'une huile polaire peut avoir des conséquences significatives non seulement sur la température d'inversion de phase (PIT) du système mais également sur la stabilité des émulsions en raison d'une accélération du mûrissement d'Ostwald. L'impact des alcools terpéniques sur la position du point « X » défini par (T^* , C^*) dans les diagrammes de Fish pour les systèmes formulés par les tensioactifs C_8E_4 et $C_{10}E_4$, trois huiles modèles : le dodécane, l'eicosane et l'octaméthylcyclotétrasiloxane (D4) et l'eau avec un rapport eau/huile constant sont mesurés. L'influence de la concentration en géraniol et en pélargol est étudiée et comparée à un alcool linéaire : *n*-octanol dans le cas de la microémulsion à base de silicone. Le choix de ces deux alcools terpéniques en tant que molécule-modèles de parfum n'est pas fortuit, puisqu'ils sont massivement employés en création, et bien qu'ils soient tous deux des alcools primaires, ils possèdent une grande analogie structurelle car le géraniol est en fait le tétrahydropélargol, le pélargol étant lui-même le dérivé 3,7-diméthylé de l'octanol. Ces spécificités permettent la mise en évidence de l'effet de l'insaturation et de la double méthylation de l'alcool linéaire correspondant. La poursuite de l'étude des émulsions est développée par une approche analogue. Premièrement, un tensioactif pur, le C_8E_4 est employé pour mesurer l'impact du pélargol sur la PIT de l'émulsion du système C_8E_4 / dodécane / eau puis les résultats sont comparés à ceux de la microémulsion précédente. Une relation linéaire entre les valeurs de T^* et de PIT est démontrée dans l'intervalle de concentration considérée.

Deuxièmement, l'influence de divers dérivés terpéniques sur la PIT d'une émulsion formulée par un tensioactif industriel avec le système Brij30 / octane / eau en fonction de leurs concentrations est rapportée et discutée. L'équation du HLD rationalise l'effet du parfum sur la PIT en comparant leurs paramètres $a.A$ avec une série d'alcools aliphatiques (C_1OH à $C_{16}OH$) ; l'effet de la structure de la chaîne hydrophobe et la nature de la fonction polaire sur leurs propriétés cotensioactives sont discutés. Les alcools et les phénols sont certainement les molécules les plus efficaces parmi les parfums étudiés pour diminuer la PIT des émulsions tandis que les acétals, les esters et les cétones la stabilisent ou l'augmentent très légèrement. Finalement, la stabilité de l'émulsion formulée de Brij30 / octane / eau est mesurée puis discutée de même qu'une émulsion cosmétique est préparée et sert de modèle pour évaluer l'influence des alcools terpéniques sur sa stabilité.

Titre : Influence des terpènes et des dérivés terpéniques sur les comportements des phases des micro- et macro-émulsions

Mots-clés : microémulsions, émulsions, systèmes ternaires, comportement des phases, parfum, terpènes, inversion de Phase, C_iE_j , HLD, EACN

Abstract

Understanding the basic science of the interactions between fragrances and personal care formulations represents a challenge for fragrance house. Especially, predicting the influence of fragrance molecules on the phase behavior of microemulsions and macroemulsions is a critical need for the formulator. In this context, the first chapter reviews the different concepts applied during our research and examines the literature relative to fragrance/surfactant interactions.

The second chapter is focused on the determination of the phase behavior of ternary systems based on tetraethylene glycol monoalkyl ether (C_iE_4) as surfactants and a series of mono- and sesqui-terpenes as oils by resorting to the Hydrophilic-Lipophilic Deviation (HLD) concept. Each system is studied by localizing the "X" point defined by (T^*, C^*) of the Fish diagram and the terpenes are characterized by their Equivalent Alkane Carbon Number (EACN) allowing a classification of the fragrant oils. EACN values have been rationalized by considering structural changes of the terpenes, such as number of carbons, branching, cyclization, unsaturation and aromatization. 43 hydrocarbon oils of various hydrophobicity were investigated in order to establish a QSPR model with only two molecular descriptors for the prediction of the fish-tail temperatures T^* and EACN values as a function of the chemical structure of the oils. The latter results are discussed in terms of evolution of the "effective packing parameter" of the surfactants according to temperature and oil penetration into the interfacial film.

In the third chapter, more complex micro- and macro-emulsions based on polar terpenoids are investigated. The presence of polar functions increases the monomeric solubility of polyethoxylated fatty alcohol surfactants in oil and makes possible the appearance of a co-surfactant behavior when the oil is amphiphilic (alcohols, phenols). On perfumery creation level, terpenoids are more appealing than terpenes because they offer access to a range of more pleasant and diversified fragrant notes. The addition of terpenoids to emulsions formulated with alkanes or silicones has significant consequences not only on the phase inversion temperature (PIT) of the system but also on the emulsion stability because they accelerate the "Ostwald ripening". The impact of geraniol and pelargol on the position of the "X" point of the Fish diagrams are measured. The influence on the PIT of an emulsion Brij30/octane/water of various terpenoids and functionalized fragrant molecules as a function of their concentrations is reported and discussed. The HLD equation used to rationalize the effect of fragrances on PIT by comparing the $a.A$ parameter of a series of aliphatic alcohols (C_1 to C_{16}). The effect of the hydrophobic chain structure and of the nature of the polar function on co-surfactant properties is discussed. Alcohols and phenols are the most efficient molecules among fragrances to decrease the PIT of emulsions while acetals, esters and ketones have no effect or slightly increase it. Finally, the stability of brij30/octane/water emulsion is studied and a cosmetic emulsion is prepared and served as a model to evaluate the influence of fragrant terpene alcohols on its stability.

Title: Influence of terpenes and terpenoids on the phase behavior of micro- and macro-emulsions

Keywords: Microemulsions, Emulsions, Ternary System, Phase Behavior, Fragrance, Terpenes, Phase Inversion, C_iE_j , HLD, EACN

TABLE OF CONTENTS

ACKNOWLEDGMENTS	3
RESUME EN FRANCAIS	5
ABSTRACT	7
TABLE OF CONTENTS	9
GENERAL INTRODUCTION	12
I. FRAGRANCES IN EMULSIONS, MICROEMULSIONS AND LIQUID CRYSTALS	21
1. Fragrances	21
1.1. Odorants	21
1.2. Fragrance notes & olfactory families	24
1.3. The studied fragrance molecules: structure and choice	26
1.3.1. Terpene and terpenoid structures	26
1.3.2. Choice of the molecules	30
2. Emulsions and microemulsions – general concept	32
2.1. Definition	32
2.2. Surfactants	32
2.2.1. Phase behavior of surfactant / oil / water systems	34
2.3. The Winsor R ratio	37
2.4. The Phase Inversion Temperature from Shinoda (PIT)	38
2.5. Fish diagrams (Kalhweit) and their corresponding Winsor microemulsion types	39
2.6. The packing parameter	41
2.7. The Hydrophilic Lipophilic Deviation concept (HLD)	42
2.8. The Equivalent Alkane Carbon Number (EACN)	43
3. Fragrances and surfactant systems interactions: a literature review	43
3.1. Fragrances in SOW ternary systems as oil or additives	44
3.2. Diagram of optimization and effect of fragrances type alcohol	47
3.3. Perfumes location in liquid crystal phases	50
3.4. Influence of the HLB temperature of fragrances on surfactants/oil/water systems	52
3.5. Effect of the addition of alcohols and polyols on phase diagrams containing fragrance as oil	53
4. References of chapter I	57

II. FISH DIAGRAM AS A TOOL TO FORMULATE FRAGRANCE MICROEMULSIONS 65

1. Classification of terpene oils according to the Equivalent Alkane Carbon (EACN) scale	66
1.1. Introduction	66
1.2. Results	68
1.2.1. Fish temperatures T^* and critical concentrations C^* for the C_iE_4 /n-alkane/water systems	69
1.2.2. Fish temperatures and critical concentrations for the C_iE_4 /terpene/water systems	72
1.3. Discussion	74
1.3.1. Structure effects on EACN value	74
1.3.2. Comparison of fish diagrams of terpenes and n-alkanes	76
1.3.3. Influence of the nature of the oil on the value of C^*	77
1.4. Conclusion	79
2. Prediction of the “fish-tail” temperature of C_iE_4/water/polar hydrocarbon oil systems	81
2.1. Introduction	81
2.2. Results	82
2.2.1. Phase behavior of C_iE_4 ($i = 6, 8, 10$)/polar hydrocarbon oil/water systems	82
2.2.2. Influence of the surfactant alkyl chain length on T^*	85
2.2.3. Influence of oil hydrophobicity on T^*	88
2.2.4. Determination of the EACN of hydrocarbon polar oils	89
2.3. Discussion	91
2.3.1. Evolution of the effective packing parameter with temperature and oil penetration	91
2.3.2. QSPR prediction for T^*	94
2.3.3. QSPR prediction for C^* for C_6E_4 surfactant	99
2.4. Conclusion	105
3. Experimental	105
3.1. Chemicals	105
3.2. Synthesis of tetraethylene glycol monoalkyl ethers $C_{10}E_4$, C_8E_4 and C_6E_4	106
3.3. Determination of “fish-tail” temperatures (T^*) of the C_iE_4 /oil/water systems	106
3.4. Determination of the Gibbs diagram of the C_6E_4 / α -pinene/water system	107
3.5. Data and calculation methods	107
4. References of chapter II	109

III. INFLUENCE OF TERPENOIDS ON EMULSIONS AND MICROEMULSIONS	117
1. Introduction	119
2. Influence of terpene alcohols on the “X” point (T*, C*) of C_iE₄ / oil / water systems	120
2.1. Results	120
2.1.1. Alkane-based microemulsions	120
2.1.2. Silicone-Based microemulsions	122
2.2. Discussion	124
3. Influence of terpenoids on the Phase Inversion Temperature of emulsions	125
3.1. Correlation between T* and the PIT of C8E4 / dodecane / water / pelargol system	126
3.2. Alkane-based emulsions	131
3.2.1. Influence of n-alcohols on the PIT of the Brij30 / octane / water system	131
3.2.2. Influence of fragrances on the PIT of the Brij30 / octane / water system	134
3.3. Silicone-based emulsions	139
4. Emulsion stability	143
4.1. Composition-formulation maps	143
4.2. Effect of geraniol on the creaming of the Brij30 / octane / water emulsion	148
5. Influence of terpenoid alcohols on the PIT of a cosmetic emulsion	152
6. Conclusion	156
7. Experimental	157
7.1. Chemicals	157
7.2. Determination of fish temperatures (T*) and optimal concentrations (C*) of the C _i E ₄ / oil / water systems	157
7.3. PIT measurement for surfactant / oil / water systems	158
7.4. Preparation of the commercial emulsion	159
8. References of chapter III	161
GENERAL CONCLUSION	164

General Introduction

This dissertation history takes place at Givaudan (Shanghai) with a patent [1] published in 2004 as a technical background. This patent described the rules to combine fragrance and silicone responsible for the sensory properties of shampoo into one single product by mixing fragrance with polydimethylsiloxane prior to emulsification by nonionic surfactants. The resulting highly concentrated fragrance silicone emulsion helps to boost the deposition of fragrance raw materials onto scalp and increases the overall olfactory performance of the product. On the other hand, the extreme complexity of the latter system and particularly the broad range of chemical compounds used in perfumery lead somehow to unusually results difficult to understand at once. Few months later, Givaudan sponsored me for a PhD course, and gives me the possibility to investigate deeper our previous challenge. We thus approached Professor Jean-Marie Aubry and his collaborator Professor Veronique Rataj from the Laboratory Oxydation and physico-chimie de la formulation based at Lille to discuss the different options. Among the French Laboratory, Lille appears to be the best choice for two reasons, the first one, because of its 20 years of research in emulsions, micro-emulsions and their more recent experience with fragrance molecules, the second one was because I did my master degree in this laboratory 15 years ago.

In personal care products, fragrance, in addition to its functional role (odor masking), lead to a real sensory experience which is currently used to support advertisement and packaging claims. As the sense of smell is directly linked to the limbic system (the part of the brain associated with emotions and memory), fragrances play a key role in all kind of care products. It forms an essential part of brand differentiation and communication with consumers: the trigger for repurchasing. Cosmetic forms such as creams, lotions or shampoos often contain a trickle down scent from a successful fine fragrance perfume that creates the line extensions. Stability, cost and technical issues are the main trigger for shifting from fine fragrance to the technical one. The challenge for the perfumer is to keep the character of the fragrance as close as possible to the original, while matching all the crucial technical and economic requirements [2]. Perfumers learn how to meet these challenges through experience and by a long trial and error practice. For instance, they change a natural essence by a less expensive quality or they shift an unstable ester by an alcohol or ketone. Technical team also plays a key role by collecting experimental data such as deposition on different substrates, solubility parameters, water/surfactants partition, etc, which are supportive to the fragrance development team [2].

Surfactants are regularly involved in personal care formulations. Depending on the system complexity, they could be mixed with oil and water such as in creams and lotions forming a single or multiple emulsion or simply water like in shampoos and shower gels forming aqueous surfactants self-assembly. Surfactant molecules are mainly localized at the water interface and form a thermodynamically stable system that, by virtue of its two distinct active sites (hydrophilic and hydrophobic), prevents polar and nonpolar solvents from contacting each other. Types of thermodynamically stable systems include: micelles, micro-emulsions and liquid crystals. The polar and nonpolar parts of a surfactant provide affinities for aqueous and organic oils respectively.

Main surfactants functions in Personal Care products

The mechanism of surface activity is similar between all types but the intended use ultimately determines the appropriate surfactant or surfactant combination choice. Everyday uses include:

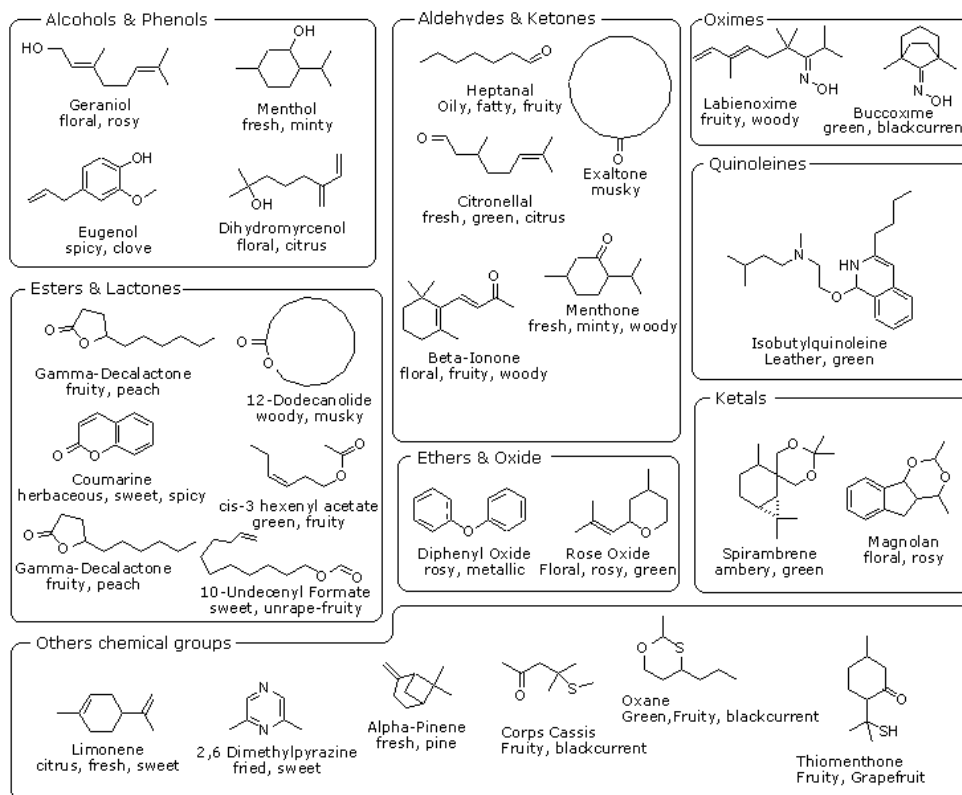
- Detergency to remove soil—e.g., in shampoos and soaps;
- Wetting to improve the contact angle between a solution and a substrate—e.g., in hair coloring or permanent wave lotions;
- Foaming for visual effects—e.g., in shampoos, bubble bath and hand wash;
- Emulsification to form a stable mixture of two incompatible phases such as oil-in-water, water-in-oil and multiple phases; and clear micro, alcoholic, nano- and refractive index matching—e.g., in skin and hair creams and lotions;
- Solubilization of insoluble components to improve their compatibility—e.g., in perfumes and flavors;

Commercial surfactants are not pure and often characterized by a range of molecular weights [3]. The situation is further problematical because fragrance can be present at concentrations high enough so that their impact on formulation cannot be considered as negligible. Table 1 provides the approximate percentages fragrance and surfactant in common consumer products.

Table 1 – Fragrance and Surfactants Level in Common Consumer Products [4]

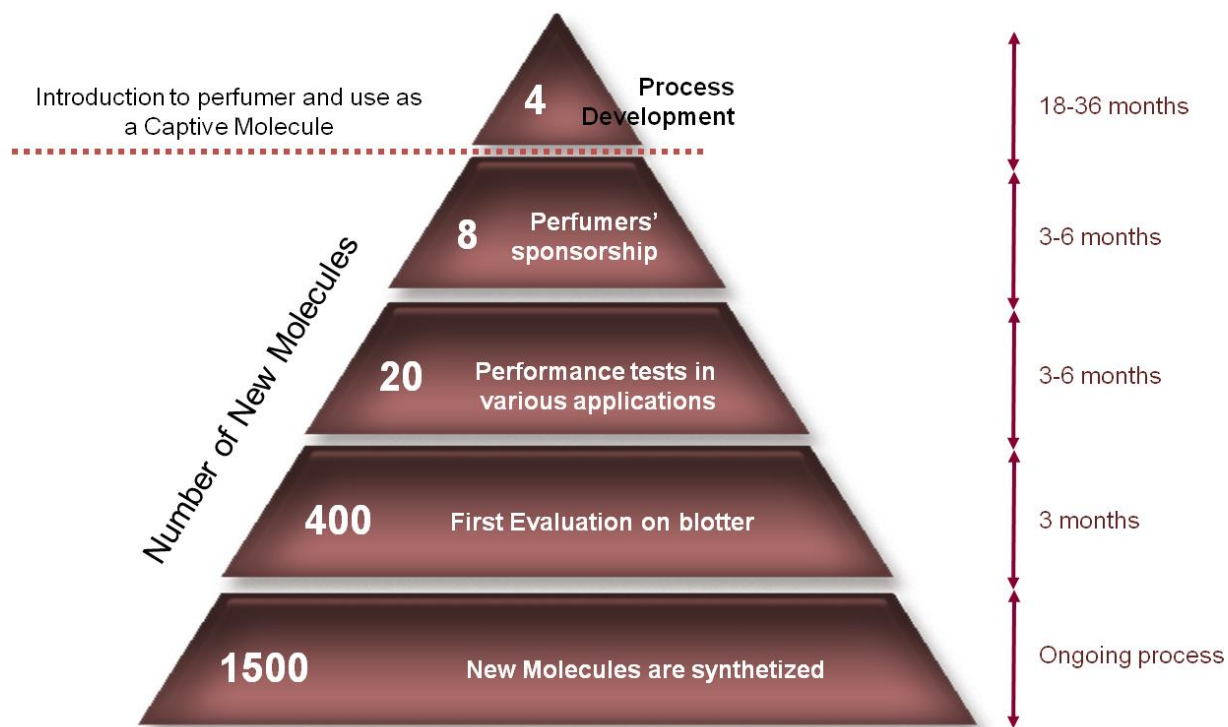
Consumer product	Fragrance %	Surfactant %
Shampoo	0.3 to 1.2	10 to 30
Fabric Softener	0.2 to 0.8	10 to 15
Cream	0.1 to 0.3	5 to 10
Liquid Laundry Detergent	0.3 to 0.6	15 to 25
Toothpaste	0.5 to 1.0	0.5 to 2

A fragrance is a creative combination of individual aroma chemicals. The performance of the complete fragrance composition in different media can be approached by characterizing these chemicals separately, and then combining their effects. Important properties of fragrance chemicals include polarity, volatility, surface activity and chemical stability. Each fragrance component interacts with the chemical and structural environment to determine the aesthetic and the physical characters of the final system. Until the end of the 19th Century, the perfumers worked with a relatively limited palette of natural raw materials such as essential oils produced by extraction and distillation of natural bark, woods, flowers. Advanced technologies have been developed to improve such extraction and distillation processes. The 20th Century and its rapid growth of modern organic chemistry allow a tremendous breakthrough; perfumers saw their possibilities of creation massively extended. Fragrances encompass virtually all organic functional groups as illustrated in Scheme 1 which also shown the diversity of in the hydrocarbon chains (macro, poly and heterocyclic, unsaturated, aromatic structures and/or combination of).



Scheme 1 – Main Structures and Functional groups in Fragrance raw materials – Scheme structure derived from paper [5].

Besides, synthetic products have some great advantages: a steady olfactory profile and they are not exposed to frequent interruptions of extraction due to abnormal climatic condition, disease, economic or politics issues. Modern fragrance chemistry is now focusing on molecules that deliver uniqueness, increase the performance of the consumers' products or have high impact; they are also used to replace regulatory restricted or banned natural molecules. Three classes of synthetic fragrance could be identified: *the commodities* which are produced in low cost manufacturing countries like China or India due to cost pressure. These molecules are no longer often cover by patent protection and they are produced in mass quantities. *The specialties* are linked to an exclusive manufacturing process or special technology so these limitations give to its producers a competitive advantage. The most important synthetic molecules for perfumery house are called *captive*; they enjoy a fully patent protection, and give fragrance composition the uniqueness, which makes it difficult to counterfeit. They are not sold outside the company and keep for internal development; they sometimes represent 20% of the total palette of the perfumer. The leading manufacturers are Givaudan, Firmenich, IFF and Symrise.



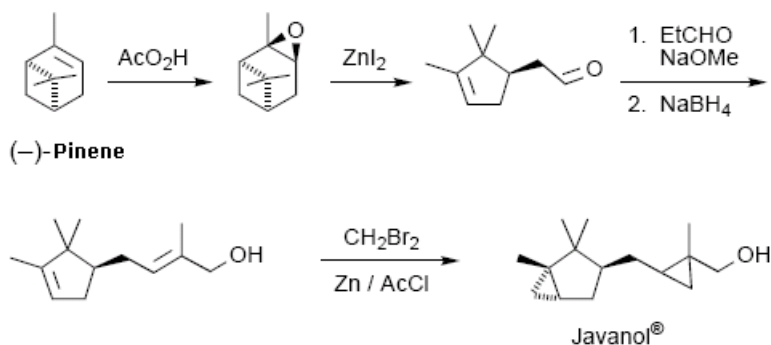
Scheme 2 – Introduction of new fragrance molecules accessible for perfumer in Givaudan

As shown in Scheme 2, the introduction of a new fragrance raw material to the palette of the perfumer follows a very specific channel which is very similar to pharmaceutical industry. From the laboratory to the final use, the validation process could take between 2 and 5 years.

For instance, the organic synthesis of Javanol[®] derived from α -pinene is shown in Scheme 2. It is the most powerful sandalwood type molecule ever synthesized. Current price of natural sandalwood is around 1500 USD/kg and corresponds to an increase cost of 10 fold in 20 years. Natural Sandalwood is reserved exclusively to fine fragrance development. The name Javanol[®] has been selected to evoke the excellent quality of Java's sandalwood oil, which is, unfortunately, no longer available for perfumery creations. As shown in Scheme 3, Javanol[®] is prepared from turpentine, which is a non-petrol-derived starting material; it contributes also to sustained development and indirectly protects S. Album [6].



Sandalwood nursery in India



Scheme 3 – Synthesis of Javanol[®] [6]

The interaction of emulsions or water surfactant self-assembly systems with fragrance reveal most of the important issues, which occur in fragrance applications. The breakings of emulsions, the insolubility or the viscosity changes in surfactant systems are key indicators of product integrity. Besides, new regulations (environmental or toxicological purpose), fast moving economical situation, new consumer needs often imply the replacement of product raw materials of existing formulation. These leveraging actions shuffle the card (in the final system) and unluckily often lead to new instabilities. A number of personal care product manufacturers take care of perfumes selection at the latest stage of the product formulation development. Seldom but a potentially critical issue happens when the formulator develops a formulation including their stability tests without considering the fragrance as a critical part of the formula aspect at earlier stage of the development. Instability issue involving fragrance is particularly emphasis when it concerns low surfactant waterborne formulation system. For that reason, the most difficult part for these systems resides in the possibility to encompass a complete picture of the relation of the chemistry of fragrance oil components to the structure of such surfactants/oil/water systems. This goal is rather ideal and difficult to approach with real products since most of consumer products of importance are multi-component systems, sometimes containing several surfactants and others ingredients, such as mineral pigments, salts, polymers, hydrotropes, waxes, mineral or silicone oils.

Understanding the basic science of interactions between fragrances and personal care formulation matrix represents a strong need for perfumery house, consequently predicting the influence of fragrance molecules on the phase behaviour of emulsions and micro emulsions at equilibrium or non-equilibrium is therefore a critical challenge for the formulator in a competitive context of delivering a successful market product [6].

In this framework, we have chosen to specifically work with fatty alcohol polyethoxylated surfactants (abbreviated as C_iE_j) systems to investigate the phase behavior of C_iE_j /oil/water systems as C_iE_j are easy to produce at lab scale with high purity. Oils have been chosen among terpenes for fragrance molecules and silicones oils for its specificity in cosmetics. Actually natural terpenes, terpenoids and their derivatives are very abundant in perfumery and silicone oil are central in cosmetics for their specific spreading properties and feeling and more generally in personal care products such as shampoos and shower gels. Therefore, this manuscript is separated into three chapters. Chapter one is informative and particularly dedicated to the studied fragrance molecules (terpenes and terpenoids), it reviews the different definitions and concepts mostly orientated on microemulsions and macroemulsions systems, it finally examines the literature related to fragrances involved in

surfactant systems (micellar solution, emulsion, microemulsion and liquid crystal). Chapter two is contributed to explain how terpene oils can be classified using the fish diagrams and the Equivalent Alkane Carbon Number (EACN) scale and how the "Fish Tail" Temperature of C_iE_4 /water/unsaturated and/or cyclic hydrocarbon oils systems with the help of a simple QSPR Model can be predicted; the results exposed into the first two sections have been published respectively in *Colloids and Surfaces A* [7] and *Langmuir* [8]. Chapter three is more dedicated to surfactant/oil/water/fragrance system at non-equilibrium, and more particularly the influence of terpene alcohols on the Phase Inversion Temperature of emulsions based on alkane or silicone oils, including the study of a commercial emulsion.

1. Vedantam, K., Bouton, F., WO/**2006**/012767
2. Herman, S.J. *Chemistry and Technology of flavors and fragrances* Blackwell Publishing Ltd; **2005**, chapter 13
3. Fournial, A.G., Molinier, V., Vermeersch, G., Aubry, J.M., Azaroual, N., High resolution NMR for the direct characterisation of complex polyoxyethylated alcohols (C_iE_j) mixtures, *Colloids Surf. A*, **2008**, 331 (1-2) p16-24
4. Solubilization of fragrances by Surfactants *Surfactants in Cosmetics*; Marcel Dekker Inc: New York, **1997**, 68, p617
5. Herrmann, A., Controlled Release of Volatiles under Mild Reaction Conditions: From Nature to Everyday Products *Angew. Chem.*, **2007**, 46 (31), p5836-63
6. Bajgrowicz, J., Gaillard, A., Perfumer's notes: Javanol. Fragrance creation with sandalwood oil substitutes, *Perfumer & Flavorist*, **2007**, 32 (1), p32-37
7. Bouton, F., Durand, M., Nardello-Rataj, V., Serry, M., Aubry, J.-M., Classification of terpene oils using the fish diagrams and the Equivalent Alkane Carbon (EACN) scale, *Colloids Surf. A*, **2009**, 338 (1-3), p142-147
8. Bouton, F., Durand, M., Nardello-Rataj, V., Borosy, A.P., Quellet, C., Aubry J.M., A QSPR Model for the Prediction of the "Fish-Tail" Temperature of C_iE_4 /Water/Polar Hydrocarbon Oil Systems, *Langmuir*, **2010**, 26 (11), p7962-7970

Chapter I

I. Fragrances in emulsions, microemulsions and liquid crystals

This chapter is dedicated to the studied fragrance molecules (terpenes and terpenoids), it also reviews the different concepts and definitions mostly orientated on macroemulsion and microemulsion system that were applied during our research, it finally examines the literature relative to fragrances/surfactant interactions.

1. Fragrances

1.1. Odorants

Odor is the result of an interaction between a chemical stimulus (odorant) and an olfactory receptor system causing biological and psychological effects in a living organism. The molecules of nearly all chemical substances can act as odor stimuli if they are sufficiently volatile to be present in air. Since most odorous substances are liquids or solids, the release of odorant molecules from the liquid or solid state into the surrounding air is a prerequisite for any material to become odorous [1].

During inhalation, a fraction of air reaches the olfactory epithelium in the upper part of the nose, where the sensory cells (receptors cells, olfactory neurons) are located. While passing over the mucous layer that covers the olfactory epithelium, odorant molecules partially solubilize in the aqueous phase and migrate through the mucus where they meet the receptor sites. They are located at the hair-like endings (cilia) of sensory cells (dendrites) which protrude in the mucous layer.

During the contact between odorants molecules and receptor cells the olfactory stimulation and signal transduction process, which is not yet fully understood, take place: odorant molecules are supposed to react specifically with binding proteins at the receptor cell membrane. During this interaction, a series of complex biochemical processes take place, in the course of which electrical receptor potentials are built up and rhythmic bursts of action potentials are induced.

The resulting electrical impulses are conducted from the peripheral end of the receptor cells via the nerve fibers (axons) to the olfactory bulb, where the central-nervous processing of the signals starts.

Via synaptic connections these signals are further transmitted to other parts of the brain, where the primary chemosensory information is translated into physiological and behavioral effects and finally, by comparison with memory contents, into a conscious experience, which we call olfactory perception [1].

Theories on Olfaction

The complexity of the neurophysiologic aspects of olfaction has limited the number of possible studies of molecular mechanisms of the odorant features. A few hypotheses have been suggested, especially those linked to the molecular structure of the odorant. The most well known are the steric theory of odor and the vibrational model [2]. The understanding of the organization of olfactory systems and their odorant receptors has seen tremendous improvement with the work of Buck and Axel.

The Vibrational Theory of Odor

In 1938, Dyson [3] suggested that the infrared resonance (IR) which is a measurement of a molecule's vibration might be associated with odor. R.H. Wright popularized this idea in the mid 1950's as infrared spectrophotometers became generally available for such spectral measurements that Wright [4] was able to correlate with certain odorants.

During the 60's and early 70's, vigorous debate raged as to the validity of each theory for classifying chemical odorants. By the mid-70's, it appeared that Wright's theory had failed a critical test. The optical enantiomers of Menthol [5] and of Carvone [6] smelled distinctly different, although the corresponding infrared spectra were identical, and hence this theory fell from favor.

The Steric Theory of Odor

John Amoore [7] completed the idea of a "Steric Theory of Odor" originally proposed by R.W. Moncrieff [8] in 1949 that confirmed airborne chemical molecules are smelled when they fit into certain complementary receptor sites on the olfactory nervous system. This "lock and key" approach was an extension from enzyme kinetics. Amoore proposed primary odors (ethereal, camphoraceous, musky, floral, minty, pungent and putrid). The molecular volume and shape similarity of various odor chemicals were compared (by making hand prepared molecular models and physically measuring volume and creating silhouette patterns - there were no computer molecular modeling programs in that period). The steric theory is well suited to the idea that the odorant receptor proteins accept only certain

odorants at a specific receptor sites. The receptor is then activated and couples to the G-protein and the signal transduction cascade begins.

The discovery of olfactory receptors

In 2004, Linda Buck and Richard Axel [9] are rewarded by the Nobel price of Physiology or Medicine for their discoveries of odorant receptors and the organization of the olfactory system". They discovered a large gene family, comprised of some 1,000 different genes (three per cent of our genes) that give rise to an equivalent number of olfactory receptor types. These receptors are located on the olfactory receptor cells, which occupy a small area in the upper part of the nasal epithelium and detect the inhaled odorant molecules.

Each olfactory receptor cell possesses only one type of odorant receptor, and each receptor can detect a limited number of odorant substances. Our olfactory receptor cells are therefore highly specialized for a few odors. The cells send thin nerve processes directly to distinct micro domains, glomeruli, in the olfactory bulb, the primary olfactory area of the brain. Receptor cells carrying the same type of receptor send their nerve processes to the same glomerulus. From these micro domains in the olfactory bulb the information is relayed further to other parts of the brain, where the information from several olfactory receptors is combined, forming a pattern (see below Figure I-1). Therefore, a human being can consciously experience the smell of a lilac flower in the spring and recalls this olfactory memory at other times.

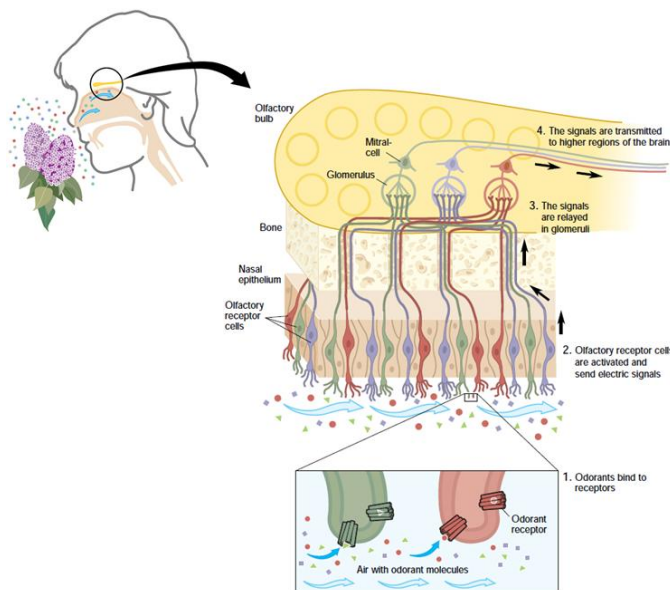


Figure I—1 Odorant Receptors and the organization of the olfactory system extracted from [9].

1.2. Fragrance notes & olfactory families

A note is the characteristic odor of a single material. Accords are a balanced blend of three or four notes that lose their individual identity to create a completely new, unified odor impression.

G.W.S. Piesse [10] states: "Scents, like sounds, appear to influence the olfactory nerve in certain definite degrees. There is, as it were, an octave of odors like an octave in music; certain odors coincide, like the keys of an instrument. Such almond, heliotrope, vanilla, and orange-blossoms blend together, each producing different degrees of a nearly similar impression. Again, we have citron, lemon, orange-peel, and verbena, forming a higher octave of smells, which blend in a similar manner".

He developed theories relating specific odors to notes on a musical scale in an attempt to categorize the spectrum of smells. Fragrances began to be described in a structural form with the adoption of top, middle and bottom note terminology after W.A. Poucher [11] began to classify fragrance materials in 1924. He published in 1955 a list of 300 in order of their volatility, eventually sub-dividing his materials into those with coefficients 1 to 14 as Top Notes; those from 15 to 60 as Middle Notes; and those from 61 to 100 as Basic Notes.

Top notes are essentially responsible for the initial smell of perfumes and are typically the most volatile compounds. The middle notes (or heart notes) contains the common components that have some volatility are responsible for the main aroma of the fragrance, generally lasting several hours. Bottom notes (or base notes) contain the least volatile compounds and have aromas lasting most of the day. In perfumery, we often represent the olfactory description of a fragrance with a pyramid as shown in Figure I-2.

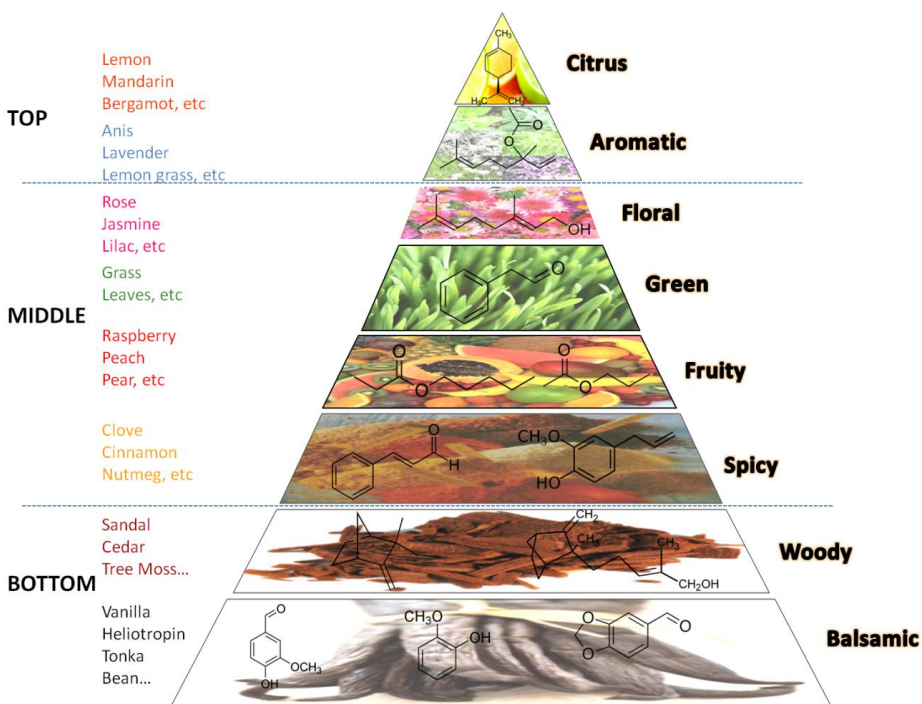


Figure I—2 - Pyramidal representation of the main fragrance families.

Accord used in perfumery

The olfactive classification of a scent, from fine to functional fragrance, is a complex task, even if professional technician undertakes it. Indeed, each perfume presents various facets, the perception of which varies according to each nose, so that a same “accord” can be felt and described in a different way according to the individual evaluator. Fortunately, a certain number of almost irrefutable references allow an objective synthesis. These benchmarks are based on simple products that belong to our natural environment such as flowers, fruits and natural products or a raw materials association (natural or synthetic) that all perfumery house professionals recognize as the basic accord of perfumery (Table I-1).

Table I-1 – Main accords used in traditional perfumery.

Floral	Other
Carnation	Chypre
Hyacinth	Cologne
Jasmine	Fougere
Lilac	Oriental
Lilly of the valley	
Orange Blossom	
Rose	
Tuberose	
Violet	

1.3. The studied fragrance molecules: structure and choice

1.3.1. Terpene and terpenoid structures

1.3.1.1. Definition

Terpenes are a large and varied class of hydrocarbons, mainly produced by a wide variety of plants: particularly conifers wood and balm trees. The name "terpene" originates from the word "turpentine" (lat. Balsamum terebinthinae). Turpentine, the so-called "resin of pine trees", is the viscous pleasantly smelling balsam that flows upon cutting or carving the bark and the new wood of several pine tree species (Pinacea) seen at Figure I-3.

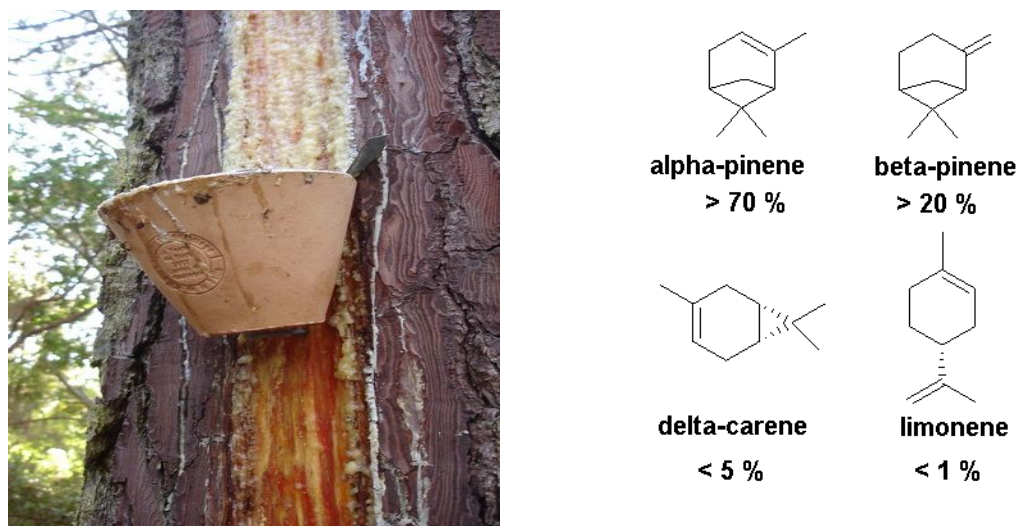


Figure I-3 – Collecting pine resin directly from a pine tree by wounding the bark and its main components including their percentages found after separation from rosin by distillation.

Terpenes originally referred to some hydrocarbons contained in Turpentine with the “resin acids”. Traditionally, all natural compounds built up from isoprene sub-units, and for the most part originating from plants, are denoted as terpenes (see Figure I-4 below for general structure). In addition to their roles as end-use products in many organisms, terpenes are major biosynthetic building blocks within nearly every living creature. Steroids, for example, are derivatives of the triterpene: squalene. Terpenes may be modified chemically, such as by oxidation or rearrangement of the carbon skeleton, the resulting compounds are generally referred to as terpenoids. Some authors will use the term terpenes to include all terpenoids. Terpenoids are also known as Isoprenoids [12]. Figure I-4 shows the different parent hydrocarbon of terpenes.

1.3.1.3. General structure

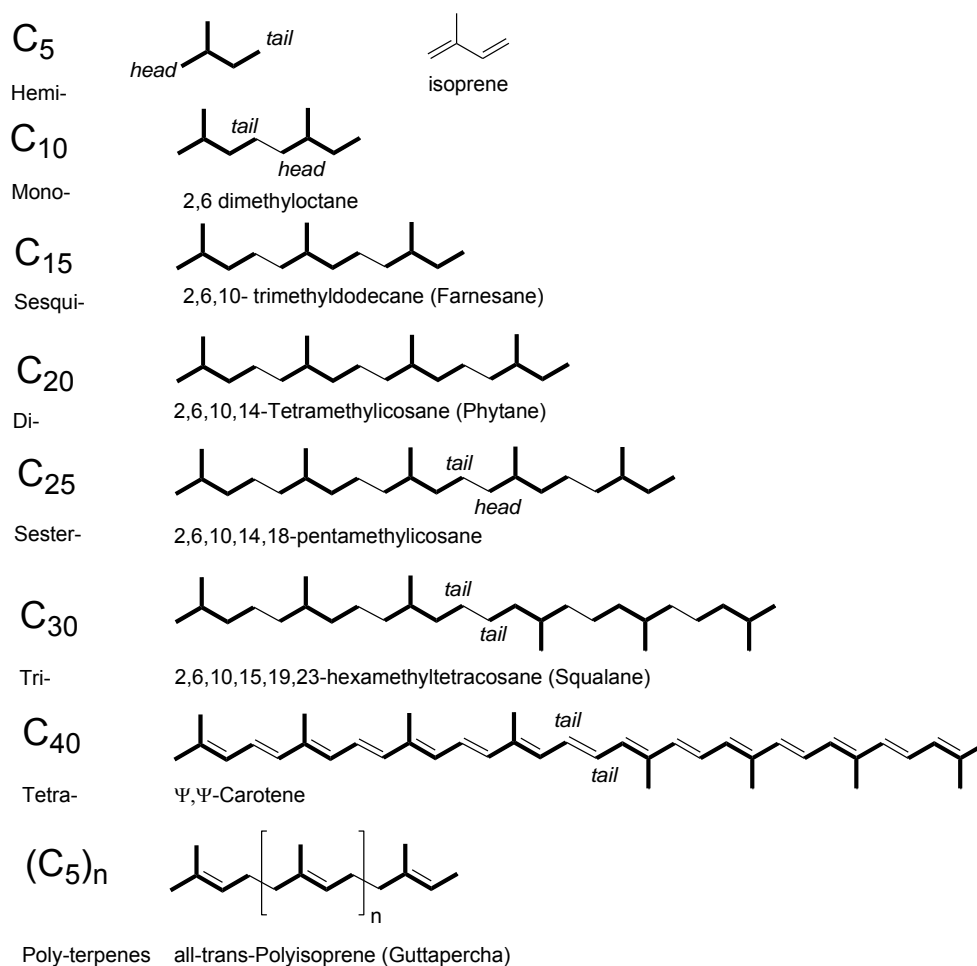


Figure I-4 – Parent hydrocarbon of terpenes (isoprenoids) [13].

Hemiterpenes [13]

Only 50 hemiterpenoids are known. A few examples of natural hemiterpenoids are shown in Figure I-5. In contrast to non-natural 2-methyl-1,3-butadiene (isoprene), 3-methyl-2-buten-1-ol (prenol) occurs in ylang-ylang oil obtained from freshly picked flowers of the Canaga tree, tiglic acid (pungent sour odor) and isovaleric acid (strong pungent cheese/sweaty smell). These molecules are the components of numerous natural esters, for example, ester "alkaloids".

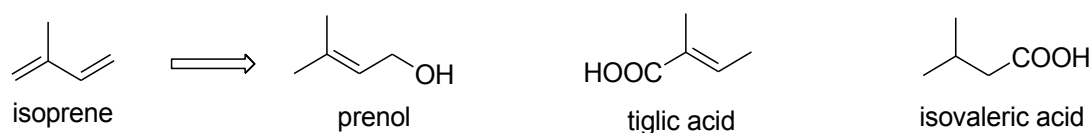


Figure I-5 – Examples of natural hemiterpenoids [13].

Acyclic monoterpenoids [13]

Most of acyclic monoterpenoids are derived from 2,6-dimethyloctane. Pelargol or (R)-3,7-dimethyloctanol is a component of the geranium oil (*Pelargonium graeveolens*). Acyclic monoterpenoid trienes such as myrcene are found in common basil leaves oil, bay leaves oil, hops oil or petitgrain (*Citrus vulgaris*) oil and several others essentials oils.

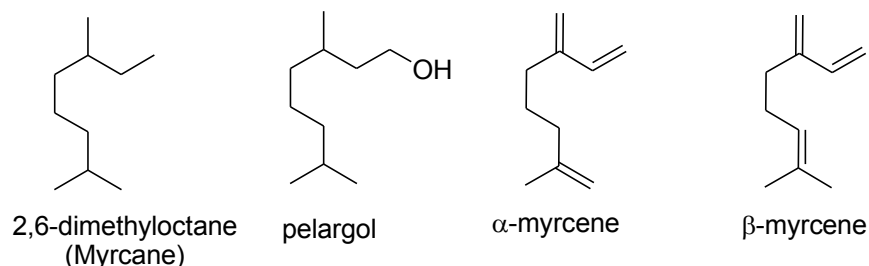


Figure I-6 – Most of acyclic monoterpenes derived from 2,6-dimethyloctane.

Monocyclic monoterpenes: cyclohexane monoterpenes [13]

Monocyclic terpenes results mostly from p-menthane derivation. Trans-paramenthane itself occurs in the turpentine oil. Limonene is an unsaturated monocyclic terpenes hydrocarbon occurring in various essential oil. Its R-(+)-enantiomer, smelling like oranges, is the dominant component of mandarin peel oil from *Citrus reticulata* and the oil of orange from *Citrus Aurantium*, respectively, while the (S)-(-)-enantiomer, concentrated in the oil of fir-cones obtained from young twigs and cones of *Abies Alba*, also smells like oranges, but is more balsamic with a terebinthinate touch.

Menthadienes such as α - and β -terpinene as well as terpinolene are fragrant components of several oils originating from Citrus, Mentha-, Juniperus- and Pinus- species.

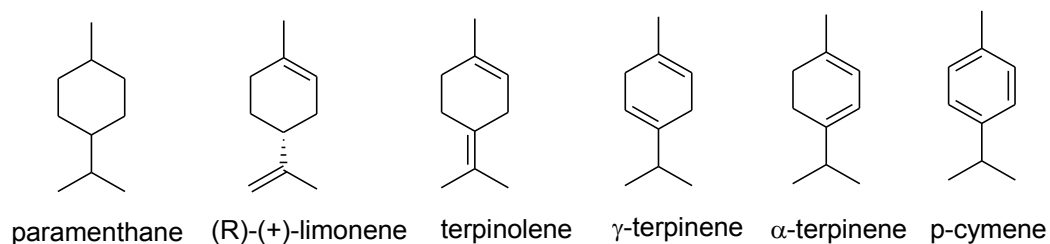


Figure I–7 - A few common monocyclic monoterpenes.

Benzenoid menthanes are referred to as cymenes. The ortho-isomer is not yet been found in nature. Meta-cymene is a constituent of the ethereal oil of blackcurrant; p-cymene occurs in the oils of cinnamon, cypress, eucalyptus, thyme, turpentine and others; both are used as fragrances in perfumery.

Bicyclic monoterpenes [13]

(+)-3-Carene is a component of the oil of turpentine from the tropical pine *Pinus Longifolia*, also occurring in some species of fir, juniperus and citrus. The oil of turpentine obtained on large scale from the wood of various pine trees and by way of cellulose production (sulfurated oil of turpentine) contains more than 70% of α -pinene and up to 20% of β -pinene.

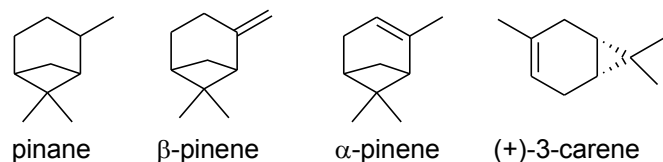


Figure I–8 - A few bicyclic monoterpenes.

Sesquiterpenes [13]

2,6,10-trimethyldodecane or farnesane as shown in figure 9, the parent compound of about 10000 sesquiterpenes is found in the oil slate. (-)- β -Caryophyllene occurs as a mixture with its cis isomer isocaryophyllene in the clove oil (up to 10%) from dried flower buds of cloves, as well as in the oils of cinnamon, rosemary, citrus, eucalyptus, sage and thyme. Clove oil, with its nicely sweet, spicy and fruity odor, is used not only in perfumery and for flavoring chewing gums, but also a dental analgesic and anti-inflammatory.

Longifolene is commonly spread in ethereal oil, present, for example, to an extent of up to 20% in Indian turpentine oil, which is produced commercially from Himalayan pine *Pinus longifolia* for the synthesis of a widely used chiral hydroboration agent.

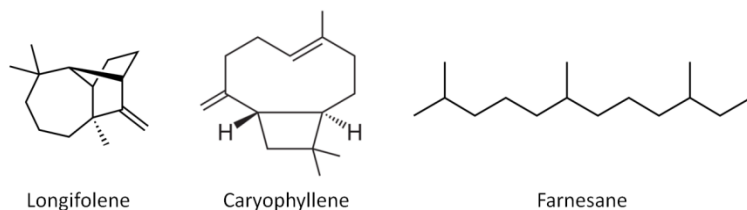
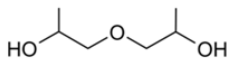
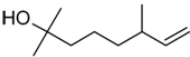
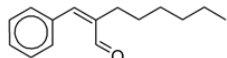
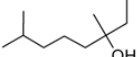
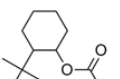
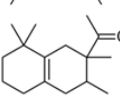
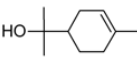
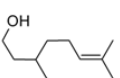
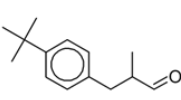
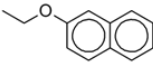
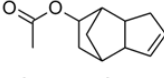
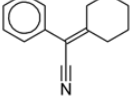
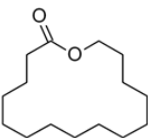


Figure I—9 – Two important natural bicyclic sesquiterpenes and farnesene.

1.3.2. Choice of the molecules

Around 4000 molecules compose the palette of the perfumer. However, the perfumer to create a technical fragrance will use only 5 to 10% of these molecules. The rationalization of the fragrance formulation is driven by the cost of each individual raw material and their performances into the final finish products. Among these two to three hundreds molecules, the captive molecules will provide the uniqueness and the performance at different stage of the end-use product. Most of the time, they are used at low level, as shown in this perfume for laundry detergent in Table I-2. The dosage of molecules like Javanol, Methyl laitone or Damascenone is around 0.02 to 0.05%. In the other hand, terpenes and terpenoids like dihydromyrcenol, tetrahydrolinalool, citronellol and terpineol represents 30% of the formulation, even more if dipropylenglycol is considered as an inert solvent and consequently do not participate to the olfactive performance of the total fragrance. Although this is just an example, it is quite representative of many technical fragrances.

Table I-2 Perfume for laundry detergent adapted from [14].

Major components	Chemical Formula	%	Minor components	%
Dipropylene glycol		26.4	Citronellyl nitrile	1.5
Dihydromyrcenol		10	Allyl amyl glycolate	0.7
Hexyl cinnamic aldehyde		8	Coumarine	0.5
Tetrahydrolinalool		8	Aldehyde C110 undecylic	0.4
Verdox (IFF)		7	Triplal (IFF)	0.4
Iso E super (IFF)		6	Florydral (Givaudan)	0.3
Terpineol		6	Manzanate	0.3
Citronellol		6	Ethyl methyl-2 butyrate	0.2
Lilial (Givaudan)		5	Cis-3 hexenol	0.1
Neroline		4	Styrallyl acetate	0.1
Verdyal acetate		4	Javanol (Givaudan)	0.1
Peonile (Givaudan)		3	δ-Damascenone	0.1
Cyclopentadecanolide		2	Methyl Laitone (Givaudan)	0

In the other hand, terpenes and terpenoids are the primary constituents of many essential oils [12-13] that are widely used as fragrances in perfumery; they contribute to the freshness and impact of the top notes. Most importantly, synthetic variations and derivatives of natural terpenes also greatly expand the variety of bouquet used in perfumery [14]. Hundreds of them are very easy to source at reasonable cost and with high purity. As shown in figure 4, their carbon backbones are entirely based on the isoprene structure, also an important concept that will be developed in.

This means for each family, at equal number of carbons, a few dozens of structural possibilities, and regarding phase behavior of surfactant / oil / water (SOW) system, this is an opportunity for studying the influence of variation in the oil chemical structure having a same number of carbon atoms.

2. Emulsions and microemulsions – general concept

2.1. Definition

An emulsion could be defined as a heterogeneous system of two immiscible liquid phases (usually water and oil) where one of the phases is dispersed in the other as colloidal size droplets (roughly 1-10 μm). There are different types of emulsions, the so-called oil-in-water (O/W) and water-in-oil (W/O) which are the simplest ones whereas multiple ones like W/O/W and O/W/O may also be formed in some conditions. Emulsions made by simple stirring of the pure immiscible liquids are very unstable and break quickly to the bulk phases. The addition of surface-active material facilitates such emulsions formation and helps in stabilization through a combination of surface activity and arrangement formation at the interface. Such surface-active materials that are used as stabilizer or emulsifiers belong to surfactant family.

2.2. Surfactants

The term surfactant is shorthand for the more cumbersome "surface active agent". Surfactants are functional ingredients and their molecular amphiphilic structure as shown Figure I-10 composed of a hydrophilic or polar moiety (head) and a lipophilic or nonpolar moiety (tail). The surfactant head can be charged (anionic or cationic), dipolar (zwitterionic), or non-charged (nonionic). **I.** Sodium dodecyl sulfate (SDS), **II.** cetyltrimethylammonium bromide (CTAB), **III.** Laurylbetaine and **IV.** tetraethyleneglycol n-dodecyl ether (C_{12}E_4) are typical examples of anionic, cationic, zwitterionic and nonionic surfactants, respectively (Figure I-10). The surfactant tail is usually a long chain hydrocarbon residue and less often a halogenated or oxygenated hydrocarbon or siloxane chain [15-16].

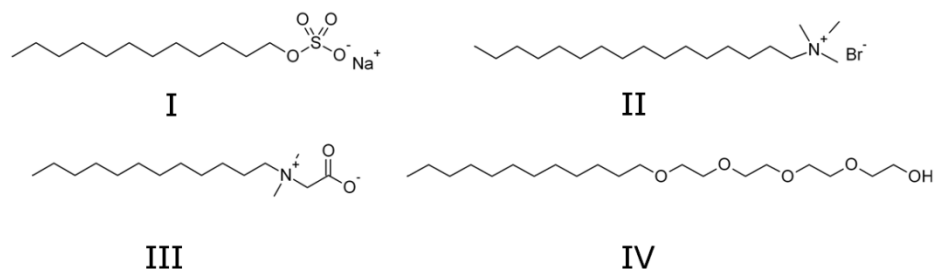


Figure I—10 - Examples of surfactants from each main family: anionic (I), cationic (II), zwitterionic (III) and nonionic (IV).

In aqueous solution, with an increase in concentration of surfactant, a spontaneous association of molecules makes aggregates termed "micelles" (Figure I-11). The concentration at which surfactants start forming micelle is called the "critical micellar concentration" (CMC). In a micelle, the hydrophobic tails flock to the interior in order to minimize their contact with water, and the hydrophilic heads remain on the outer surface in order to maximize their contact with water (Figure I-11) [17-18].

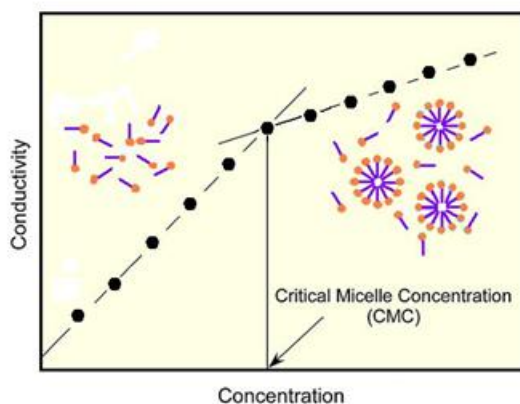


Figure I—11 - Illustration of the Critical Micellar Concentration phenomenon / Change in conductivity for an ionic surfactant solution as a function of its concentration.

The micellization process in water is the result from a delicate balance of intermolecular forces which includes hydrophobic, steric, electrostatic, hydrogen bonding and van der Waals interactions. The main attractive force results from the hydrophobic effect associated with the nonpolar surfactant tails, and the main opposing repulsive force results from steric interactions and electrostatic interactions between the surfactant polar heads. Whether micellization occurs and, if so, at what concentration of monomeric surfactant, depends on the balance of the forces promoting micellization and those opposing it [18-19]. A surfactant, when present at low concentrations in a system, adsorbs onto surfaces or

interfaces significantly changing the surface or interfacial free energy. Surfactants usually act to reduce the interfacial free energy, although there are occasions when they are used to increase it [16]. Preparation of emulsion requires surfactant and energy to form. A larger number of emulsifying process is based on droplet break-up under shear. The break-up of a droplet is possible when the deforming force exceeds the interfacial force that maintains the shape [20]. The surfactant is absorbed in the interface between the two liquids, forming a film between both products: due to their structure, the polar part of the emulsifier molecule has an affinity with water and the non-polar part (fatty chain) tends to be attracted to the oily phase. This imply a considerable reduction of the interfacial tension between the oil and the water phase (approximately 25 to below 2.5 mN/m for W/O emulsions and lower than 0.25 mN/m for O/W emulsions) thus forces one of the liquids into separate droplets, suspended and dispersed within the other liquid [20]. Because these droplets are “shielded” by the emulsifier molecules surrounding them, they are kept apart from each other, ensuring the two substances do not separate in a kinetically stable mixture.

In the other hand, when surfactant concentration exceeds a certain value, micro-emulsion can form spontaneously provided that the w/o interfacial tension is lower than 10^{-2} mN/m [21]. They are thermodynamically stable dispersions of surfactants, oil and water. Initially studied by Schulman (1959) their characteristic particle sizes comprise between 5nm to 50nm make them optically transparent or translucent. Microemulsions also differ from emulsions, as they do not require the input of considerable amounts of energy for their formation, hence, emulsion can only be stable in a kinetic sense. However, many systems of oil + water + surfactant that form microemulsions may be emulsified to emulsions by changing formulation parameter.

2.2.1. Phase behavior of surfactant / oil / water systems

Phase behavior studies are fundamental for the study of surfactant/oil/water system determined by using phase diagram that provide information on the boundaries of the different phases as a function of composition variables and temperatures, and, more important, structural organization can be also inferred. Phase behavior studies also allow comparison of the efficiency of different surfactants for a given application. The boundaries of one-phase region can be assessed easily by visual observation of samples of known composition. Long equilibrium time could be the main disadvantage of this technique, especially if liquid crystalline phase is involved.

Binary diagram

Due to their amphiphilic molecular structure, surfactants have a tendency to aggregate in aqueous or oily environments, e.g. to form micelles or liquid crystals, as shown in Figure I-12.

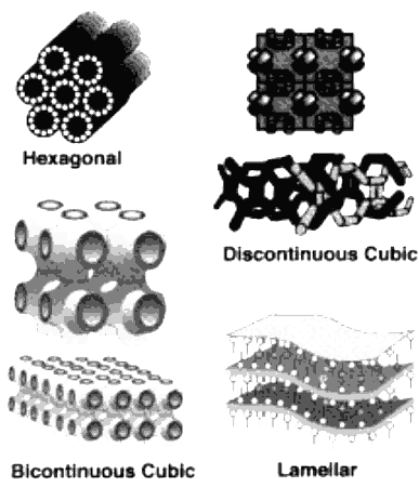


Figure I-12 - Classes of surfactant liquid crystals extracted from [28].

These aggregates form thermodynamically stable phases that can also change the macroscopic appearance of an emulsion; table 3 summarizes the abbreviation and notation of the different phase structure found in literature.

Table I-3 – Most common liquid crystal structures in surfactant systems with their abbreviations and different notations adapted from [23].

Phase Structure	Abbreviation	Notation
Micellar	mic	L_1, S
Reversed micellar	rev mic	L_2, S
Hexagonal	hex	$H_1, E, M_1, \text{middle}$
Reversed hexagonal	rev hex	H_2, F, M_2
Cubic (normal micellar)	cub_m	I_1, S_{1c}
Cubic (reversed micelle)	cub_m	I_2
Cubic (normal bicontinuous)	cub_b	I_1, V_1
Cubic (reversed bicontinuous)	cub_b	I_2, V_2
Lamellar	lam	$L_\alpha, D, G, \text{neat}$
Gel	gel	L_β
Sponge phase (reversed)	spo	$L_3 \text{ (normal)}, L_4$

In 1980, Lang and Morgan [22] have reported an accurate detailed binary phase diagram for aqueous mixtures of the monodispersed surfactant $C_{10}E_4$. They interpreted that phase diagram by correlating thermodynamics to molecular interactions and chemical structure. This diagram (Figure I-13) served as an introduction to rationalize more complicated multi-component systems containing these two constituents. This multi-component system will be discussed further in subsequent chapters.

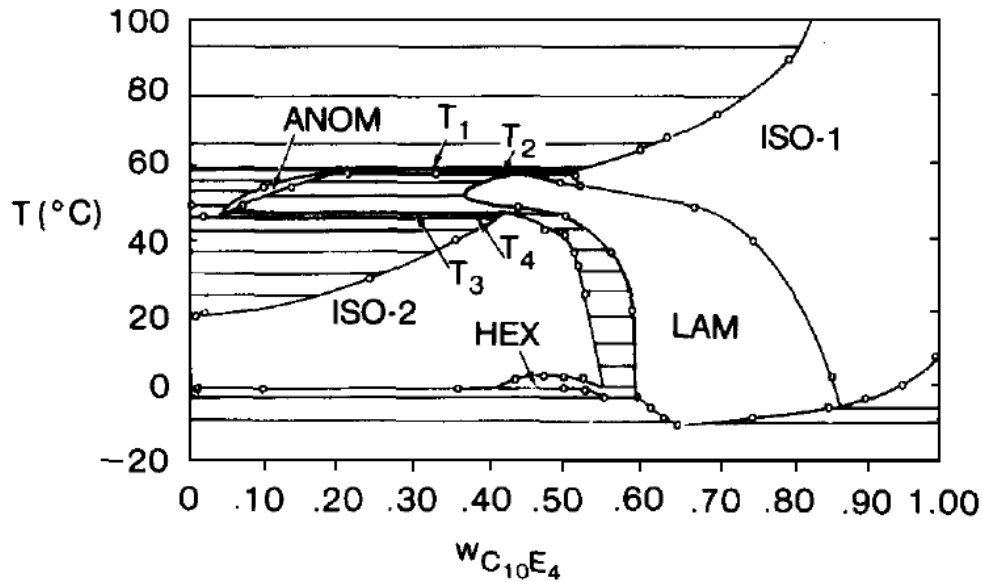


Figure I—13 – Phase diagram of $C_{10}E_4$ - H_2O in the “temperature – mass fraction of surfactant” space extending from -20 °C to 100 °C. ISO-1 and ISO-2 designate two isotropic phases which at some temperatures are distinct; HEX is an hexagonal and LAM is a lamellar birefringent liquid crystalline phase; AMON is anomalous phase $T_{1,2,3,4}$ are phase transition temperatures adapted from [22].

Ternary diagram

The type of surfactant and oil, the mixing ratios, and the external conditions such as temperature and salt or solvent content determine which macroscopic phases can occur in a certain surfactant/oil/water system. These complex relationships can be represented graphically in the form of phase diagrams, as shown for a three-component system Brij30/oil/Water as shown in Figures I-14a and I-14b.

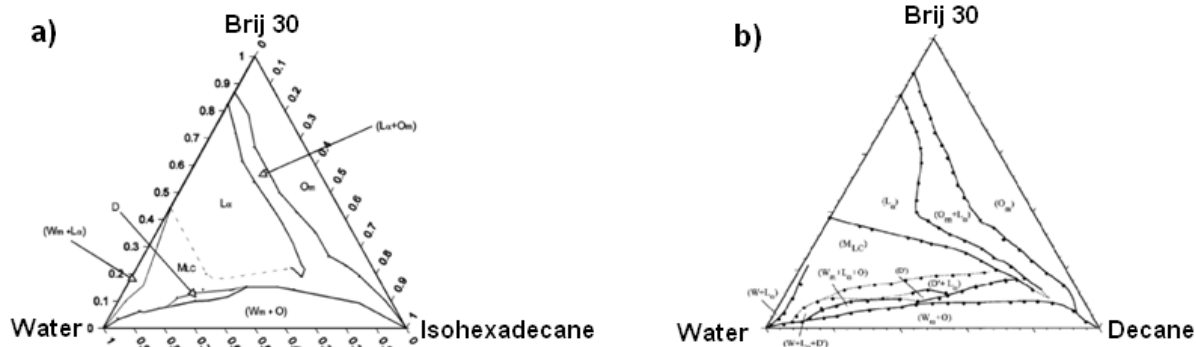


Figure I–14 – (a) Pseudo ternary phase diagram at 25 °C of the system water / brij30 / isohexadecane. W_m , isotropic bluish liquid phase (micellar solution or O/W microemulsion); L_a , anisotropic phase (lamellar liquid crystalline phase); O , isotropic liquid colorless oil phase; O_m , isotropic liquid colorless phase (inverse micellar solution or W/O microemulsion); D , isotropic bluish liquid phase (microemulsion); M_{LC} , multiphase region (equilibrium not determined). (b) Phase behavior of water / Brij 30 / decane system at 25 °C: O_m , isotropic liquid phase; L_a , lamellar liquid crystalline phase; D' , shear birefringent liquid phase; W_m , bluish liquid phase (O/W microemulsion); W , aqueous liquid phase; O , oil liquid phase; M_{LC} , multiphase region including lamellar liquid crystal extracted from [24-25]

2.3. The Winsor R ratio

Winsor first proposed the R ratio [30] and it corresponds to the proportion of cohesive interactions energies (miscibility) of surfactant with the vicinity of oil (A_{co}) and water (A_{cw}) in microemulsion or micellar solutions system. This R ratio compares the tendency for a surfactant layer to disperse in oil to its tendency to dissolve into water. The interfacial region tends to take on a definite curvature if one phase is favored. More precisely,

$$R = \frac{(A_{co} - A_{oo} - A_{LL})}{(A_{cw} - A_{ww} - A_{HH})} \quad (1)$$

The energy of cohesion in between two molecules X and Y, for example, is defined as A_{xy} , which has a positive value when the interactions between molecules are positive.

A_{oo} Cohesive energy between oil molecules

A_{ww} Cohesive energy between water molecules

A_{HH} Cohesive energy between hydrophilic group of surfactants molecules

A_{LL} Cohesive energy between lipophilic group of surfactants molecules

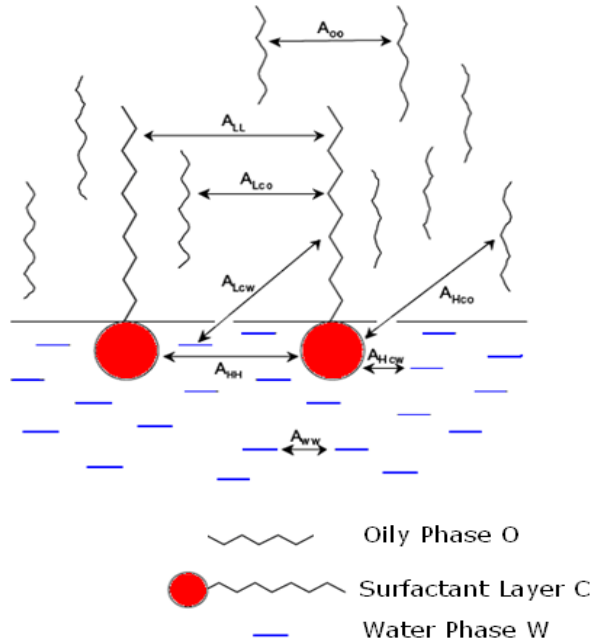


Figure I—15 Interaction energies in the interfacial region for a surfactant/oil/water system adapted from [31].

Besides, A_{co} is defined as the sum of A_{LCo} and A_{HCo} while A_{cW} is defined as the sum A_{LcW} and A_{HcW} . A_{LcW} quantifies the interaction between the nonpolar parts of water and surfactant (typically London Forces) and A_{HcW} represents the polar interactions, more precisely the hydrogen bonds and the Coulomb interactions. A_{HCo} and A_{LcW} are generally small values and therefore often neglected. The energy of A_{co} cohesion translates the miscibility of the molecules of surface-active with the area oils and A_{cW} with water. In addition A_{oo} and A_{LL} are opposed to miscibility with oil while A_{WW} and A_{HH} are opposed to miscibility with water [31].

To summarize, R ratio of cohesive energies, stemming from interaction of the interfacial layer with oil divided by energies resulting from the interactions with water, determines the preferred interfacial curvature. As a result, if $R > 1$, the interface tends to increase its area of contact with oil while decreasing its area of contact with water so those surfactant molecules have more affinity with oil. $R = 1$ means a balanced interfacial layer and $R < 1$ means surfactant has more affinity with water which represents the continuous phase of the system.

2.4. The Phase Inversion Temperature from Shinoda (PIT)

Polyethoxylated nonionic surfactants are well known for their special solubility behavior: the interaction of the ethoxylate groups with water decreases with increasing temperature,

i.e. a surfactant with better solubility in water, forming micelles in the water, becomes a surfactant with better solubility in oil when the temperature is increased [32]. This property of ethoxylated nonionic surfactants is revealed in the phase behavior (see fish diagram).

In 1968, Shinoda and Saito named this empirical correlation [33] with polyethoxylated surfactants: Phase Inversion Temperature (PIT). The authors demonstrated that the same surfactant can act as an O/W or a W/O emulsion stabilizer. At low temperatures, over the Winsor I region, O/W emulsion can be easily formed and are quite stable. On raising temperature, the O/W emulsion stability decreases, and the emulsion finally resolves when the system reaches Winsor III state. Within this region, W/O and O/W emulsions are unstable, with the minimum of stability as the ethoxylated surfactant is just balanced. At high temperatures, over the Winsor II region, W/O emulsion become stable. The median temperature of the inversion range is considered as the PIT of the emulsion. In practical, the determination of the PIT is usually followed by conductivity measurement as function of temperature [34], or measurement of emulsion droplets size below PIT and at the PIT [35] measurement as function of temperature, by viscosity change or light backscattering.

2.5. Fish diagrams (Kalhweit) and their corresponding Winsor microemulsion types

Shinoda, then Kalhweit and Strey have shown that the phase behavior of the ternary system consisting of non-ionic surfactant / oil / water / temperature can be completely represented in a phase prism [39-40]. Its base specifies the composition of the ternary system; its vertical edge is the temperature axis (see system in Figure I-16).

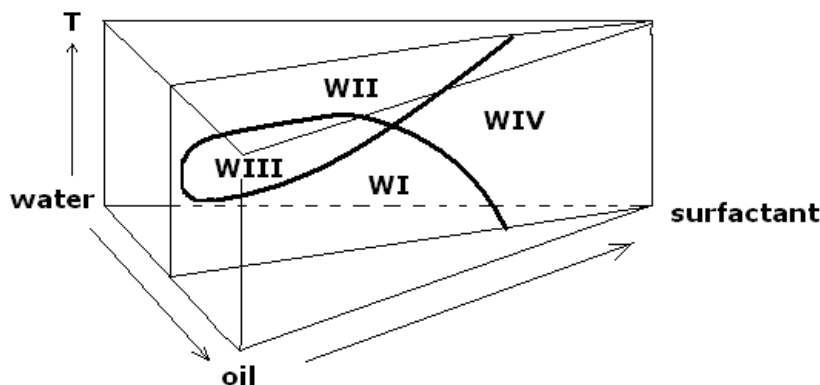


Figure I—16 – Fish cut in SOWT prism adapted from [39-41]

The perpendicular cut through the surfactant corner at a fixed oil/water-ratio of 1 (see Figure I-16 and below Figure I-17) shows the dependence of the phase behavior upon temperature.

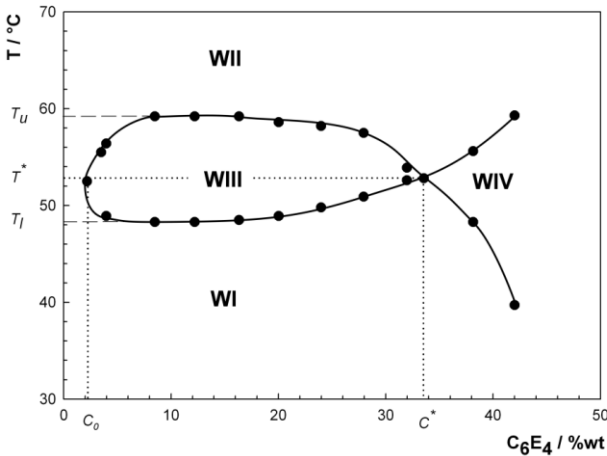


Figure I—17 –Fish diagram of the C₆E₄ / α-pinene / water system extracted from [29]

The so-called “Fish diagram” is the bi-dimensional temperature-surfactant concentration section of the tri-dimensional prism SOWT, where T is the temperature. The determination of the X point localized between the body and the tail of the fish diagram give the “optimal temperature”, noted T^* and “optimal concentration” noted C^* . This point corresponds to the intersection of the four Winsor micro-emulsion systems, the so-called Winsor I (WI), II (WII), III (WIII) and IV (WIV) and serves as a measurement of the phase inversion temperature (PIT \leftrightarrow T^*) and surfactant efficiency (C^*) as shown in figure 17. In the Winsor I system, the surfactant is preferentially soluble in water, and an oil-in-water O/W microemulsion is formed in equilibrium with an excess oil phase. On the contrary, the Winsor II system corresponds to water-in-oil W/O microemulsion, rich in surfactant, in equilibrium with an excess aqueous phase. In the Winsor III system, a three-phase system is formed where a surfactant-rich middle-phase coexists with both excess water and oil surfactant-poor phases. The middle-phase microemulsion is often characterized by a randomly distributed oil and water micro domains and discontinuity in both oil and water domains leading to a bicontinuous microemulsion. Finally, for higher surfactant concentrations, a single-phase (isotropic) microemulsion, the so-called Winsor IV system, can form. In the case of temperature-sensitive surfactants, such as polyethoxylated alcohols noted C_{*j*}E_{*j*}, the phase transitions WI→WIII→WII can occur by raising the temperature resulting from a more and more hydrophobic interface. An “optimal formulation” is thus defined for a given temperature at which the non-ionic surfactant has the same affinity for

water and oil [41]. This optimal formulation corresponds to a WIV system characterized by a maximal cosolubilization of water and oil in the microemulsion phase with the minimum amount of surfactant.

2.6. The packing parameter

The curvature alteration of the surfactant layer at the interface can be explained by the geometrical structure of surfactant with the interface. The obtained curvature is a function of the surface of the surfactant's head a_0 and its hydrophobic chain length l . Israelachvili introduced the concept of packing parameter (a dimensionless figure). It helps to classify the surfactant but also to understand how they aggregate [19].

$$P = \frac{V}{a_0 \times l} = 1 - \frac{l}{2} \left(\frac{1}{R_1} + \frac{1}{R_2} \right) + \frac{l^2}{3R_1 R_2} \quad (2) [43]$$

with V : volume of lipophilic chain of the surfactant

a_0 : area of the polar Head of the surfactant at the interface.

l : length of the lipophilic chain of the surfactant.

R_1 and R_2 : principal curvatures at the interface.

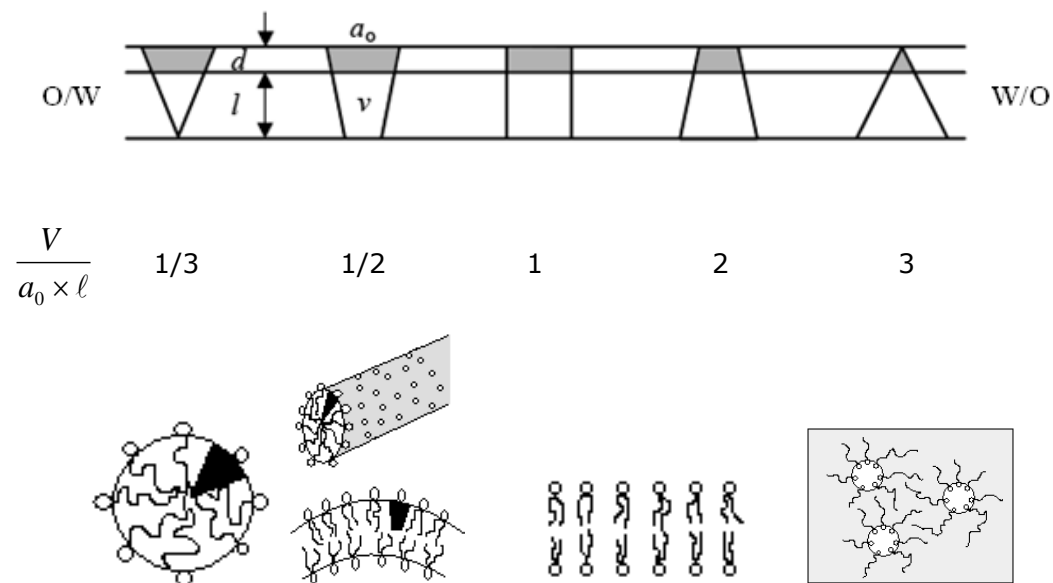


Figure I—18 - Effect of the geometry of the surfactant on the packing parameter from [19, 31]

This parameter increases while the structure changes from hydrophilic to lipophilic [42]. In a surfactant/oil/water system, it is important to notice that the volume of the polar head of the surfactant is actually the volume of the hydrated head and the volume of the lipophilic chain corresponds to the volume of the chain solubilized in oil.

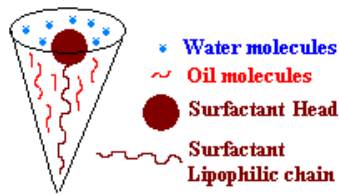


Figure I—19 - Surfactant molecule environment

2.7. The Hydrophilic Lipophilic Deviation concept (HLD)

In the beginning of 70's, consequently to the oil crisis, intensive research on Enhanced Oil Recovery (EOR) techniques based on surfactant/oil/water (SOW) systems at equilibrium has been developed to sustain the supply of crude oils. Among the proposed methods were low-tension surfactant flooding processes, in which a surfactant solution was injected into the oil reservoir to produce a low interfacial tension between the crude oil and water, in order to reduce capillary pressure resistance. The researchers were aiming at an "optimal surfactant formulation" at which the interfacial tension has a minimum, i.e.: at the balanced surfactant composition. The systems studied represented very complex mixtures, containing polydisperse surfactants, alcohols, salts, hydrocarbons and water. Elaborate empirical equations were proposed to evaluate the location of the balanced point of these compositions. Salager et al. [41] suggested an empirical correlation known as the hydrophilic-lipophilic deviation (HLD) as a dimensionless form of the thermodynamically derived surfactant affinity difference (SAD) equation to describe microemulsion systems [43]. Hydrophilic Lipophilic Deviation is based on the determination of the so-called optimum formulation. At this optimum formulation, the surfactant affinity to the polar and apolar pseudo phase of a micro-emulsion is equal, which thermodynamically means that the free energy change of a surfactant molecule, when transferred from oil-phase to water-phase, is zero. In addition, interfacial tension between oil and water has reached a minimum, it corresponds to the triphasic system introduced by Winsor (Winsor III: oil/micro-emulsion/water). At this optimal formulation, the value of HLD is set to zero; it is the reference state for the system. Any modification of the system will imply a change of the HLD value from zero (reference state) to a negative or positive value respectively depending on surfactant affinity for oily phase (hydrophobic behavior) or water phase (hydrophilic behavior). By any modification, we mean a change of temperature, type of surfactants and oil, addition of salt or co-surfactant.

For nonionic surfactants, the HLD value of a SOW system is defined as:

$$\text{HLD} = (\alpha - \text{EON}) + bS - k\text{ACN} + a.A + t\Delta T \quad (3)$$

where ACN is the alkane carbon number of the n-alkane used as oil, otherwise an EACN (Equivalent Alkane Carbon Number) scale is used; EON is the ethylene oxide number of the nonionic surfactant; S and b are respectively salt concentration and a constant characteristic of the type of salt; $a.A$ are two characteristic parameters linked to the nature, type and behavior of alcohols as a function of its concentration A , α and k are constants for a given type of surfactant, t is a temperature coefficient, ΔT is the temperature deviation from a reference (25 °C). Originally HLD equation was developed for ionic surfactants [43].

2.8. The Equivalent Alkane Carbon Number (EACN)

Cash et al. [44] originally described the concept of Equivalent Alkane Carbon Number (EACN). They have been extensively applied this concept to enhanced oil recovery to facilitate the characterization of crude oil. EACN corresponds to the number of carbon atoms of the linear alkane showing an equivalent lipophilicity to the given oil. Queste et al. [45] recently revisited the concept using the phase behavior of ternary systems based on monodispersed tetraethylene glycol monodecyl ether (C_{10}E_4) as surfactants and a series of oils such as alkanes, alkylcyclohexanes and alkylbenzenes. Each ternary system was studied by localizing the critical point (T^* , C^*) in the fish diagram. T^* has been used to characterize each oil by their Equivalent Alkane Carbon Number (EACN). This method set up the basis of an absolute EACN scale for the classification of oils.

3. Fragrances and surfactant systems interactions: a literature review

It is well established now in formulation development that the addition of fragrance, particularly the most polar ones (alcohols, phenol, aldehydes, amines, amides) may have a significant effect on the product formulation stability. The latter often implies substantial changes in the complex surfactant microstructure that has in general not been quantified. In the same time, their impact upon the self-assembly in surfactants and their influences on surfactant/oil/water systems are documented in a relatively limited bibliography. In early 90's, a basic research on the solubilization of perfumes by aqueous surfactant system has been initiated by cosmetic companies such as Kao and Colgate Palmolive due to the new regulation imposed to control VOC [46-47]. Friberg is one of the pioneer scientists who have extensively worked on the influence of fragrances on various surfactants systems, abundant

literatures regarding on vapor pressures and amphiphilic association structures are reported [48-57].

Saito et Al. [58] reported the investigation of the volatility of some synthetic fragrances (benzyl formate, benzyl acetate, benzyl propionate) from Pluronic P-85 in aqueous solution (a difunctional block copolymer surfactant terminating in primary hydroxyl groups) by the dynamic headspace method. The trial outcome showed that the volatility of hydrophobic fragrance was strongly reduced by Pluronic P-85. This volatile behavior was elucidated by the solubilization constants of fragrances between the micelle and bulk phase by semi equilibrium dialysis method.

3.1. Fragrances in SOW ternary systems as oil or additives

Early 90's, the solubilization of synthetic perfumes [59] by different hexadecyl polyoxyethylene ethers aqueous solution has been studied in terms of cloud point, maximum additive concentration, solubilizing capacities, distribution coefficient, and micellar size by Tokuoka et al. Three years later, the same author investigated the phase diagram of hexadecyl polyoxyethylene ether/synthetic perfume/water ternary system and discussed the interaction between surfactants and synthetic perfumes in relation to variations in phase regions; in particular, the micellar solution, inverse micellar solution and lamellar liquid crystal phases. This study is particularly relevant as many industrials products are based on such concentrated surfactants system and particularly detergents and cosmetics. Tokuoka et al. have selected fragrances by chemical functions of different polarities (hydrophilicity). In order to compare two very different systems using fragrance as oil, a monocyclic monoterpene - limonene, which is slightly more hydrophilic than alkanes [26] - and another class of plant-derived phenylpropanoid family: - eugenol, is emphasized here [59].

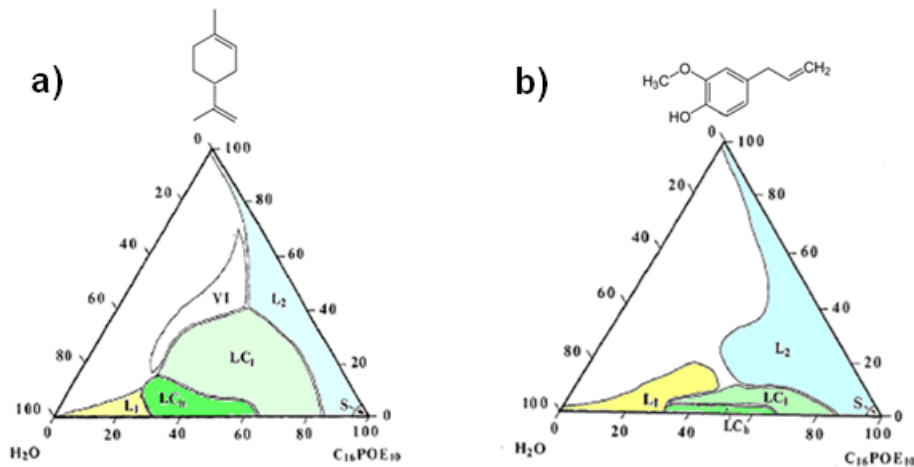


Figure I—20 -C₁₆POE₁₀ / limonene / water system (b) C₁₆POE₁₀ / eugenol / water system at 30 °C from reference [59]

The diagrams are composed by different phases: micellar solutions L₁ and L₂ (direct micelles and reverse), liquid crystal LC_n, LC₁ and V₁ (viscous isotropic solution). The unnamed region corresponds to a multiphase region. The region L₁ increases with the hydrophilic character of fragrance raw material as seen in Figure I-20. This behavior could suggest that a hydrophilic perfume is more easily solubilized in a micelle than hydrophobic perfume. While in the region L₁, perfume is solubilized in water, L₂ form of reverse micelles solubilizing water with perfume as continuous phase. In fact, the region L₂ also increases with the hydrophilicity of the molecule. When amount of surfactant is increasing, the micellar region L₁ vanishes and is transformed successively into two liquid crystal phases: LC_n (hexagonal phase) and then LC₁ (lamellar structure).

These two regions shrink with the increasing of the hydrophilicity of the molecule (which is the opposite for L₁ and L₂). In addition, the maximum concentrations of each synthetic fragrance dissolved in LC₁ decreases with their hydrophilicities, this implies that the more hydrophobic molecule produces a more stable lamellar structure at higher concentrations. Finally, the cubic phase disappears completely in the system which is involving eugenol as oil. To rationalize these observations, the authors introduced the Fujita ratio [59] (I/O) which defines the hydrophilicity of both molecules: perfume and surfactant. The more I/O of fragrances and surfactants are similar, the more they have affinity for each other so the regions L₁ and L₂ are larger. The higher the I/O ratio, the more perfume is considered as co-surfactant. Indeed, the limonene is soluble in the oily phase while eugenol, with I/O close to that of surfactant, tends to be at the interface due to the presence of phenolic OH group, which have strong affinity with water. The region L₁ is larger in the phase diagram for the

compounds considered as co-surfactants (case of eugenol) because they increase the interfacial surface occupied by surfactant and thus help to form a higher number of swollen micelles. The same assumption can be made for the increase of the region L_2 . This observation is confirmed by determining the concentration of perfume in the swollen micelles in the presence of another surfactant as shown in Figure I-21 [60].

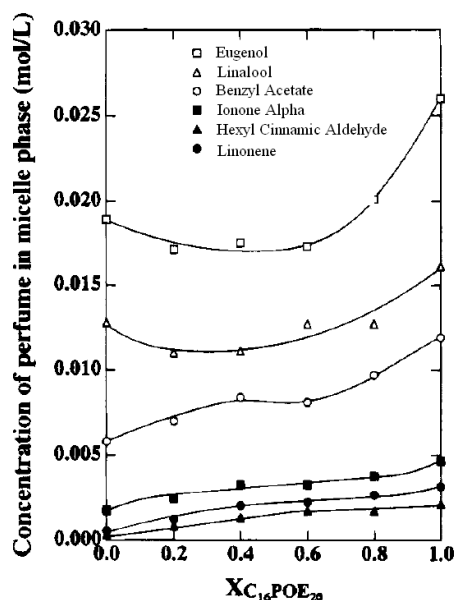


Figure I-21- Concentration of fragrance in the micellar phase as a function of the mole fraction of $C_{16}POE_{20}$ in the system SDS- $C_{16}POE_{20}$ extracted from [60].

The higher the fragrance I/O ratio (high hydrophilic property), the more it solubilizes in the micelles. In general, the higher the concentration of surfactant, the more perfume is dissolved. This phenomenon is less obvious for lipophilic perfume [60]. A smaller liquid crystals area in the phase diagram can also be explained by this location of perfumes. In fact, co-surfactants molecules may weaken the liquid crystal structure by altering the curvature and flexibility of the film and thus, the crystal structure break more quickly. Polar oils such as long chain alcohols segregate at the interface and may cause a change sign of the curvature, which is, became less positive which affects, more or less the crystal structure [61]. It is important to notice that eugenol is slightly lipophilic and will therefore strengthen the lipophilic character at the interface, and thus brings about a negative curvature. The cubic phase disappears completely when the fragrance penetrates in the interface [62].

However, among the liquid crystal structure, the lamellar phase is the one, which has the greatest change. According to the equation (1) A_{CW} , A_{WW} , A_{HH} and A_{II} are independent from the properties of perfumes, only A_{CO} and A_{OO} can be changed in this case. Taking into

account the presence of a phenolic group, A_{OO} value of eugenol should be rather more important because of its intermolecular interaction with the hydroxyl groups. Besides, eugenol's Fujita ratio value is close to that of surfactant, it should have a strong affinity for $C_{16}POE_{10}$; hence, the term A_{CO} should consequently increase. For a ternary system containing a hydrophilic perfume, the Winsor R ratio becomes very large compared to unity. The lamellar region clearly decreases when the hydrophilic properties of the perfume increases [59].

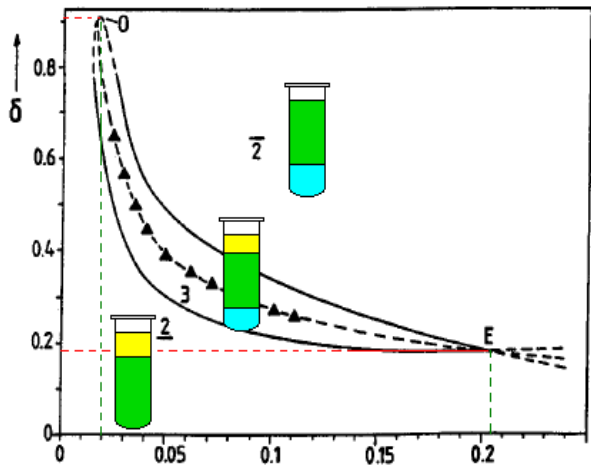
3.2. Diagram of optimization and effect of fragrances type alcohol

Various techniques - such as the addition of additives, variation of temperature - can modify the phase behavior of SOW system, and act directly at the interface (on the surfactant layer) to change the spontaneous curvature or increase the solubilization of organic compounds. Thermally stable microemulsions can be obtained using surfactants such as alkylpolyglucosides, C_nG_m with $m \geq 1$. In these systems, the temperature has only a slight influence on the size of the different regions of the diagram. This temperature stability is due to the strength of hydrogen bonds between hydroxyl groups of glucose and water molecules which prevents dehydration of the surfactant's head with a temperature increase; therefore the phase behavior depends essentially on the nature of the interfacial film. In the case of C_8G_1 / cyclohexane / water / geraniol system, the perfume will act as an additive. Stubenrauch, Paepflow and Findeneg studied the behavior of geraniol in this system using the interpretation of an optimization diagram (Figure I-22) [63].

The author are used notation introduced by Kahlweit to characterize the composition of the sample:

$$\alpha = \frac{B}{A+B} \quad (4) \quad \delta = \frac{B}{A+B} \quad (5) \quad \gamma = \frac{C+D}{A+B+C+D} \quad (6)$$

with α : mass fraction of oil in the binary water (A) - oil (B = cyclohexane) and δ : mass fraction of alcohol (D = geraniol) in the amphiphilic surfactant mixture (C = Octylmonoglucoside) - Alcohol (D) and γ : mass fraction of amphiphilic surfactant mixture (C) - Alcohol (D) in the quaternary system.



- $\underline{2}$ Winsor I - microemulsion oil droplets in water with an excess of oil
- $\bar{2}$ Winsor II - microemulsion of water droplets in oil with an excess of water
- 3 Winsor III - microemulsion with excess water and oil

Figure I—22 - Diagram optimization system C_8G_1 / cyclohexane / water / geraniol at 25 °C
 1:1 oil-water $\rightarrow \alpha = 0.44$ [63]

As co-surfactant, geraniol is segregated into the interfacial layer, and therefore changes the curvature of the amphiphilic interfacial layer: it goes from positive values (oil on the concave side of the interfacial layer) to negative (water on the concave side of the interfacial layer). It is therefore expected to cause a transition $\underline{2}$ to $\bar{2}$. In the same time, geraniol, as hydrophobic co-solvent, is present in high proportion in the oil thus responsible for an increase of its polarity. The C_8G_1 (hydrophilic surfactant) is progressively more solubilized into the oil phase where it can create a W/O micro emulsion. Geraniol leads to a phase inversion $\underline{2} - 3 - \bar{2}$. The solubility of fragrant alcohol changes the polarity of the oil phase but also the composition of the interface. The twisted shape of the fish (Figure I-22) is a direct consequence of competition between the incorporation of geraniol into the interfacial film and its solubility in the oil phase. When a surfactant-alcohol mixture is introduced into an oil-water mixture, a portion of alcohol is dissolved into oil. The alcohol is not available as co-surfactant and decreases the lipophilicity of the interface therefore the water molecules can enter the disordered interface.

The geraniol fraction in the oil increases with decreasing the proportion of alcohol-surfactant γ mixture in the system. Therefore, it will require a relatively large quantity of geraniol, in the alcohol-surfactant mixture (δ) to act as a co-surfactant.

The region of coexistence of three phases (WIII) starting at low δ and high γ (fish tail) and ends when the microemulsion phase disappears (head of fish).

At the optimum point, the quantities of surfactant and alcohol are at their minimum amount required to create a single-phase microemulsion (without water or oil excess). The composition of the amphiphilic phase (surfactant + alcohol) is obtained by subtracting from the total amount involved, the quantity dissolved in oil (solubility of the alcohol and surfactant are known). Thus, the fraction of alcohol present at the interface for zero curvature can be estimated as two molecules of alcohol for five of surfactants as shown in

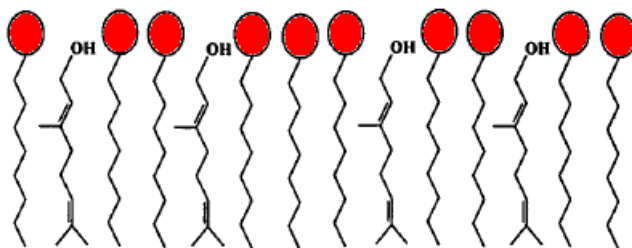


Figure I-23.

Figure I—23 - Organization at the interface of C_8G_1 and geraniol adapted from [63].

It is important to notice that this ratio depends on the nature of the surfactant and alcohol but also the entire system (oil + water). The presence of methyl groups at the end geraniol molecule increases its efficiency; in fact, the area occupied by this molecule is quite large and can easily reduce the curvature of the film. The fish, as shown in Figure I-22, is twisted because of the dual role of alcohol. Initially geraniol dissolves in the oil phase then starts to segregate at the interface. The authors suggested to pre-saturate cyclohexane with surfactant at 0.32% and geraniol at 3.24% avoiding the distortion of the fish (Figure I-24). The effect of solubility is removed by oil pre-saturation so that geraniol can fully play its role of co-surfactant, when incorporated into the interface, it changes the spontaneous curvature.

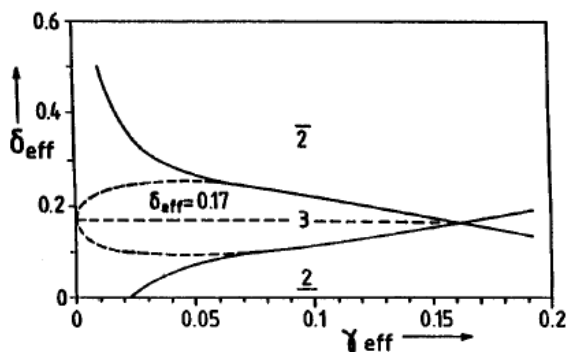


Figure I—24 - Optimization Diagram of C_8G_1 / cyclohexane / water / geraniol / 1:1 system oil-water $\alpha = 0.44$ at 25 °C and with the system Pre-saturation C_8G_1 and geraniol adapted from [63].

3.3. Perfumes location in liquid crystal phases

The location of the fragrance raw material into a surfactant/oil/water system is required to predict evaporation profile of fragranced emulsion but also to predict the product stability during their manufacturing [64]. There are different methods of investigation to determine the nature of Liquid Crystal phases. However, the most common technique is the SAXS (Small-Angle X-ray Scattering). It allows characterizing the structure of a fluid or solid at the nanometer scale by obtaining quantitative information on the size, shape and dynamics of the components. The principle is to irradiate the sample with a very well defined monochromatic X-rays beam (Figure I-25). Indeed, the sample must be irradiated by forming small angles to the surface to be characterized, as this process may allow it to be observed at large distances (see Figure I-25). The structure of monodisperse and polydisperse systems, such as liquid crystals can be studied, by this technique.

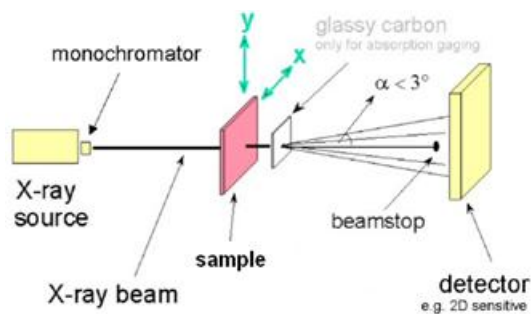


Figure I—25 - Diffraction of X-ray radiation extracted from [65]

Depending on the type of fragrance and the phase in which it is dissolved; there are two possible locations for the oil solubilization in liquid crystals. Firstly, the oil molecules can penetrate into the surfactant layer, which increases the surface a_0 of the surfactant. The second possibility is the solubilization of oil molecules inside the micelle (swelling effect) as shown in Figure I-26. In this case, the hydrocarbon part of the surfactant remains in the same state and a_0 is unchanged. In general, the volume of the lipophilic part of surfactant and its surface increase during the penetration of oil molecules within the chains of surfactants. To minimize this phenomenon, the increase in the curvature parameter, P , is energetically favorable: the curvature of the film becomes negative (or less positive) and a phase transition towards more lipophilic systems takes place [62].

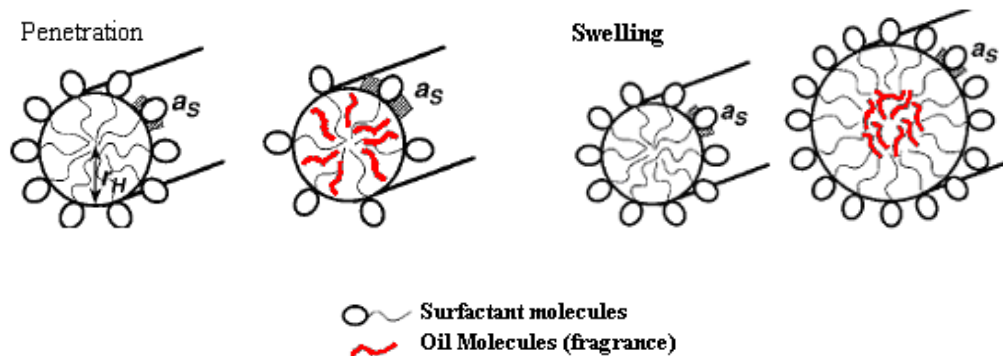


Figure I–26 - Schematic representation of the penetration phenomena and swelling by oil in the hexagonal phase adapted from [62].

The assessment of the radius r of the hydrophobic aggregate and the surface a_0 allow comparing the different liquid crystals phases as function of added perfumes. In all cases, the addition of perfume in the hexagonal phase increases the a_0 value: Some of the fragrance molecules therefore penetrate into the layer of surfactant. For the lamellar phase, L_α , a_0 increases more slowly by adding the fragrance, and with limonene, it even remains constant. The increase of a_0 is greater in the case of geraniol and linalool compared to limonene. This can be explained by the fact that limonene is a hydrophobic molecule while the two others are more hydrophilic and thus tend to segregate themselves at the interface. The value of a_0 increases when the “amphiphilic” character of the fragrance rises. More specifically, when both parameters r and a_0 increase, the perfume is located in micellar aggregate (swelling); however only if a_0 increases, so the fragrance is localized in the interfacial layer [66]. In the case of swelling, a_0 should not be modified but the fragrance molecules are not completely hydrophobic and they are still segregated along the chains of surfactants. Limonene belong to these molecules, it does not participate in the formation of the interface and is located in the apolar area [64]. Linalool, geraniol, eugenol have a hydroxyl group in their chain and act as a lipophilic co-surfactant. They enter largely into the surfactant layer and increasing the value of a_0 , so they influence the interface and make the curvature negative (more lipophilic). The hydrophilicity of the surfactant should increase to compensate the effect of the perfume and maintain the curvature at zero. A classification of perfumes can then be made. Depending on their properties, they change the penetration of the swelling in this order: d-limonene > aldehyde α -Hexylcinnamic > β -ionone > benzyl acetate > linalool > geraniol > eugenol > cis-3-hexenol.

In fact, the hydrophilicity of the perfume is not the only factor affecting the location of the solute particles in the aggregates. Indeed, the size and shape of molecules, their interactions with water and surfactants are also important. Therefore, the entire system must be taken into account in order to determine the location of perfumes [67]. Indeed, if the surfactant possesses chemical group with strong interactions (e.g., cholesterol groups), the perfume cannot penetrate the interfacial film and it will dissolve within the aggregates [66]. One more way to explain the solubilization of perfume molecules is to consider the measurement the HLB temperature.

3.4. Influence of the HLB temperature of fragrances on surfactants/oil/water systems

The HLB temperature is the temperature at which the solubilization of oil or fragrance compounds into the micelle reaches its maximum. This temperature coincides with the phase inversion temperature (PIT) in the emulsion except for areas rich in water and oil. The curvature of the surfactant layer at HLB temperature is zero for a bicontinuous microemulsion, with excess water and oil in same proportion [61]. The determination of HLB temperature is a significant datum for understanding the solubilization of fragrance molecules and the phase behavior of polyethoxylated nonionic surfactants in the presence of perfume. Oil types also influence the HLB temperature of these surfactants. In the case of saturated hydrocarbon compounds, the HLB temperature decreases with decreasing the oil molecular weight. Regarding fragrance, the carbon number for α -hexylcinnamic aldehyde is the same as decane; however, its HLB temperature is lower than decane [61]. This observation implies that the HLB temperature for perfumes molecules which have a double bond is lower, compared to ordinary hydrocarbon systems.

In addition, the nature of the different functional group present in a fragrance molecule has an influence on the HLB temperature of the system, for example, the effect of aldehyde or ketone group is minimal compared to that of a terminal hydroxyl group. This means that the fragrance molecules with an "amphiphilic" nature tend to lower the HLB temperatures. A classification of perfumes by their HLB temperature can be done as follow: linalool, geraniol, and eugenol < α -Hexylcinnamic aldehyde, β -ionone, and limonene. The phase diagrams of some of these fragrances are shown in Figure I-27. The HLB temperature of the system with limonene is 46 °C, with linalool is lower (10 °C) and geraniol is not even observable (< 0 °C). The HLB temperature of these perfumes is extremely low compared to classical alkane hydrocarbon.

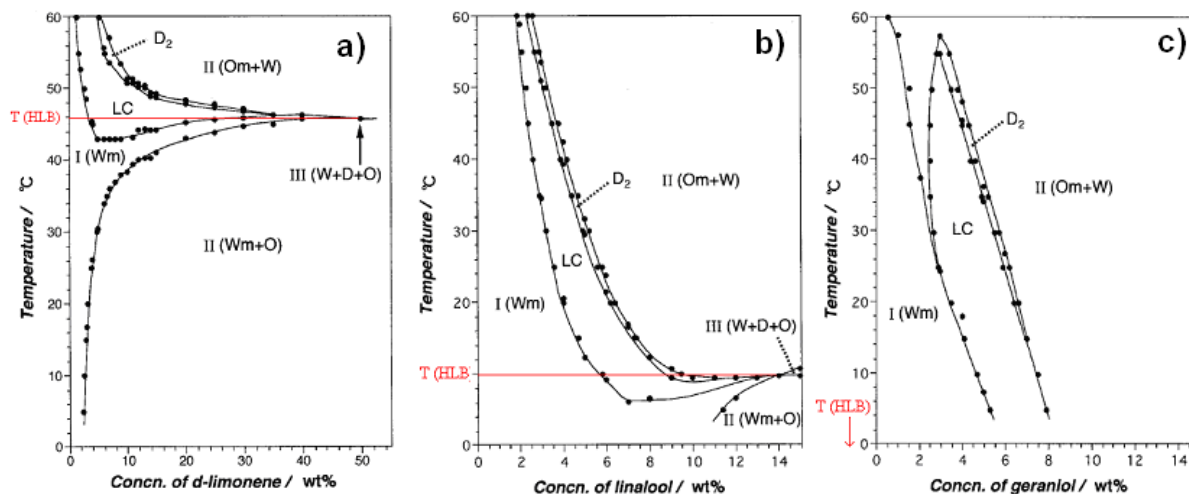


Figure I–27 - Phase diagram of the system water / $C_{12}EO_8$ (10%) / perfume depending on temperature (a) $C_{12}EO_8$ /limonene/water system (b) $C_{12}EO_8$ / linalool / water system (c) $C_{12}EO_8$ / geraniol / water system [61]

At HLB temperature, the curvature of the film is zero. Some fragrance molecules tend to penetrate into the surfactant film and involve a negative curvature. In the presence of oil with low molecular weight or with amphiphilic properties, the HLB temperature of the systems is low. This molecule tends to make the interface more lipophilic and changes the curvature. In other words, if oil has a strong tendency to penetrate into the surfactant layer, the HLB temperature will decrease.

3.5. Effect of the addition of alcohols and polyols on phase diagrams containing fragrance as oil

Polyols and alcohols alter H_0 and increase the flexibility of surfactant film. They modify the polarity of the current phases and go through the interface by increasing its flexibility and destabilizing the liquid crystal phase.

Addition of *n*-alcohols

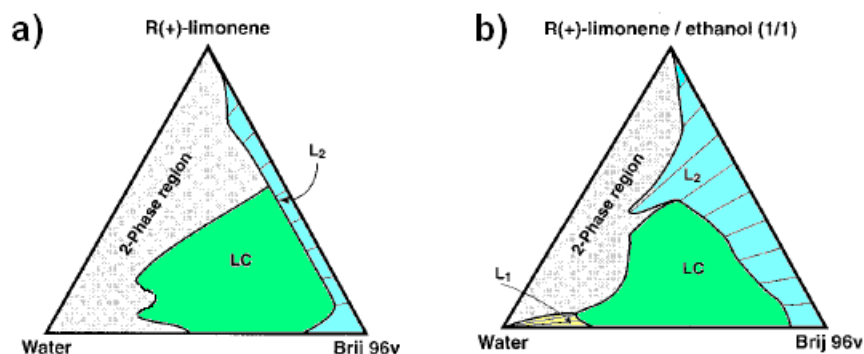


Figure I—28 - Phase diagram of Brij96 / R(+)-limonene / water system at 25°C; (a) R-(+)-limonene alone and (b) R-(+)-limonene / ethanol (1:1) [68]

The action of a monoalcohol is explained by taking the example of Brij96 / R-(+)-limonene / water system. As demonstrated in Figure I-20, the liquid crystal phase (LC) in the presence of ethanol (b) decreases in favor of L_2 (water in oil microemulsion formed along the area of liquid crystals). This implies that a considerable part of ethanol entering the interfacial film. In addition to the formation of larger L_2 area, a small region of microemulsion O/W occurs (phase L_1). This can be explained by the favorable solubility of ethanol in the three components of the system, which leads to the solubilization of oil in the water. The contraction of the LC phase means that the fragrance solubilization enhancement into the aqueous phase affects the spontaneous curvature at the interface and the amphiphilic layer elasticity [68]. The chain length of alcohol is an important factor in the achievement of more or less hydrophilic system.

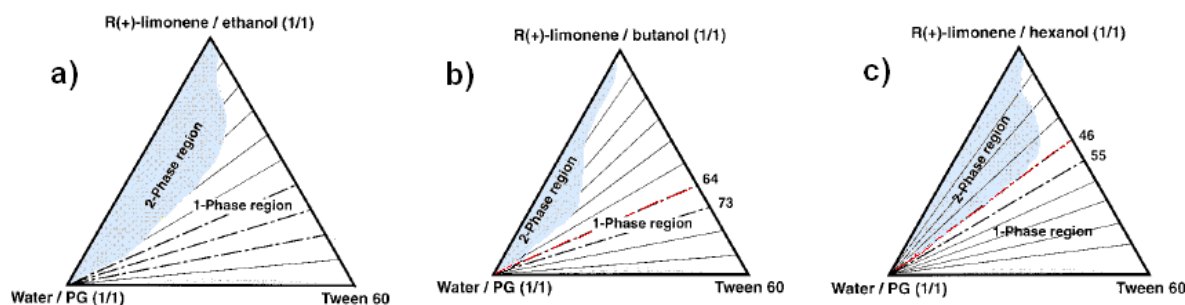


Figure I—29 - Phase diagram Tween 60 / limonene / alcohol / water / PG system at 25 °C; (a) R-(+)-limonene / ethanol (1:1), (b) R-(+)-limonene / butanol (1:1) and (c) R-(+)-limonene / hexanol (1:1)

Hydrophobic alcohols as butanol appear to be less effective because the monophasic area is less important. The addition of long-chain alcohol such as pentanol or hexanol decreases the solubilization capacity by increasing the interaction between the droplets. As a result, in order to formulate a fully water-soluble microemulsion, addition of short chain alcohols requires a significant amount of surfactants while for longer chain alcohols, this quantity is reduced. A larger microemulsion area do not mean an optimal composition, it will depend on the shape of the biphasic zone [69].

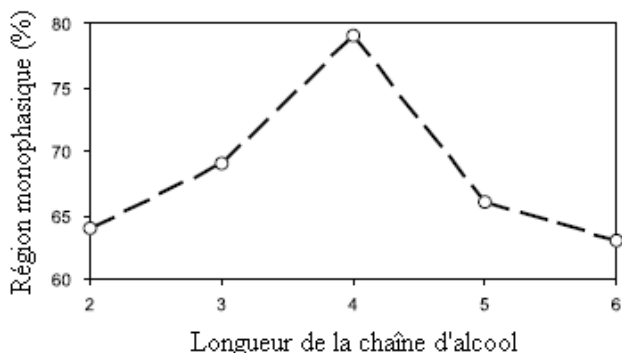


Figure I—30 - Alcohol chain length effect on the monophasic area (A_T) at 25 °C [69].

Addition of polyols

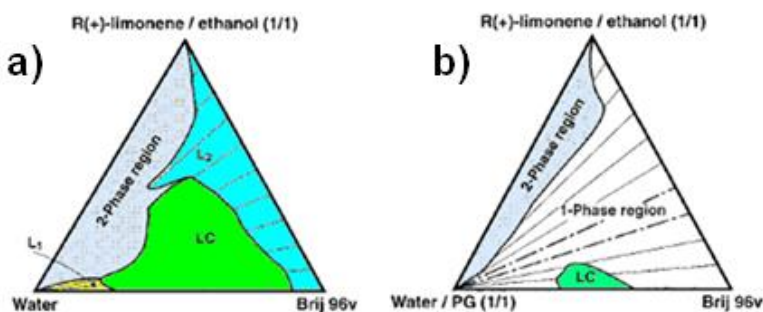


Figure I—31 - Phase diagram of Brij96 / R (+)-limonene / ethanol (1: 1) / water system at 25°C; (a) Brij96 / R-(+)-limonene / ethanol (1:1) / water and (b) PG (1:1) / Brij96 / R(+)-limonene / ethanol (1: 1) / water systems

Surfactant molecules aggregate also in polar protic solvents such as propylene glycol, formamide or glycerol. These solvents similar to water, form also hydrogen bonds, and have a relatively high dielectric constant. They are immiscible in apolar solvents like hydrocarbons. When these solvents are used as substitutes for water, their penetration into the surfactant interface can break or minimize the liquid crystals area.

Part of propylene glycol is incorporated in the interfacial layer and the other part can lower the polarity of the water. It is important to notice that this system is temperature-independent thanks to the solubility of nonionic surfactant in propylene glycol-water mixture. At any temperature, the surfactant is more soluble in the aqueous phase than in the oily phase (no increase of hydrophobicity with temperature). In the system propylene glycol / water / R(+)limonene / ethanol / Brij 96, the single-phase isotropic region (L_1 and L_2) is very wide and filled almost the entire phase diagram to the disadvantage of the liquid crystal as shown in Figure I-31 a. By increasing the proportion of propylene glycol, a total dilution of the oil in the aqueous phase is possible. It seems that this additive acts as a coupling agent between the regions of microemulsion O/W and W/O: phases L_1 and L_2 are joined and there is no phase transition in this region. The addition of additives in the oil phase (short-chain alcohol) or in the aqueous phase (polyols) significantly increases the area of microemulsion by changing the properties of interfacial film. The flexibility of the film is increased (the presence of asymmetry) because of the destabilization of the LC phase (organizational structure) for the benefit of the microemulsion. Ethanol has mainly an action on the surfactant film rigidity while polyols affect mainly the polarity of the aqueous phase. In all cases, polyols and short chain alcohols have an effect salting-in "and act as co-surfactants [69].

4. References of chapter I

1. Neuner-Jehle, N., Etzweiler, F., *Perfumes: Art, Science & Technology*, Chapman & Hall, **1994**, p153-206
2. Leffingwell Reports, Vol. 2 (No. 1), *Olfaction - Update No. 5*, May **2002**, www.leffingwell.com
3. Dyson, G.M., The Scientific Basis of Odor, *Chem. Ind.*, **1938**, 57, p647-651
4. Wright, R.H., *The Sense of Smell*, CRC Press, Boca Raton, FL, **1982**
5. Leffingwell, J.C., Comment in Gustation and Olfaction, G. Ohloff and A. Thomas, Ed., Academic Press, NY, **1971**, p144
6. Langenau, E.E., *Olfaction and Taste*, Vol. III., C. Pfaffman, Ed., Rockefeller University Press, New York, **1967**
7. Amoore, J.E., *Molecular Basis of Odor*, C.C. Thomas, Pub., Springfield, **1970**
8. Moncrieff, R.W., What is Odor? A New Theory, *Am. Perfumer*, **1949**, 54, p453
9. Buck, L. and Axel, R. *Cell*, **1991**, 65, p175-187
10. Piesse. S., *The art of perfumery - Longman London*, **1857**
11. Poucher, W. A., A classification of odors and its uses. *Am. Perf. Essent. Oil Rev.*1955, 66.
12. Sacchettini, J.C., Poulter, C.D., Creating Isoprenoid Diversity, *Science*, **1997**, 277(5333), p1788-1789
13. Breitmaier, E., *Terpenes* Wiley-VCH, **2006**
14. Bajgrowicz, J., Gaillard, A., Perfumer's notes: Javanol, Fragrance creation with sandalwood oil substitutes, *Perfumer & Flavorist*, **2007**, 32 (1), p32-37
15. Jones, M.N., Chapman, D., *Micelles, monolayers and biomembranes*, Wiley-Liss Inc, New York, **1995**
16. Rosen, M.J. *Surfactants and interfacial phenomena*, 2ed., John Wiley & Sons, New York, **1989**
17. Chevalier, Y., Zemb, T., The structure of micelles and microemulsions, *Rep. Prog. Phys.*, **1990**, 53, p279-371

18. Tanford, C., The hydrophobic effect: Formation of micelles and biological membranes, Wiley, New York, **1980**
19. Israelachvili, J.N., Intermolecular and surface forces, 2ed. Academic Press, London, **1991**
20. Forster, T., Principles of Emulsions Formation, Surfactants in Cosmetics: Second Edition, Revised and Expanded Ed.: Martin M. Rieger and Linda D. Rhein, Marcel Dekker Inc, New York, **1997**, 68, 4, p105-123
21. Sottmann, T., Strey, R., Ultralow interfacial tensions in water–n-alkane–surfactant systems, *J. Chem. Phys.*, **1997**, 106, p8606
22. Lang, John C.; Morgan, R. D., *J. Chem. Phys.*, **1980**, 73 (11), p5849
23. Tadros, T.F., Colloids in Cosmetics and Personal Care, Vol. 4, Wiley VCH, **2008**
24. Izquierdo, P., Esquena, J., Tadros, Th.F., Dederen, C., Feng, J., García, M.J., Azemar, N., Solans, C., *Langmuir*, **2004**, 20, p6594–6598
25. Forgiani, A., Esquena, J., Gonzalez, C., Solans, C. *Langmuir*, **2001**, 17 (7), p2076-2083
26. Bouton, F., Durand, M., Nardello-Rataj, V., Serry, M., Aubry, J.-M., Classification of terpene oils using the fish diagrams and the Equivalent Alkane Carbon (EACN) scale, *Colloids Surf. A*, **2009**, 338 (1-3), p142-147
27. Tokuoka, Y., Uchiyama, H., Abe, M., Ogino, K., *J. Colloid Interface Sci.*, **1992**, 152, p402–409
28. Scamhorn, J.F., Sabatini D.A., Harwell, J.H., *Surfactant, Part I: Fundamentals*, *Encyclopedia of Supramolecular Chemistry*, Ed. by J.L. Atwood and J.W. Steed, Marcel Dekker Inc, New York, **2004**, vol. 2, p1458
29. Bouton, F., Durand, M., Nardello-Rataj, V., Borosy, A.P., Quellet, C., Aubry J.M., A QSPR Model for the Prediction of the “Fish-Tail” Temperature of C₁₂E₄/Water/Polar Hydrocarbon Oil Systems, *Langmuir*, **2010**, 26 (11), p7962–7970
30. Winsor, P.A., Binary and multicomponent solutions of amphiphilic compounds. Solubilization and the formation, structure, and theoretical significance of liquid crystalline solutions. *Chem. Rev.* **1968**, 68 (1), p1-40
31. Eastoe, J., Microemulsions, Colloids Science Principles, methods and applications, Ed. by Terence Cosgrove, Blackwell Publishing Ltd, **2005**, Chap.5, p77-97

32. Shinoda, K., Arai, H., The correlation between Phase Inversion Temperature in Emulsion and Cloud Point in solution of Nonionic Emulsifier, *J. Phys.Chem.*, **1964**, 68, p3485-3490
33. Shinoda, K.; Saito, H., Stability of O/W (oil/water) type emulsions as functions of temperature and the HLB [hydrophilic-lipophilic balance] of emulsifiers: the emulsification by PIT (phase inversion temperature)-method, *J. Colloid Interface Sci.* **1969**, 30 (2), p258-63
34. Lee, J.M, Shin, H.J., Lim, K.H., Morphologies of three-phase emulsions of the ternary nonionic amphiphile/oil/water systems and their determination by electrical method, *J. Colloid Interface Sci.*, **2003**, 257, p344–356
35. Salager, J.L., Pérez-Sánchez, M., Garcia, Y., Physicochemical parameters influencing the emulsion drop size, *Colloid Polym. Sci.*, **1996**, 274, p81–84
36. Allouche, J., Tyrode, E., Sadtler, V., Choplin, L., Salager, J.L., Simultaneous conductivity and viscosity measurements as a technique to track emulsion inversion by the phase-inversion-temperature method, *Langmuir*, **2004**, 20, p2134–2140
37. Tyrode, E., Allouche, J., Choplin, L., Salager, J.L., Emulsion catastrophic inversion from abnormal to normal morphology 4. Following the emulsion viscosity during three inversion protocols and extending the critical dispersed-phase concept, *Ind. Eng. Chem. Res.* **2005**, 44, p67–74
38. Pizzino, A., Rodriguez, M.P., Xuereb, C., Catté, M., Van Hecke, E., Aubry, J.M., Salager, J.L., Light backscattering as an indirect method for detecting emulsion inversion, *Langmuir*, **2007**, 23, p5286–5288
39. Kahlweit, M., Strey, R., Haase, D., *J. Phys. Chem.*, **1985**, 89, p163-171
40. Kahlweit, M., Strey, R., Haase, D., Kunieda, H., Schmeling, Faulhaber, T.B., Borkovec, M., Eicke, H.F., Busse, G., Eggers, F., Funck, Th., Richmann, H., Magid, L., Södermann, O., Stilbs, P., Winkler, J., Dittrich, A., Jahn, W.J., *J. Colloid Interface Sci.*, **1987**, 118, p436
41. Salager, J.L., Anton, R., Anderez, J.M., Aubry, J.M., *Techniques de l'Ingénieur, Génie des Procédés, J2157*, **2001**, p1-20
42. Kunieda, H, Kazuyo, O., Huang, K.L., Effect of oil on surfactant molecular curvatures in liquid crystals, *J. Phys. Chem. B*, **1998**, 102, p831-838
43. Salager, J.L., Marquez, N., Graciaa, A., Lachaise, J., *Langmuir*, **2000**, 16, p5534-5539

44. Cash, L., Cayias, J. L., Fournier, G., MacAllister, D., Schares, T., Schechter, R. S., Wade, W. H., The application of low interfacial tension scaling rules to binary hydrocarbon mixtures, *J. Colloid Interface Sci.*, **1977**, 59 (1), p39-44
45. Queste, S., Salager, J.L., Strey, R., Aubry, J.M., The EACN scale for oil classification revisited thanks to fish diagrams, *J. Colloid Interface Sci.*, **2007**, 312 (1), p98-107
46. Labows, J.N., Brahms, J.C., Cagan, R.H., *Surf. Sci. Ser.*, **1997**, 68, p605-619
47. Labows, J.N., Brahms, J.C., Cagan, R.H., Solubilization of fragrances by surfactants, *Surfactants in Cosmetics: Second Edition, Revised and Expanded Ed.: Martin M. Rieger and Linda D. Rhein*; Marcel Dekker Inc: New York; **1997**, 68, 28, p605-618
48. Friberg, S.E., Ge, L., Guo, R., Swelling of water/nonionic surfactant lamellar liquid crystals: A model, *J. Dispersion Sci. Technol.*, **2008**, 29, 5, p735-739
49. Friberg, S.E., Yin, Q., Aikens, P.A., Vapor pressures and amphiphilic association structures, *Colloids Surf. A*, **1999**, 159, 1, p17-30
50. Friberg, S.E., Yin, Q., Aikens, P.A., Vapor pressures of phenethyl alcohol and limonene in systems with water and Laureth-4, *Int. J. Cosmet. Sci.*, **1998**, 20, 6, p355-367
51. Friberg, S.E., Young, T., Mackay, R.A., Oliver, J., Breton, M., Evaporation from a microemulsion in the water-aerosol OT-cyclohexanone system, *Colloids Surf. A*, **1995**, 100, p83-92
52. Friberg, S.E., Zhang, Z., Gan Zuo, L., Aikens, P.A., Stability factors and vapor pressures in a model fragrance emulsion system, *J. Cosmet. Sci.*, **1999**, 50, 4, p203-219
53. Zhang, Z., Friberg, S.E., Aikens, P.A., Change of amphiphilic association structures during evaporation from emulsions in surfactant-fragrance-water systems, *Int. J. Cosmet. Sci.*, **2000**, 22, 3, p181-199
54. Friberg, S.E., Effect of relative humidity on the evaporation path from a phenethyl alcohol emulsion, *J. Colloid Interface Sci.*, **2009**, 336, 2, p786-792
55. Friberg, S.E., Evaporation from a fragrance emulsion, *J. Dispersion Sci. Technol.*, **2006**, 27, 5, p573-577
56. Friberg, S.E., Aikens, P.A., Constant vapor pressure emulsions evaporation: Linalool/water stabilized by Laureth-4, *J. Colloid Interface Sci.*, **2009**, 333, 2, p599-604

57. Friberg, S.E., Al-bawab, A., Bozeya, A., Aikens, P.A., **2009**, Geranyl acetate emulsions: Surfactant association structures and emulsion inversion, *J. Colloid Interface Sci.*, **2009**, 336, 1, p345-351
58. Saito, Y., Miuraa, K., Tokuokab, Y., Kondob, Y., Abeb, M., Satoa, T., Volatility and solubilization of synthetic fragrances by Pluronic P-85, *J. Dispersion Sci. Technol.*, **1996**, 17, 6, p567-576
59. Tokuoka, Y., Uchiyama, H., Abe, M., Phase diagrams of surfactant/water/synthetic perfume ternary systems, *Colloid Polym. Sci.*, **1993**, 272, p317-323
60. Tokuoka, Y., Uchiyama, H., Abe, M., Christian, S.D., Solubilization of some synthetic perfumes by anionic-nonionic mixed surfactant system, *Langmuir*, **1995**, 11, p725-729
61. Kanei, N., Tamura, Y., Kunieda, H., Effect of Types of Perfume Compounds on the Hydrophile-Lipophile Balance Temperature, *J. Colloid Interface Sci.*, **1999**, 218, p13-22
62. Kunieda, H., Kazuyo, O., Huang, K.L., Effect of oil on surfactant molecular curvatures in liquid crystals. *J. Phys. Chem. B.* **1998**, 102, p831-838
63. Stubenrauch, C., Paepflow, B., Findenegg, G.H., Microemulsions supported by monoglucoside and geraniol: The role of the alcohol in the interfacial layer, *Langmuir*, **1997**, 13, p3652-3658
64. Kayali, I., Khan, A., Lindman, B., Solubilization and location of phenethyl alcohol, benzaldehyde, and limonene in lamellar liquid crystal formed with block copolymer and water, *J. Colloid Interface Sci.*, **2006**, 297, p792-796
65. Leibniz Institute of Polymer Research Dresden, X-Ray Lab web site: <http://www.ipfdd.de/X-ray-Lab.197.0.html>, **2010**
66. Kanei, N., Watanabe, K., Kunieda, H., Effect of added Perfume on the stability of discontinuous cubic phase, *J. Oleo Sci.*, **2003**, 52, p607-619
67. Szekeres, E., Acosta, E., Sabatini, D.A., Harwell, J.H., A two-State Model for Selective Solubilization of Benzene-Limonene Mixtures in Sodium Dihexyl Sulfosuccinate Microemulsions, *Langmuir*, **2004**, 20, p6560-6569
68. Garti, N., Yaghmur, A., Leser, M.E., Clement, V., Watzke, H.J., Improved oil solubilization in oil/water food grade microemulsions in the presence of polyols and ethanol, *J. Agric. Food Chem.*, **2001**, 49, p2552-2562

69. Yagmur, A., Aserin, A., Garti, N., Phase behavior of microemulsions based on food-grade non-ionic surfactants: effect of polyols and short chain alcohols, *Colloids Surf. A.*, **2002**, 209, p71-81

Chapter II

II. Fish diagram as a tool to formulate fragrance microemulsions

This second chapter is focused on the phase behavior of different polar oils, especially odorous terpenes. The first section of this chapter is dedicated to the determination of the phase behavior of ternary systems based on tetraethylene glycol monoalkyl ether (C_iE_4) as surfactants and a series of mono- and sesquiterpenes as fragrance oils by resorting to the HLD (Hydrophilic–Lipophilic Deviation) concept. Each ternary system was studied by localizing the critical point (T^* , C^*) in the fish diagram and the terpenes were characterized by their Equivalent Alkane Carbon Number (EACN) allowing a classification of the fragrant oils. EACN values have been rationalized by considering structural changes of the terpenes, such as number of carbons, branching, cyclization, unsaturation and aromatization. The case of a sesquiterpene (caryophyllene) has been studied in detailed and compared with *n*-hexane since both of them exhibit a similar EACN although they have 15 and 6 carbons respectively.

In the second section, the fish-tail temperatures (T^*) have been determined or collected for 85 ternary systems based on 3 tetraethylene glycol monoalkyl ethers C_iE_4 ($i = 6, 8, 10$), water and 43 hydrocarbon oils of various hydrophobicities. 14 fragrant mono- and sesquiterpenes in addition to 29 model oils, including *n*-alkanes, cyclohexenes, cyclohexanes and alkylbenzenes were investigated in order to establish a QSPR model for the prediction of T^* as a function of the chemical structure of the oils. Only two molecular descriptors related to branching (Kier A3) and polarizability (Average Neg Softness) of the molecules are necessary to model and predict the values of T^* and EACN of unsaturated and/or cyclic, and/or branched hydrocarbons exhibiting an EACN ranging from -1.2 and 28. Prediction of C^* for C_6E_4 /oil/water system is also established and qualitatively discussed. Results are discussed in terms of evolution of the effective packing parameter of the surfactants according to temperature and oil penetration into the interfacial film. The results shown in this chapter have been published respectively into: *Colloids and Surface A* for section 1 [46] and *Langmuir* for section 2 [78].



1. Classification of terpene oils according to the Equivalent Alkane Carbon (EACN) scale

1.1. Introduction

Fragrances play a key role in many consumer products such as detergents, cosmetics, foods, pharmaceuticals, personal care products. Though they encompass virtually all organic functional groups, these molecules of different polarities exhibit generally a hydrophobic feature and their solubilization, especially in water-based formulations, is not straightforward [1]. Many methods have been developed to solve this problem using inclusion complexes, e.g. cyclodextrins, vesicles and liposomes [2,3]. However, the usual route to solubilize perfume molecules in water involves surfactants, particularly non-ionic ones such as polyethoxylated alcohols C_iE_j [4,5]. Solubilization of perfume molecules with surfactants in aqueous systems is generally performed in micellar solution [6,7]. Some studies also report their solubilization in hexagonal [8], cubic [9] or lamellar [10] liquid crystalline phases. Kunieda and coworkers [9] showed that, in a cubic phase of aqueous polyoxyethylene dodecyl ether $C_{12}E_{25}$, the solubilization capacity of the perfume strongly depends on its hydrophobicity. Kayali et al. studied the solubilization and location in the association structures of limonene, benzaldehyde and phenethylalcohol in lamellar [10] and hexagonal [8] liquid crystals formed with a triblock amphiphilic copolymer and water. It was shown that amphiphilic fragrance molecules tend to penetrate in the surfactant palisade layer, inducing a more negative surfactant curvature leading to lower fish temperature values, whereas hydrophobic fragrance molecules are localized inside the core of the apolar domain. Their influence on the surfactant palisade layer is subsequently lower, leading to higher fish temperature values.

Cosolubilization of water and perfume molecules can also be achieved efficiently through the formation of one-phase microemulsions [11-17]. Most of the time, a cosurfactant, e.g. short chain alcohols or glycols, is added. Kanei et al. [18] studied the influence of added synthetic fragrance molecules on the phase behavior of the octaethylene glycol dodecyl ether $C_{12}E_8$ /water/perfume systems. They demonstrated that the fish temperature is directly linked to the degree of penetration of the fragrance oil molecules into the surfactant palisade layer.

The behavior of surfactant–oil–water (SOW) systems can be rationalized by resorting to the HLD (Hydrophilic–Lipophilic Deviation) concept [19], originally described by Salager et al. [20] as SAD (Surfactant Affinity Difference). Queste et al. [21] revisited recently the HLD concept thanks to the so-called “fish diagram”, i.e. the bi-dimensional temperature–surfactant concentration section of the tri-dimensional prism SOWT, where T is the temperature. The optimal temperature, noted T^* , is no longer determined at an arbitrarily fixed value of surfactant concentration but at the X point localized between the body and the tail of the fish diagram. This point corresponds to the intersection of the four Winsor microemulsion systems, the so-called Winsor I (WI), II (WII), III (WIII) and IV (WIV).

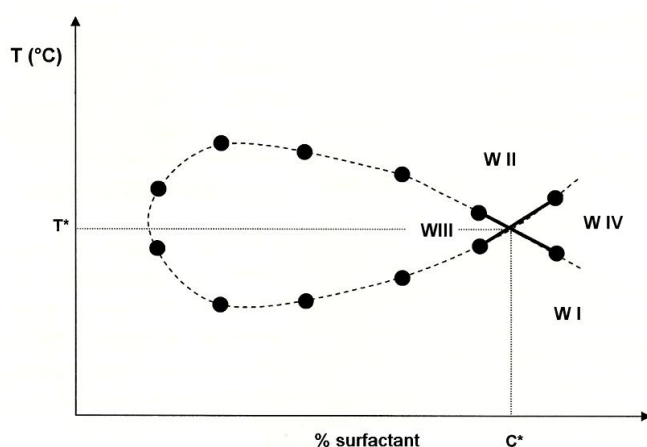


Figure II–1 - Determination of the X point by construction of the fish diagram Temperature / % surfactant. Experimental points (\bullet) are used to delimit the form of the fish (---). (C^*/T^*) is located by the cross (intersection of the Winsor I, II, III and IV)

In the present work, the phase behavior of ternary systems based on tetraethyleneglycol monoalkyl ether, noted C_7E_4 , as surfactants and fifteen mono- and sesqui-terpenes as fragrance oils was investigated by resorting to the HLD concept. The ternary systems, for each terpene have been studied by localizing the X point in the fish diagram and have been characterized by their Equivalent Alkane Carbon Number (EACN). Complete fish diagram of the C_8E_4 /water/caryophyllene system has been established and compared with hexane, i.e. the alkane of closest ACN. Finally, the effect of the chemical structure of the terpenes on the EACN values has been rationalized by considering structural changes of the terpenes, such as number of branching, double bonds or cyclic content. EACN is a key parameter to design stable emulsions or microemulsions.

1.2. Results

Phase behavior of equilibrated surfactant–oil–water systems can be described according to the Winsor classification (type I, II, III and IV) [22,23] and quantitatively rationalized by the HLD concept [19-21]. In the Winsor I system, the surfactant is preferentially soluble in water, and an oil-in-water O/W microemulsion is formed in equilibrium with an excess oil phase. On the contrary, the Winsor II system corresponds to water-in-oil W/O microemulsion, rich in surfactant, in equilibrium with an excess aqueous phase. In the Winsor III system, a three-phase system is formed where a surfactant-rich middle-phase coexists with both excess water and oil surfactant-poor phases. The middle-phase microemulsion is often characterized by a randomly distributed oil and water microdomains and discontinuity in both oil and water domains leading to a bicontinuous microemulsion. Finally, for higher surfactant concentrations, a single-phase (isotropic) microemulsion, the so-called Winsor IV system, can form. In the case of temperature-sensitive surfactants, such as polyethoxylated alcohols noted C_iE_j , the phase transitions $WI \rightarrow WIII \rightarrow WII$ can occur by raising the temperature resulting from a more hydrophobic interface. An “optimal formulation” is thus defined for a given temperature at which the non-ionic surfactant has the same affinity for water and oil [20]. This optimal formulation corresponds to a WIV system characterized by a maximal cosolubilization of water and oil in the microemulsion phase.

HLD, for Hydrophilic–Lipophilic Deviation, is a dimensionless number expressed, for non-ionic surfactants, by the following relation:

$$HLD = (\alpha - EON) + bS - kACN + aA + t \Delta T \quad (1)$$

where ACN is the carbon number of the n -alkane (replaced by EACN for non-alkane oils), A and S are alcohol and salt concentrations, a and b are constants characteristic of type of alcohol and salt, a and k are constants for a given type of surfactant, t is a temperature coefficient, ΔT is the temperature deviation from a reference (25 °C).

The HLD value takes into account not only the hydrophilic/lipophilic balance of the surfactant, as the HLB number does, but also the temperature, the nature and the concentration of cosurfactant, the electrolyte and the nature of the oil phase. The HLD value is of particular interest as it is directly related to the phase behavior of SOW systems [24,25]. Therefore, it is a key parameter to formulate micro- and macro-emulsions

according to a rational approach. In the absence of electrolyte and alcohol, the HLD equation is simplified as follows:

$$\text{HLD} = cst + tT^* - kACN \quad (2)$$

which becomes, at the optimal formulation:

$$0 = cst + tT^* - kACN \quad (3)$$

where *cst* stands for "constant value".

As a consequence, temperature scans performed at several surfactant concentrations allow the detection of the *X* point, i.e. the intersection of the four Winsor regions, characterized by the optimal temperature T^* and by the optimal surfactant concentration C^* [26]. In comparison with *n*-alkanes of well-defined ACN, such experiments allow the determination of the Equivalent Alkane Carbon Number of more complex oils like the terpene fragrance molecules.

1.2.1. Fish temperatures T^* and critical concentrations C^* for the C_iE_4/n -alkane/water systems

Polyethoxylated alcohols C_jE_j were chosen as surfactants because their hydrophilicity decreases when temperature increases, which is actually a sensitive, accurate and reversible formulation variable, particularly convenient for the study of the phase behavior of SOW systems using the HLD concept. Among the large choice of possible C_jE_j , those bearing at the most four ethylene oxide groups can be easily purified by distillation. Hence, tetraethylene glycol monoalkyl ether, noted C_iE_4 where $i = 6$ (C_6E_4), 8 (C_8E_4) and 10 ($C_{10}E_4$) of high purity (> 99%) were synthesized on laboratory scale using a modified version of the known procedure [21] and [29] in order to obtain the highest yield of C_iE_4 . The tetraethylene glycol/bromoalkanes molar ratio was equal to 10/1 instead of 20/1 and the elimination of unwanted compounds, such as dialkyl derivatives, alcohols and unreacted E_4 , could be optimized thanks to repeated extractions with a mixture of toluene/petroleum ether. These improvements allowed the recovery of more than 80% of the desired C_iE_4 with an excellent purity as attested by their cloud point (40.85 °C at 7.1% in water for C_8E_4) [30]. The phase behavior of the tetraethyleneglycol monoalkyl ether / *n*-alkane / water systems was plotted in a two-dimensional diagram, as a function of the formulation, i.e. temperature, (ordinate) and surfactant concentration (abscissa).

This leads to the typical fish-shaped diagram as illustrated in Figure II-2 for *n*-hexane.

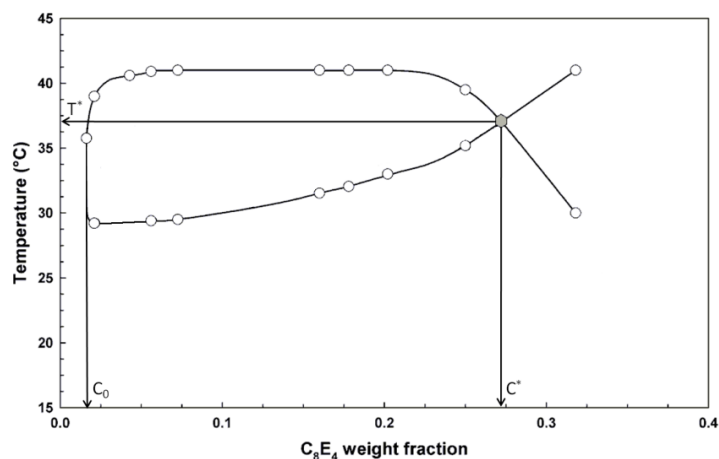


Figure II-2 - Fish diagram of the C_8E_4/H_2O /hexane systems.

From this fish diagram, the optimal formulation corresponding to a one-phase microemulsion (Winsor IV) obtained with the minimum surfactant concentration can be readily detected. The associated point, further named X point, is characterized by its two coordinates, the fish temperature T^* and the optimal surfactant or critical concentration C^* . T^* and C^* values reported in the literature [21], [27] and [31] for different C_iE_4/n -alkane/water systems are summarized in Table II-1 and compared with our values. Figure II-3 shows the evolution of the fish temperatures T^* for the C_iE_4 /oil/water systems as a function of the ACN of alkanes and of the EACN of terpenes.

Table II-1 - Fish temperatures $T^*(^{\circ}C)$ and critical concentrations $C^*(wt. \%)$ for C_iE_4/n -alkane/water systems at a water-to-oil ratio = 1

Alkanes	$C_6E_4^a$		C_8E_4				$C_{10}E_4$			
	T^*	C^*	T^{*a}	C^{*a}	T^{*b}	C^{*b}	T^{*c}	C^{*c}	T^{*d}	C^{*d}
Hexane	65.8	47	37.4	25.7	34.5	21.2	19.5	8	19.4	10.7
Heptane	71.4	51.6	-	-	-	-	-	-	-	-
Octane	77.5	53.7	46.1	29.3	41.3	24.1	25	10.5	24.3	13.6
Nonane	82	60.9	50.5	32.9	-	-	-	-	-	-
Decane	-	-	54.5	35.7	48	29.2	30.5	14.1	30.2	17
Dodecane	-	-	63.9	44.1	54.6	34	35.5	17	35.4	21.5
Tetradecane	-	-	71.3	49.1	61	41.3	41.5	21.7	40.2	-
Hexadecane	-	-	77.9	55	68.1	49.1	47	24.5	-	-

^a our work, ^b Kahlweit work [27], ^c Queste work [21], ^dBurauer work [31]

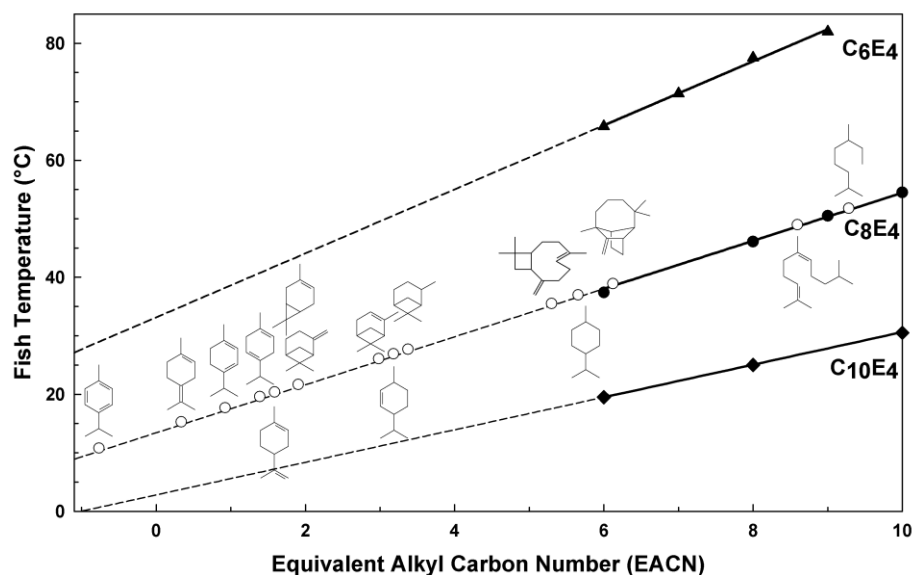


Figure II—3 Linear evolution of the fish temperatures T^* for the systems C_iE_4/n -alkanes/water as a function of the Alkyl Carbon Number (ACN) of the alkane: solid lines, C_6E_4 (▲), C_8E_4 (●), $C_{10}E_4$ (◆). Equivalent Alkyl Carbon Number (EACN) are determined by intersecting their fish temperatures T^* with the extrapolated straight line (dotted line) obtained with n -alkanes for C_8E_4 (○) and C_6E_4 (not shown).

This is worth noting that both optimal concentration C^* and fish temperature T^* reported by Kahlweit for the C_8E_4/n -alkanes/water systems [27] are significantly lower than our values. This discrepancy could be explained by the method used and the purity of the surfactant. To determine the X point, Kahlweit reported a water-to-oil ratio expressed in volume whereas we considered the ratio in weight, which might led to limited differences in the position of the optimal formulation [21].

Impurities coming from synthesis for surfactants like octanol and tetraethyleneglycol (E_4) in the case of C_8E_4 might lead to decrease the fish temperature (and optimal concentration as well)in a much more extensive way. A deliberate addition of 0.3 wt.% of octanol and E_4 in the system was found to decrease the fish temperatures by 5 °C. Furthermore, it was found that commercially available C_8E_4 (e.g. from Fluka) often used to build fish diagrams has a much lower cloud point (37.45 °C) than the one of our synthesized sample (40.85 °C) which is very close to the value reported by Schubert et al. for a highly purified C_8E_4 (40.8 °C).

At the X point, both the curvature of the interfacial film and the HLD value are equal to zero. Equation (2) can be then expressed as follow:

$$\text{HLD} = 0 = \sigma + \beta \text{ACN} - T_{CE4}^* \quad (4)$$

When the X point is determined for a series of alkanes, e.g. from hexane to hexadecane, there are enough data to fit Equation (4) with a linear regression [26] and [28]. The corresponding best fits are summarized in Table II-2 which reports the values of the σ and β coefficients as well as the EACN range of oils attainable with the C_iE_4 ($i = 6, 8, 10$) under study for fish temperatures T^* easily reachable in normal conditions, i.e. between 10 and 100 °C.

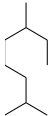
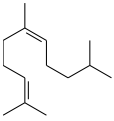
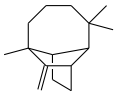
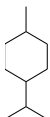
Table II-2 Coefficients σ and β for C_iE_4 surfactants and EACN range of oils attainable with the C_iE_4 for T^* between 10 °C and 100 °C

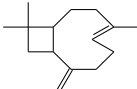
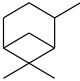
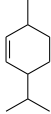
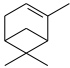
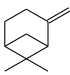
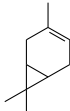
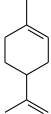
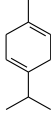
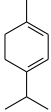
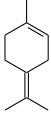
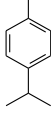
C_iE_j	σ	β	EACN Range
$C_{10}E_4$	3	2.7	3 to 35
C_8E_4	15.5	4.0	-1 to 21
C_6E_4	32.8	5.5	-4 to 15

1.2.2. Fish temperatures and critical concentrations for the C_iE_4 /terpene/water systems

The following table II-3 reports the values of T^* and C^* determined with C_6E_4 and C_8E_4 for fifteen terpenes which have been selected for their chemical and structural diversities, as well as their high purity and perfumery interest.

Table II-3 Fish points (T^* , C^*) and EACN values of terpenes determined for the C_iE_4 /terpenes/water systems ($i = 6$ or 8)

Entries	Terpenes	Formula	C_6E_4			C_8E_4		
			$T^*(^{\circ}C)$	$C^*(\%)$	EACN	$T^*(^{\circ}C)$	$C^*(\%)$	EACN
1	Myrcane		88.1	60.9	10	51.8	35	9.3
2	2,6,10-Trimethyl undecane-2,6-diene		-	-	-	49	30.2	8.6
3	Longifolene		-	-	-	38.9	26.2	6.1
4	<i>p</i> -Menthane		66.9	46.9	6.2	37	23.4	5.7

5	Caryophyllene		64.1	43.5	5.7	35.5	23.8	5.3
6	Pinane		56.8	37.3	4.3	27.7	18.3	3.4
7	<i>p</i> -Menth-2-ene		-	-	-	26.9	17.2	3.2
8	α -Pinene		52.7	35.3	3.6	26.1	18.1	3
9	β -Pinene		45.8	31.5	2.3	21.7	18	1.9
10	Δ -3-Carene		48.8	33.9	2.9	21.7	18.4	1.9
11	Limonene		44.3	28.4	2	20.4	16.2	1.6
12	γ -Terpinene		43.3	28.7	1.9	19.6	17.8	1.4
13	α -Terpinene		41.1	28.9	1.5	17.7	18.3	0.9
14	Terpinolene		40.5	29.7	1.3	15.3	17.7	0.3
15	<i>p</i> -Cymene		31.6	25.9	-0.3	10.8	17.4	-0.8

C_8E_4 and C_6E_4 are suitable amphiphiles for the determination of fish temperatures of terpene oils whereas $C_{10}E_4$ [21] would lead to fish temperatures close to or even lower than the melting point of water. Figure II-4 shows that fish temperatures T^* , measured for the various terpenes, are strongly correlated for both surfactants C_8E_4 or C_6E_4 .

However, EACN values assessed with C_8E_4 are considered to be more reliable than the one obtained with C_6E_4 since this later amphiphile is more a hydrotrope rather than a true surfactant. It is expected to exhibit a high solubility in both water and terpenes, which perturbs the determination of EACN values of neat terpenes.

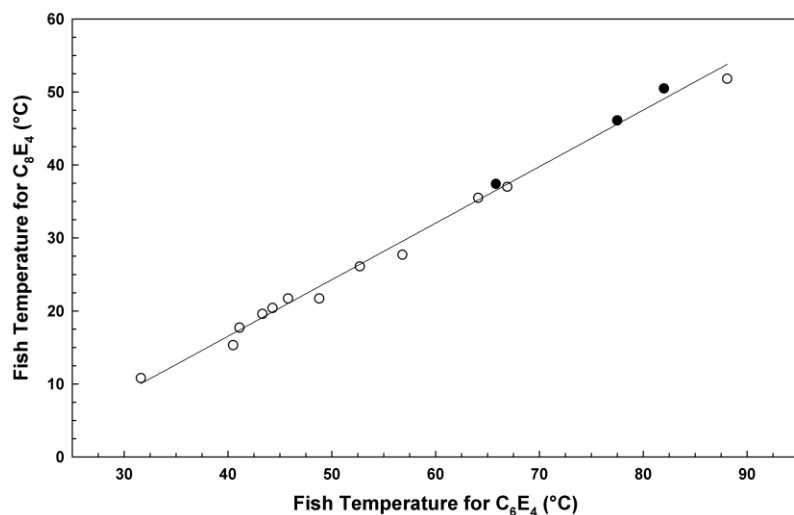


Figure II-4 Correlation between the fish temperatures T^* of alkanes (●) and terpenes (○) determined with C_8E_4 or C_6E_4 .

1.3. Discussion

1.3.1. Structure effects on EACN value

By comparing the EACN values determined for the different terpenes (Figure II-3 and Table II-3), a number of remarks can be made with regard to the effect of structural modifications of the oil (Table II-4).

Table II-4 Influence of structural change on the EACN value of terpenes

Entries	Structural modification	Δ EACN
<i>n</i> -alkanes	increasing carbon number	↗
decane \Rightarrow 1	branching	↘
1 \Rightarrow 4 and 4 \Rightarrow 6	cyclization	↘↘
4 \Rightarrow 7 and 6 \Rightarrow 9	unsaturation	↘↘
4 \Rightarrow 15	aromatization	↘↘↘

1.3.1.1. Number of carbons

The EACN scale of terpenes is calibrated using a series of *n*-alkanes of increasing chain length (from C₆ to C₁₆). By definition, one more carbon increases the ACN of the *n*-alkane of one unit. This effect does not appear clearly by comparing monoterpenes (C₁₀) with sesquiterpenes (C₁₅) since other structural effects can play a predominant role on the EACN value.

1.3.1.2. Branching

Branched alkanes are known to exhibit a slightly lower EACN value than their linear isomer because branching decreases the oil–oil interactions [26]. For instance, myrcane **1**, which bears 10 carbon atoms, has a lower EACN (9.3) than decane.

1.3.1.3. Cyclization

For similar reasons, cyclization of the chains leads to a dramatic decrease of the EACN value. Cyclohexane is known to behave as a shorter alkane than *n*-hexane [33]. This effect is observed here as the EACN value of monocyclic *p*-menthane **4** (5.7) is much lower than the one of the acyclic isomer myrcane **1** (9.3). The bicyclic isomer pinane **6** has even a much lower EACN (3.4) than *p*-menthane **4**.

1.3.1.4. Unsaturation

The EACN value dramatically decreases with the number of unsaturations. Indeed, introduction of one double bond to the *p*-menthane **4** skeleton diminishes the EACN value of 2.5 units compared to *p*-menth-2-ene, **7** (EACN = 3.2). A second double bond leads to a further decrease of 2-3 EACN units. However, the position of the double bond and the structure of the starting skeleton have also a significant influence. Endocyclic double bonds seem to have a lower influence on the final EACN value than exocyclic double bonds. Actually, β -pinene **9** has a much lower EACN (1.9) than pinane **6** (3.4) whereas EACN value of α -pinene **8** (3.0) is only slightly lower.

1.3.1.5. Aromatization

Aromatic hydrocarbons such as toluene are known to behave as much polar oils (lower EACN) than the corresponding cyclohexanes [33]. This behavior is confirmed here since *p*-cymene **15** has the lowest EACN value (−0.8) of all the set of investigated oils.

1.3.2. Comparison of fish diagrams of terpenes and *n*-alkanes

Due to the presence of two double bonds and two cycles, the sesquiterpene caryophyllene **5** exhibits a relatively low EACN value (5.3) close to the ACN of hexane (6.0). EACN of oils is an important parameter for practical applications since it can help formulators to select the appropriate surfactants to obtain micro- or macro-emulsions with the desired properties. However, it does not give any information on the efficiency of the system. To discuss this point, the whole fish bodies of caryophyllene **5** and *n*-hexane have been built (see Figure 4).

As expected, the head of the fish for caryophyllene is smaller and appears at a slightly higher concentration of C_8E_4 than the one of hexane (2.4% vs. 2.1%). This behavior indicates that the solubility of C_8E_4 in caryophyllene is higher than in *n*-hexane in agreement with the higher affinity of polyoxyethylene moiety for cyclic and unsaturated oils than for linear alkanes. On the other hand, the lower value of the critical concentration C^* for caryophyllene than for *n*-hexane (23.8% vs. 25.7%) is more surprising since both the large molecular volume of the sesquiterpene and the higher solubility of C_8E_4 in this oil were expected to shift C^* to higher values [21]. This phenomenon is explained by a better penetration of caryophyllene than hexane into the palisade of the interfacial film as discussed in detail in the next paragraph 1.3.3.

In order to confirm this effect, we performed the fish diagram of 2,6,10 trimethylundecane 2,6-diene (14 carbons), which does not belong to terpenes family. It is still interesting to see that the presence of two double bonds and 3 methyl groups on a linear 11 carbons skeleton gives to this molecule an EACN close to *n*-octane as well as a similar C^* (Figure II-5).

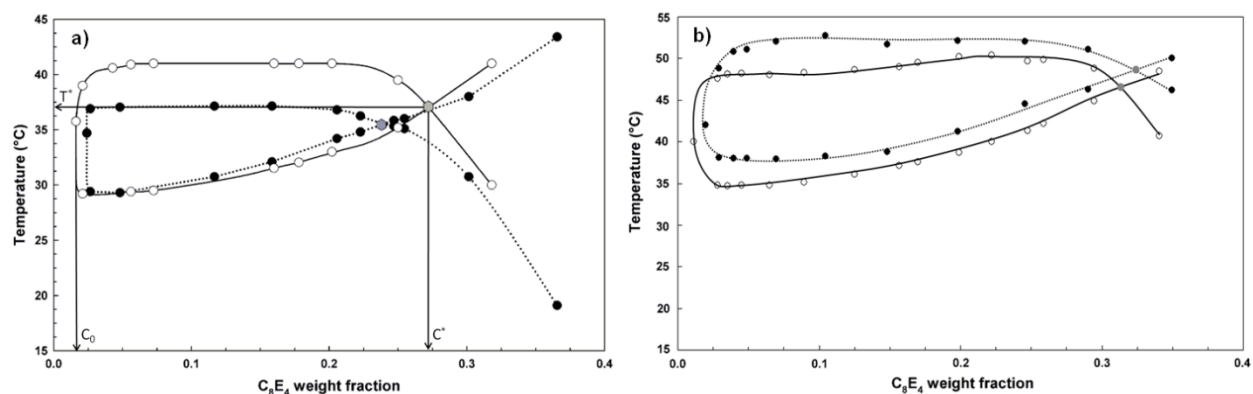


Figure II—5 (a) Comparison between the T - C section of caryophyllene (●) with the *n*-alkane exhibiting the closest ACN value: hexane (○). (b) Comparison between the T - C section of 2,6,10-trimethylundecane-2,6-diene (●) with the *n*-alkane exhibiting the closest ACN value: octane (○).

1.3.3. Influence of the nature of the oil on the value of C^*

On Figure II-5, the fish diagrams of C_8E_4 /caryophyllene/water and C_8E_4 /hexane/water systems are put side by side since these oils have close EACN values i.e.: 5.3 and 6.0 respectively. The heads of the fishes are comparable, though C_0 is slightly higher for caryophyllene, which also has a lower value of C^* . On the other hand, the body of the fish for hexane is larger than the one for caryophyllene. The solubility of caryophyllene and C_8E_4 in the excess water phase being very small, the bottom tie line of the three-phase triangle (Figure II-6) is tilted towards the water-rich corner: $\approx 0\%$ of C_8E_4 to 2.4% at 50/50 oil/water (vs. 2.1% for hexane). Besides, the monomeric solubility of the surfactant C_8E_4 in caryophyllene phase should be significantly high (a few %). For hexane, there is a shift in the whole phase diagram toward slightly higher temperature: 37.4 °C (vs. 35.5 °C for caryophyllene) whereas the shapes of the diagrams are rather similar. However comparing the lower and upper boundaries of the fishes independently, the shift in the upper boundary towards higher temperature is obviously more important for hexane than that of the lower boundary. This observation may be tentatively rationalized by using the approach developed by Kalhweit and Strey who considered that the phase behaviour of the ternary SOW systems results as a first approximation of the overlap of the three binary systems SO, SW and OW. Therefore the lower boundary of a fish diagram depends mainly on the cloud temperature of the surfactant/water system whereas the upper boundary is related to the mutual solubility curve of the oil and surfactant (SO system) [80]. Clearly, the SO system will be more dependent on the nature of the oil than the SW system. Moreover, the point of maximum solubility (C^*) for hexane moves toward higher surfactant concentration, whereas the monomeric solubility of the surfactant in the oil phase (C_0) remains almost the same (2.1% vs. 2.4%). These observations are interpreted as a significant decrease in the solubilization of the oil phase (hexane) in the amphiphilic interfacial film (see later).

More generally, our study of the critical point for ternary C_iE_4 /terpenes/water systems reveal that the value of C^* for terpenes oil (see Table II-3) first decreases as EACN decreases and then remains constant when EACN further decreases. The experimental values of the optimal concentration C^* for terpenes are shown in Figure II-6 along with alkanes for C_iE_4 /oil/water system with $i = 6,8,10$ as function of the EACN of oils.

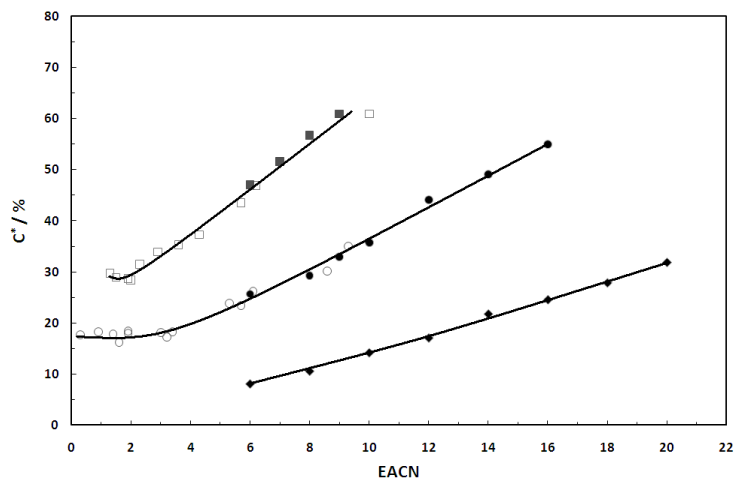


Figure II—6 Evolution of the optimal concentration C^* as function of the EACN hydrocarbon in C_iE_4 /oil/water systems. Black dots for alkanes (Table II-1) and white dots for terpenes (Table II-3); Surfactants are symbolized as follow: C_6E_4 (□), C_8E_4 (○) and $C_{10}E_4$ (◇).

This phenomenon has been reported by Queste et al. as they observed that C^* decreases as function of ACN for alkane oils and for surfactants like C_8E_4 and $C_{10}E_4$ [21] they explained this behavior by considering the interactions occurring near the oil/water interface. As the ACN of oil is increased, their intermolecular forces are stronger and as a result oils are less prone to penetrate the interfacial surfactant film. As the surfactant becomes less lipophilic, an increase of the temperature of the system is thus needed to compensate the oil effect at the interface by decreasing the hydrophilicity of the surfactant and to reach the optimal formulation. In brief, the affinity of the surfactant for oil and water decreases on both sides, so that leads to an increase of C^* .

The author also determined the EACN values of cyclic and aromatic oils and they discuss the fact that two oils of different natures which have the same EACN value ($\Leftrightarrow T^*$) do not necessarily exhibit the same C^* . The explanation of this observation is coming from the functional group polyethoxylated of the surfactant. In fact, C_iE_j solubility in the oil phase increases with the polarity of oil. Therefore, the authors give a classification of the different oils in surfactant/oil/water system by increasing C^* as follows: alkanes < alkylcyclohexanes < alkylbenzenes. The monomeric solubility of the surfactant into oil is the main factor controlling the value of the head of the fish (C_0).

In addition, the latter corresponds the amount of surfactant, which is not engaged at the interface; as a result, the surfactant loses its efficacy to co-solubilize oil and water, so the minimum amount of C_iE_j requested to reach the Winsor IV microemulsion phase: C^* is accordingly higher as shown in Table II-5.

Table II-5 Monomeric solubility of $C_{10}E_4$ in three oils of different natures with the same EACN extracted for paper [21].

Oil (EACN = 8)	$C_{10}E_4$ monomeric solubility (%)	C^* (%)
Octane	1.5	10.5
Butylcyclohexane	1.8	11.0
Dodecylbenzene	6.0	19.2

In a recent paper, the critical micellar concentration for a range of C_iE_j surfactants in heptane is reported. The data show that, for a fixed ethoxylate number, the CMC values decrease with increasing length of the alkyl chain. In contrast, for a fixed value of i the CMC values increase with increasing size of the polar moiety. Regarding the influence of the structure of C_iE_j on the micellization, the authors demonstrate that while i increases micellization is boosted, whereas increase of the ethoxylate number j counteracts micellization [79]. In order to illustrate and fit with our study, Table II-6 reports the value of used surfactants: C_iE_4 with $i = 6, 8$ and 10 .

Table II-6 Value of Critical Micellar Concentration (CMC) in mole for three C_iE_4 surfactants in heptane extracted from paper [79].

Surfactant C_iE_4	CMC in n-heptane (M)
C_6E_4	0.331
C_8E_4	0.112
$C_{10}E_4$	0.074

1.4. Conclusion

Pure C_8E_4 was used in this work to determine the EACN of a large set of well-defined mono- and sesqui-terpenes. By comparing the EACNs of these oils exhibiting a more or less complex chemical structure, some general tendencies were drawn with regard to the structural effect. Aromatization was shown to have the strongest effect on the decrease of the EACN value, as well as cyclization, unsaturation and finally branching to a lesser extent. A higher degree of penetration of terpenes into the surfactant palisade increases surfactant efficiency and requires lower amount of surfactant to generate a single-phase microemulsion to co-solubilize terpenes with water in comparison with n-alkanes.

EACN constitutes a key parameter for practical applications since it can help the formulator to select the appropriate surfactants for given oil in order to obtain microemulsions or emulsions with the desired properties.

2. Prediction of the “fish-tail” temperature of C_iE_4 /water/polar hydrocarbon oil systems

2.1. Introduction

It has been established for a long time that oil hydrophobicity is an essential parameter influencing the type and the stability of emulsions formed from surfactant/oil/water (SOW) systems [34-36]. That is the reason why Griffin introduced the concept of “required HLB” of the oil in 1949 in order to complete the HLB notion used to characterize the hydrophilic-lipophilic balance of surfactants [37]. More recently, it has also been shown that there is a correlation between the type of emulsions (O/W or W/O) obtained with a given SOW system and that of microemulsions behavior obtained in the same system, as reflected by so-called Winsor I, II and III microemulsion types [38-39].

In 1977, Wade et al. introduced the Equivalent Alkane Carbon Number concept (EACN), a dimensionless number that reflects the “hydrophobicity” of oil [40]. The EACN of oil is determined experimentally by comparing its phase behavior with that of a well-defined linear hydrocarbon in the same SOW system. By definition, the EACN value of a given oil is equal to the number of carbons of the *n*-alkane exhibiting the same phase behavior.

It has been shown that when the oil polarity increases, its EACN value decreases [41]. Since that time, reliable EACN values have been reported for various series of oils such as triglycerides [42], aliphatic or aromatic hydrocarbons [26-27], ethers or esters [43-44], chlorinated hydrocarbons [45], and terpenes [46]. This latter family is particularly interesting not only for its applications in perfumery, cosmetics, pharmaceutical, etc but also from a molecular point of view as it exhibits a wide range of chemical structures (acyclic, mono- or polycyclic, cycles of different sizes, branched, unsaturated) allowing the study of the influence of these parameters on the EACN.

In the first part of this chapter, we describe the phase behavior of ternary systems based on monodisperse tetraethylene glycol monoalkyl ethers (C_iE_4) ($i = 6, 8, 10$) as surfactants, water, and a series of mono- and sesqui-terpenes [15]. Partial fish diagrams were constructed to determine the so-called “fish-tail” temperature T^* at which the one-phase (Winsor IV), the two-phase (Winsor I and II) and the three-phase (Winsor III) regions meet. Comparison with similar SOW systems based on homologous *n*-alkanes allowed the determination of the EACN values of 15 terpenes.

It was found that structural alterations such as branching, aromatization, cyclization, unsaturations lower T^* of terpenes compared to n -alkanes having the same number of carbon atoms. From a qualitative standpoint, this confirms that terpenes exhibit a much higher polarity than the corresponding n -alkanes.

In this second part, we extend the study to 10 alkylcyclohexanes and 4 alkylcyclohexenes. Thus, the 43 hydrocarbon oils were selected among a broad range of relevant and highly pure molecules to assess various structural effects on T^* . They consist of 12 n -alkanes, 17 aromatics or branched and cyclic alkanes and alkenes as well as 14 fragrant terpenes and sesquiterpenes. The twelve n -alkanes denoted as B_x ($x = 6 - 10, 12, 14, 16, 18, 20, 24, 28$) are used as reference oils to calibrate the EACN (Equivalent ACN) scale by expressing their T^* value as a function of the carbon number x denoted as ACN'' . Then, a QSPR modeling approach based on Genetic Function Approximation is used to correlate experimental values of T^* , and indirectly the EACN, with structural molecular descriptors of the oils. Molecular descriptors represent structural and physico-chemical features of compounds. Some of them have been proposed to predict the structural basis of different properties of surfactant-based systems, such as the cloud points of non-ionic surfactants [68], the critical micelle concentration [69-72]. However, these modeling methods have never been applied to the prediction of the impact of the molecular structure of the oil on the phase diagrams of SOW ternary systems.

2.2. Results

2.2.1. Phase behavior of C_iE_4 ($i = 6, 8, 10$)/polar hydrocarbon oil/water systems

At constant pressure, a ternary C_iE_j /oil/water system (SOW) has three independent variables, namely the temperature and two composition variables. The phase behavior of such systems may be described with Gibbs diagrams at different temperatures, giving a phase prism SOW-T that shows the whole phase behavior of the ternary system (Figure II-7). If T is kept constant, the phase behavior may be mapped in isothermal Gibbs triangles as illustrated on Figure II-7 with the system C_6E_4/α -pinene/water at 52.7 °C, i.e. when the apex of the three-phase triangle (shown in grey) is localized on the median of the Gibbs triangle. α -Pinene has been chosen as typical fragrant oil because it is one of the most abundant terpene and C_6E_4 as the amphiphile since the emulsion obtained after mixing of the components are extremely unstable and the equilibrium of the system is rapidly attained. As indicated on Figure II-7, the Gibbs diagram, at this particular temperature, allows the determination of C_0 and C^* which are the minimal concentrations of C_6E_4 required

to obtain a three-phase system and the one-phase microemulsion respectively. C_0 depends on $(C_{\text{mono/w}})$ and $(C_{\text{mono/o}})$ which is the monomeric solubilities of the C_6E_4 in the excess water and oil phases respectively. For the C_6E_4/α -pinene/water system, $C_0 = 2.09\%$, $C^* = 33.1\%$, $C_{\text{mono/w}} = 0.069\%$ and $C_{\text{mono/o}} = 4.11\%$.

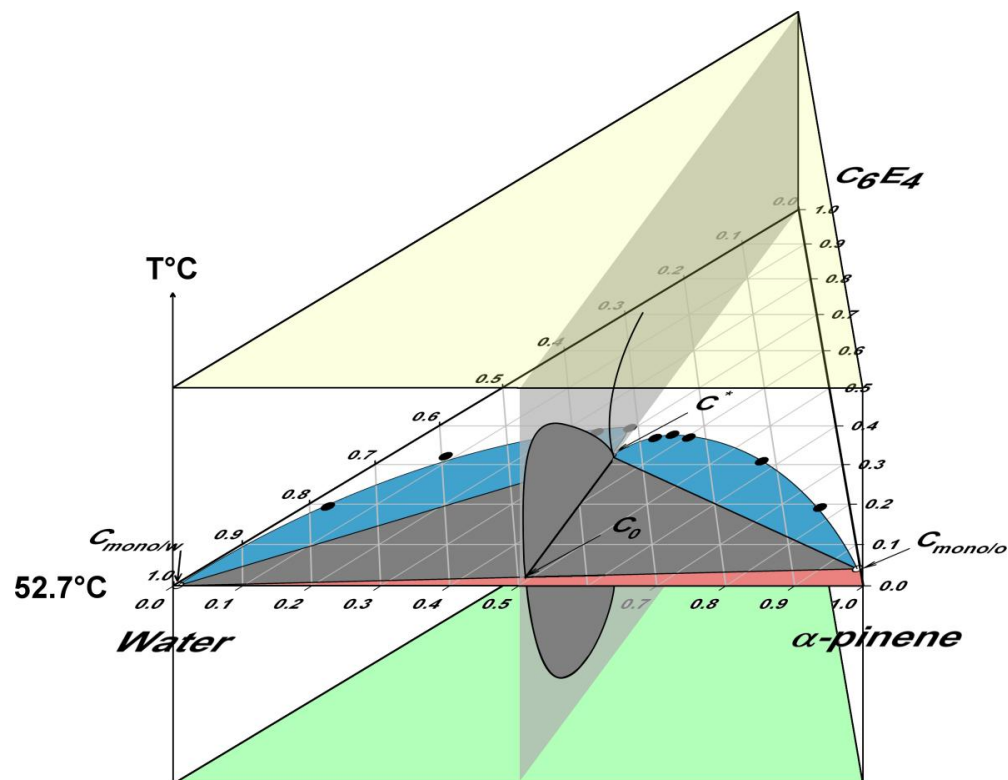


Figure II-7 C_6E_4/α -pinene/water-T phase prism defined by the stacking of Gibbs phase triangles. The dark grey area represents the three-phase region, the blue areas code the two-phase microemulsion systems and the red area corresponds to a simple biphasic system.

Kahlweit and Strey have shown that the phase behavior of ternary SOW systems is intimately related to the phase behavior of the three binary surfactant/water (SW), surfactant/oil (SO) and oil/water (OW) subsystems [59]. In our example, the binary α -pinene/ H_2O system presents a broad miscibility gap in the whole range of accessible temperatures. The binary C_6E_4 /oil systems show a lower miscibility gap with upper critical temperatures T_α equal to $40.0\text{ }^\circ\text{C}$ when the oil is n -hexadecane whereas for terpenes, such as α -pinene, the miscibility gaps and T_α are much lower than $0\text{ }^\circ\text{C}$. This result can be easily understood considering the higher polarity of such oils, that increases their affinity for C_6E_4 . The phase diagrams of the binary C_iE_4/H_2O ($i = 6, 8, 10$) system show higher miscibility gaps with lower critical temperatures (so-called cloud points) at T_β equal to 66.1 [30], 40.8 [30] and 20.5 [60] $^\circ\text{C}$ for C_6E_4 , C_8E_4 and $C_{10}E_4$ respectively.

The interplay of these three binary systems determines the phase behavior of the SOW ternary system. The H₂O/ α -pinene miscibility gap extends into the Gibbs triangle giving two-phase systems above $T_u = 59.2$ °C and below $T_l = 48.3$ °C with C₆E₄ dissolved mainly in the W/O or in the O/W microemulsion phases respectively. The system separates into three phases within the temperature interval ($T_l - T_u$), i.e. when C₆E₄ has an almost equal affinity for oil and water.

The most convenient procedure for determining the position and extension of the three-phase region within the phase prism is to draw a vertical section at a weight water-to-oil ratio equal to 1, corresponding to the fish cut shown in Figure II-7. This cut of the C₆E₄/ α -pinene/water system exhibits a three-phase body shaping a "fish" (Figure II-8). Such a "fish plot" is much easier to construct than the series of Gibbs triangles at different temperatures and it provides the essential information with regard to the SOW-T phase behavior.

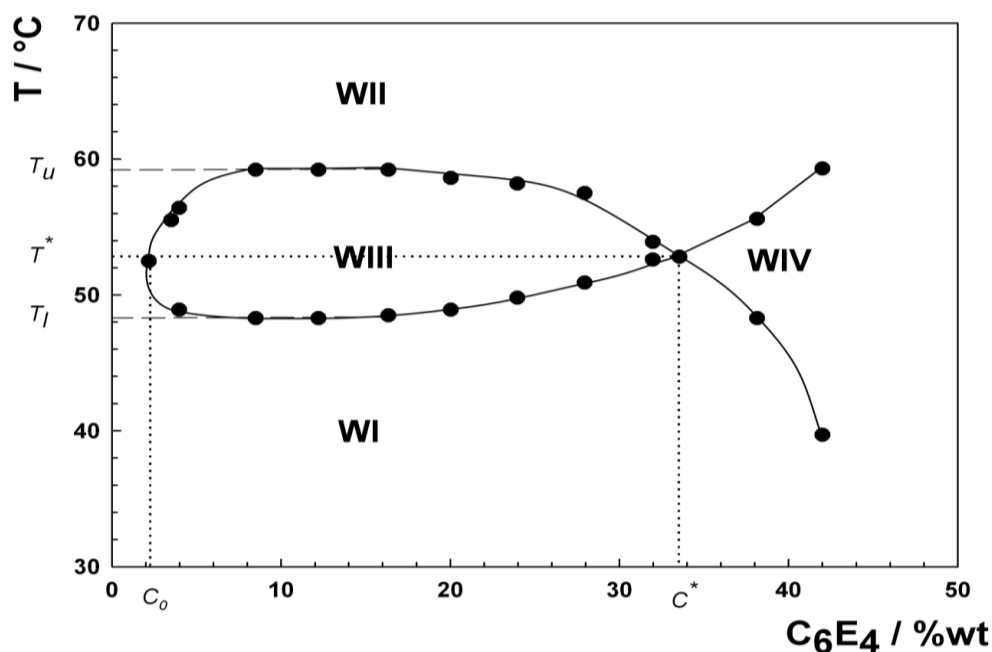


Figure II—8 Fish plot of the C₆E₄/ α -pinene/water system at a water/ α -pinene ratio equal to 1 (w/w). The different types of Winsor regions are indicated on the diagram (WI: O/W microemulsion with excess oil, WII: W/O microemulsion with excess water, WIII three-phase oil/microemulsion/water system, WIV one-phase microemulsion).

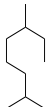
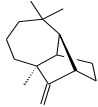
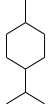
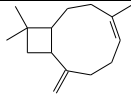
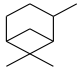
The point at which the one-phase (WIV) and the three-phase regions (WIII) meet corresponds to the "fish-tail" temperature T^* (= 52.7 °C), at which a complete co-solubilization of equal masses of water and α -pinene is obtained with the minimum concentration of C₆E₄, C^* (= 33.1%). T_l and T_u are the lowest and highest temperatures of

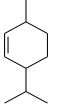
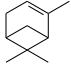
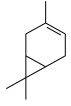
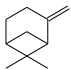
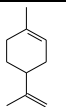
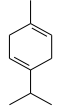
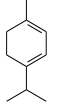
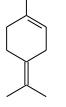
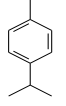
the fish body respectively whereas C_0 corresponds to the amount of C_6E_4 dissolved as monomers in the excess aqueous and oily phases of the three-phase system at the temperature T^* .

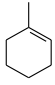
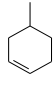
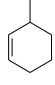
2.2.2 Influence of the surfactant alkyl chain length on T^*

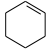
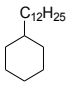
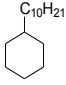
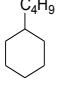
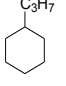
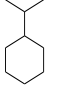
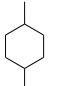
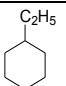
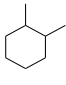
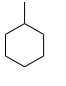
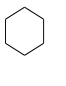
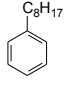
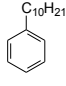
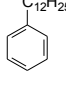
The position of T^* on the temperature scale depends on the chemical structure of both the oil and the surfactant because it is closely related to the relative positions of T_α and T_β . The more hydrophilic the surfactant, the higher the cloud point T_β and the higher the "fish-tail" temperature T^* for a given oil [59]. Hence, three surfactants of increasing hydrophilicity, $C_{10}E_4$, C_8E_4 and C_6E_4 have been used to determine T^* in order to encompass a broad range of oils including highly hydrophobic oils such as *n*-octacosane and much more polar oils such as cyclohexene. The experimental values of T^* determined in this work for model polar hydrocarbons or collected from our previous article for terpenes [46] are summarized in Table II-7.

Table II-7 "Fish-tail" temperatures T^* , EACN and values of the QSPR descriptors for saturated, unsaturated, branched, linear and cyclic hydrocarbon oils determined for the C_iE_4 /oil/water systems ($i = 6, 8$ or 10) at a water-to-oil ratio = 1 (w/w).

Terpenes ^a	Formula	EACN _{average}	T*(°C)			Average	
			C ₆ E ₄	C ₈ E ₄	C ₁₀ E ₄	Neg Softness	KierA3
Myrcane		9.7	88.1	51.8	31.0	7.97	7.00
Longifolene		6.5	69.5	38.9	-	9.16	1.02
<i>p</i> -Menthane		6.0	66.9	37.0	15.6	8.36	2.29
Caryophyllene		5.6	64.1	35.5	-	8.37	1.97
Pinane		4.0	56.8	27.7	-	8.49	0.72

<i>p</i> -Menth-2-ene		3.3	50.0	26.9	-	7.56	2.06
α -Pinene		3.4	52.7	26.1	-	7.89	0.65
Δ -3-Carene		2.5	48.8	21.7	-	7.51	0.65
β -Pinene		2.2	45.8	21.7	-	7.74	0.65
Limonene		2.0	44.3	20.4	-	6.95	1.85
γ -Terpinene		1.8	43.3	19.6	-	6.76	1.85
α -Terpinene		1.3	41.1	17.7	-	6.78	1.85
Terpinolene		1.0	40.5	15.3	-	6.79	1.85
<i>p</i> -Cymene		-0.4	31.6	10.8	-	6.13	1.65

Model Hydrocarbons	Formula	EACN	T*(°C)			Average Neg Softness	KierA3
			C ₆ E ₄	C ₈ E ₄	C ₁₀ E ₄		
1-Methyl-1-cyclohexene		0.4	37.4	12.4	-	6.58	1.25
4-Methyl-1-cyclohexene		0.4	36.3	13.2	-	6.72	1.25
3-Methyl-1-cyclohexene		-0.1	35.3	10.5	-	6.63	1.25

Cyclohexene		-1.2	26.5	< 8	-	6.21	1.06
Dodecyl cyclohexane		17.3	-	-	51.5 ^b	8.57	9.60
Decyl cyclohexane		14.4	-	-	43.0 ^b	8.51	7.86
Butyl cyclohexane		7.0 7.0 ^b	72.4	41.1	22.0	8.16	3.11
Propyl cyclohexane		5.7 5.6 ^b	65.0	35.9	18	8.01	2.38
Isopropyl cyclohexane		5.3	63.8	33.8	15.2	8.16	2.00
1,4-Dimethyl cyclohexane		4.4	58.4	30.0	-	7.96	1.80
Ethyl cyclohexane		4.2 3.8 ^b	57.8	29.7	13	7.87	1.80
1,2-Dimethyl cyclohexane		3.3	54.6	23.7	-	8.01	1.49
Methyl cyclohexane		3.2	52.3	24.4	-	7.60	1.50
Cyclohexane		2.2	46.5	20.7	-	7.28	1.33
Octylbenzene		4.3	-	-	14	6.79	5.02
Decylbenzene		6.2	-	-	19.5	7.17	6.59
Dodecylbenzene		7.9	-	-	24.5	7.38	8.23

Alkanes ^c		ACN	T* (°C)			Average Neg Softness	KierA3
			C ₆ E ₄	C ₈ E ₄	C ₁₀ E ₄ ^b		
<i>n</i> -hexane	B ₆	6.0	65.8	37.4	19.5	6.97	5.33
<i>n</i> -heptane	B ₇	7.0	71.4	43.8	-	7.17	6.00
<i>n</i> -octane	B ₈	8.0	77.5	46.1	25.0	7.34	7.20
<i>n</i> -nonane	B ₉	9.0	82.0	50.5	-	7.48	8.00
<i>n</i> -decane	B ₁₀	10.0	-	54.5	30.5	7.60	9.14
<i>n</i> -dodecane	B ₁₂	12.0	-	63.9	35.5	7.80	11.11
<i>n</i> -tetradecane	B ₁₄	14.0	-	71.3	41.5	7.95	13.10
<i>n</i> -hexadecane	B ₁₆	16.0	-	77.9	47.0	8.07	15.08
<i>n</i> -octadecane	B ₁₈	18.0	-	-	54.0	8.17	17.07
<i>n</i> -eicosane	B ₂₀	20.0	-	-	59.0	8.26	19.05
<i>n</i> -tetracosane	B ₂₄	24.0	-	-	71.0	8.39	23.05
<i>n</i> -octacosane	B ₂₈	28.0	-	-	79.0	8.49	27.04

^a Our previous work[46]. ^b Queste et al.[21] ^c B_x = n-C_xH_{2x+2}

As expected from the respective values of T_{β} of the three C_iE₄, used here, the T* values measured for a given oil are in the order $T^*_{C_6E_4} > T^*_{C_8E_4} > T^*_{C_{10}E_4}$. Therefore, in the same experimentally accessible range of temperatures, C₁₀E₄ allows the investigation of hydrophobic oils whereas C₆E₄ is suitable for the study of more polar oils. A further advantage of the shorter alkyl chain amphiphile C₆E₄ over the two others C_iE₄ is the rapidity of the phase equilibration that allows a rapid inspection of the different Winsor types.

2.2.3. Influence of oil hydrophobicity on T*

It has been recognized for a long time that, for a given C_iE_j, T* measured for a series of *n*-alkanes linearly increases with the number of carbon atoms of the oil, *i.e.* the so-called Alkane Carbon Number (ACN) [59].

Recently, Queste et al. have shown by studying the $C_{10}E_4/n$ -alkane/ H_2O systems, that the linear relationship between T^* and ACN is retained for longer n -alkanes up to octacosane (n - $C_{28}H_{58}$) [21]. This behavior can be quantitatively explained by considering the influence of ACN on the miscibility gaps of the three binary C_iE_j/H_2O , n -alkane/ H_2O and C_iE_j/n -alkane subsystems which determine the phase behavior of the ternary C_iE_j/n -alkane/ H_2O system. The first binary system does not depend on the nature of the oil, so T_α remains constant. The second one is hardly affected by ACN since it always presents a broad miscibility gap in the whole range of accessible temperatures whatever the length of the n -alkane is. On the contrary, ACN has a strong influence on the surfactant/oil binary system. Kahlweit et al. have shown that nonionic surfactants become less and less soluble in the oil phase as ACN increases [59].

The model hydrocarbon oils studied here (Table II-7) consist of 12 n -alkanes, 10 cyclohexanes, 4 cyclohexenes and 3 aromatics. The n -alkanes denoted as B_x ($x = 6 - 10, 12, 14, 16, 18, 20, 24, 28$) are used as reference oils to calibrate the EACN (Equivalent ACN) scale by expressing their T^* value as a function of the carbon number x denoted as ACN [27]. The 14 fragrant terpenes and sesquiterpenes are more complex and allow the investigation of the influence of various changes in the molecular structures including branching, cyclization (one, two or three cycles), aromatization or unsaturation (one or two double bonds at various positions). By definition, the EACN value of a given oil is equal to the number of carbons of the n -alkane exhibiting the same fish-tail temperature T^* [27]. It is most often a non-integer number since T^* of an oil generally lies between the T^* values of two successive alkanes. It may also be outside of the range of ACN values accessible with liquids n -alkanes when the oils are more polar than n -hexane.

2.2.4. Determination of the EACN of hydrocarbon polar oils

T^* values obtained for investigated oils with C_6E_4 , C_8E_4 and $C_{10}E_4$, were found to be strongly linearly correlated to each other. Figure II-9 shows the correlation between T^* measured for a same oil with the two surfactants C_6E_4 and C_8E_4 on the one hand (left Y axis) and with the two $C_{10}E_4$ and C_8E_4 surfactants on the other hand (right Y axis). Such indisputable correlation has been observed for a long time for a number of SOW systems based on a series of homologous n -alkanes and surfactants of type C_iE_j [75].

However, it was not fully expected in case of short chain amphiphiles such as C_6E_4 since the microstructure of the middle phase is far from the classical view of microemulsion consisting of oily and aqueous micro-domains separated by a well-defined interfacial layer of

amphiphilic molecules [76]. Nevertheless, fish-tail temperatures appear to be highly correlated for $C_{10}E_4$, C_8E_4 as well as for C_6E_4 , suggesting that the main features of three-phase bodies based on short chain amphiphiles are similar to those found with “true” surfactants irrespective to the particular microstructure of the phases and to the chemical structures of the complex oils studied herein.

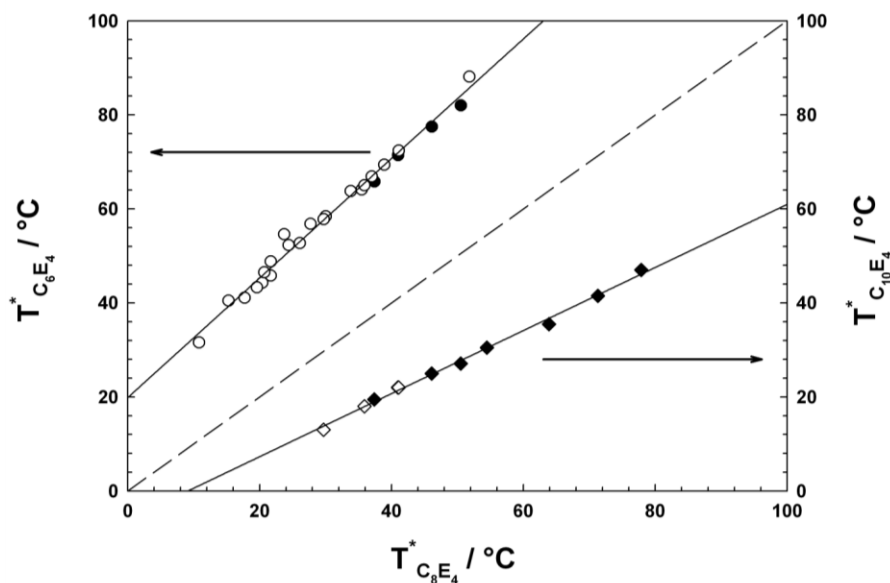


Figure II—9 Correlation between the “fish-tail” temperatures determined either with C_8E_4 (abscissa) or with C_6E_4 (left ordinate and upper series of dots) or with $C_{10}E_4$ (right ordinate and lower series of dots). Black dots correspond to n -alkanes and white dots to branched and/or cyclic and/or unsaturated and/or aromatic hydrocarbons.

Therefore, the classification of these oils inferred from experiments conducted with any of the three C_iE_4 will not depend on the nature of the surfactant and can be confidently expressed according to the EACN (Equivalent Alkane Carbon Number) scale [19]. At the fish-tail point, the curvature of the interfacial film is equal to zero and T^* is linearly related to EACN according to equation (5) [19,27,46]:

$$T^*_{C_iE_4} = \alpha + \beta EACN \quad (5)$$

When the fish-tail point is determined for a series of n -alkanes, e.g. from n -hexane to n -octacosane, there are enough data to fit Equation (5) with a linear regression. The corresponding best fits are summarized in Table II-8 which reports the values of the a and b coefficients as well as the EACN range of oils that can be determined with the three C_iE_4 ($i = 6, 8, 10$) by measurement of T^* under normal conditions, *i.e.* between 10 and 100 °C.

Table II-8 Coefficient α and β for C_iE_4 surfactants and EACN range of oils attainable with the C_iE_4 for T^* between 10 and 100 °C

C_iE_4	α	β	EACN range
$C_{10}E_4$	1.71	2.87	3 to 35
C_8E_4	12.83	4.15	-1 to 21
C_6E_4	33.15	5.47	-4 to 15

The average EACN of the present hydrocarbon oils have been calculated from T^* of different C_iE_4 when available, leading to an average standard deviation of 0.3 EACN unit. This uncertainty is notably due to the calibration step, which is made with a narrow range of alkanes, especially in the case of C_6E_4 (only from hexane to nonane). As polar hydrocarbon EACNs are extrapolated, a small deviation on the calibration line may lead to significant deviation in the EACN value.

2.3. Discussion

2.3.1. Evolution of the effective packing parameter with temperature and oil penetration

The evolution of the T^* -values according to the chemical structure of the oil and to the hydrophilicity of the surfactant can be rationalized in terms of the so-called "effective packing parameter". Israelachvili et al. have introduced the concept of "packing parameter" in 1976 to rationalize the type of surfactant assemblies formed in aqueous solutions as a function of the surfactant structure [61]. The packing parameter P of a binary SW system is defined as $P = v_s / \sigma_s l_s$ where v_s and l_s are respectively the volume and the length of the hydrophobic tail respectively and σ_s is the equilibrium area per surfactant molecule in the micelles. The surfactant packing parameter depends on variables such as temperature and electrolytes (nature and concentration) that modify σ_s .

For more complex SOW ternary systems, additional parameters, such as the nature of the oil or the presence of co-surfactant, also influence the apparent packing parameter of the surfactants. In this paper, the resulting packing parameter will be referred to as "effective" packing parameter \bar{P} , i.e. the total packing parameter, which takes into account the entire physico-chemical environment of the surfactant [61]. It is nowadays well admitted that most oils are prone to penetrate into the surfactant palisade layer [62]. In particular, Requena et al. [63] and Chen et al. [64] showed that in the case of n -alkanes with a chain length shorter than that of the surfactant, the oil tends to penetrate the interfacial layer and to increase the effective volume of the surfactant tail, as schematized in figure II-10.

The restriction about the length of the alkane is somewhat questionable, as Queste et al. demonstrated that the linearity between T^* and ACN is maintained even when the ACN is twice the number of carbons of the hydrophobic tail of the surfactant [27]. Thus, we may assume that all the oils are able to penetrate more or less the interfacial film, even in the case of very hydrophobic oils such as long n -alkanes.

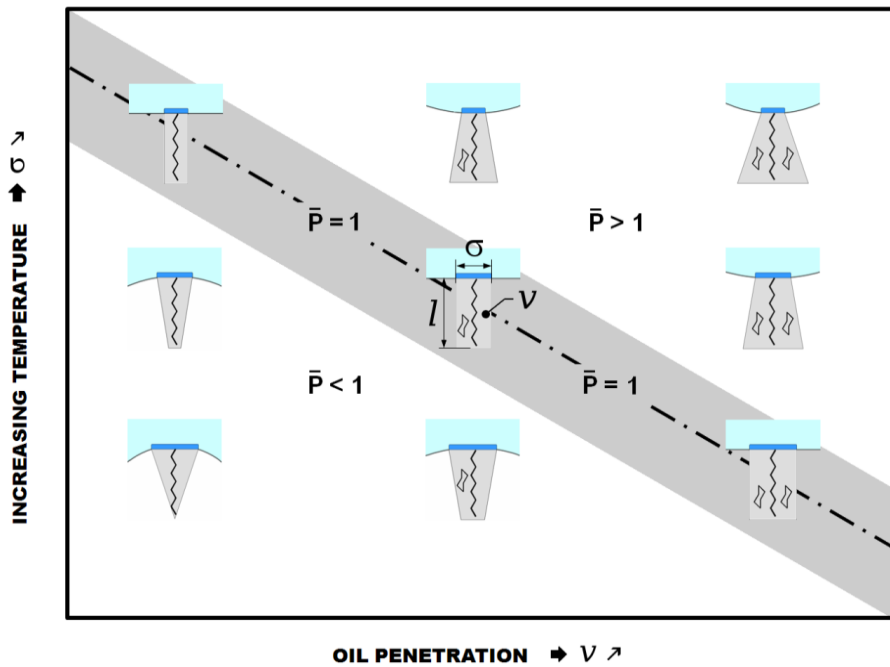


Figure II-10 Schematic description of the evolution of the effective packing parameter \bar{P} of the surfactant as a function of the temperature and of the oil penetration

On the other hand, when a second surfactant is added to a binary SW system, complete penetration occurs, increasing both the volume of the hydrophobic tail and the area of the hydrophilic part. In this case, the effective packing parameter \bar{P} of the mixed layer may consequently be expressed as [65]:

$$\bar{P} = \left(\frac{\nu}{\sigma_s l_s} \right) = \frac{x_{s1} \nu_{s1} + x_{s2} \nu_{s2}}{(x_{s1} \sigma_{s1} + x_{s2} \sigma_{s2}) l_{max}} \quad (6)$$

where x is the mole fraction of the respective species present in the aggregate and l_{max} , the critical length of the longer component.

In the case of polar oils, the systems are more complex as such oils exhibit very different degrees of penetration, as shown by Kanei et al. [18]. By studying the penetration of fragrance within C₁₂E₈ liquid crystal structure, they showed that fragrant molecules can exhibit different behaviors varying from an oil-like (localization in the hydrocarbon core of the surfactant assembly) to a co-surfactant-like (localization in the surfactant palisade layer). In the present systems, the fragrance concentration is much higher as it constitutes the oil phase and the resulting assemblies cannot be studied by X-ray diffraction making Kanei's approach unworkable. More recently, Tchakalova et al. [66] studied the addition of fragrance molecules to the decane/C₁₀E₅/water system. First, they demonstrated that the wedge model [67] was not able to describe the evolution of the packing parameter as a function of the fragrance addition. Actually, in this model, the area per surfactant molecule is supposed to be constant and the oil is assumed to be unable to penetrate the surfactant hydrophobic chains. In order to overcome the limitations of this model, Tchakalova et al. developed the Constant Interfacial Thickness model (CIT) to describe the behavior of decane/C₁₀E₅/water/fragrance quaternary systems. Unlike the wedge model, the CIT model allows the addition of solutes to cause changes in the volume and area per surfactant molecule. The sole hypothesis is relative to the thickness of the hydrophobic layer, which is assumed to remain constant and equal to the length of the surfactant tail l_s . The interfacial adsorption of a solute leads to the formation of a mixed (surfactant + solute) monolayer, so the area per surfactant molecule increases. In the ternary systems studied here, no co-extraction (extraction of oil by the solute into the film) can occur. The CIT equation can consequently be simplified as:

$$\bar{P} = \frac{v_S + \tau v_0}{(\sigma_S + \tau \sigma_0) l_S} \quad (7)$$

where v_0 is the known molecular volume of the oil, σ_0 is the area occupied per oil molecule at the S/W interface and $\tau = N_0^I / N_S^I$ is the number of oil molecules per surfactant molecule at the interface.

Unfortunately, this valuable approach cannot be directly applied to the present system, as spherical assemblies are needed to determine the characteristic parameters of the oil. The bicontinuous structure of microemulsions at T^* corresponds to interpenetrated domains of oil and water for which no simple mathematical model can further be used. However, based on their conclusion, EACN can be rationalized in a similar matter.

Oil is prone to adsorb within the interfacial surfactant layer and change the interfacial curvature, providing additional surface and volume that lead to an increase of the effective area per molecule and of the chain volume in the interfacial layer. Nevertheless, with saturated hydrocarbons and terpene oils, no polar or hydrophilic functions are present. As a result, the oil contribution to the total equilibrium area per surfactant molecule ($+ \tau\sigma_o$) is small and does not compensate for the increase of the apparent volume of the hydrophobic core ($+ \tau\nu_o$). This assumption is validated by the results of Tchakalova et al. [66] who showed that fragrances always increase \bar{P} of the microemulsion droplets. Consequently, \bar{P} increases as a function of the oil penetration (X-axis of Figure II-10). Moreover, with ethoxylated alcohols, the packing parameter of the surfactant is highly dependent on the temperature since an increase of temperature decreases the hydrophilicity of the ethoxylates through a dehydration phenomenon. Therefore, σ_o decreases and \bar{P} increases with temperature (Y-axis of Figure II-10). The bicontinuous microemulsions obtained at T^* correspond to an effective packing parameter equal to 1. The more the fragrance is prone to penetrate in the interfacial film, the lower the temperature needed to obtain an effective parameter of 1 (Figure II-10). In other words, a higher T^* must compensate for the non-penetrating ability of the oil. In our case, we studied true ternary systems whereas Tchakalova et al. added a fourth compound to a fixed ternary mixture. The simplicity of our approach and the great number of oils investigated provide a large amount of precise data which enables us to study the influence of molecular structure and polarizability of the oil on the film curvature (packing parameter) and to predict T^* variations from molecular descriptors.

2.3.2. QSPR prediction for T^*

Molecular descriptors represent structural and physical-chemical features of molecules. They have been extensively used for developing statistical models such as Quantitative Structure Property Relationships (QSPR) models. Some of them have been proposed to predict the structural basis of different properties of surfactant-based systems, such as the cloud points of non-ionic surfactants [68], the critical micelle concentration [69-72]. However, these modeling methods have never been applied to the prediction of the impact of the molecular structure of the oil on the phase diagrams of SOW ternary systems.

QSPR models were built for the T^* data for C_6E_4 , C_8E_4 and $C_{10}E_4$ reported in Table II-7. First, a split of the polar hydrocarbon oils into training (26 candidates) and test (4 candidates) sets has been performed. Multiple QSPR was then built applying Genetic Function

Approximation on the training set and the uninformative variables have been eliminated. At a second stage, the robustness model has been validated with a test set of molecules. For example, in the case of C₆E₄ a training set of 26 molecules have been constituted and a test set of 4 molecules have been used to validate the model. Finally, the model has been refined using the entire dataset (training + test), leading to the following best-fit equation (8):

$$T_{C_iE_4}^* = a \times \text{Average negative softness} + b \times \text{KierA3} - c \quad (8)$$

Table II-9 reports the values of the coefficients a, b and c for C₆E₄, C₈E₄ and C₁₀E₄.

Table II-9 QSPR model for C₆E₄, C₈E₄ and C₁₀E₄

C _i E ₄	a	b	c	R ²
C ₁₀ E ₄	10.02 ± 1.79	2.35 ± 0.13	-67.10 ± 13.74	0.965
C ₈ E ₄	10.2 ± 0.67	3.84 ± 0.11	-58.20 ± 5.05	0.979
C ₆ E ₄	14.27 ± 0.55	5.04 ± 0.20	-65.3 ± 4.21	0.981

Strikingly, only two descriptors (from a set of more than 1000 descriptors) are sufficient to calculate T* satisfactorily. Indeed, both Average negative softness and Kier A3 terms are the relevant molecular descriptors linking the molecular structure of the oil to the fish temperature and a, b and c are the parameters of the linear regression.

The Kier A3 descriptor is the third alpha modified Kier and Hall kappa shape index [73,74]. It equals $(s-1)(s-3)^2 / p_3^2$ for odd n , and $(s-3)(s-2)^2 / p_3^2$ for even n , where n denotes the number of non-hydrogen atoms in the molecule $s = n + a$. The value for a is $(r_i/r_c - 1)$ where r_i is the covalent radius of atom i , and r_c is the covalent radius of an (sp³) carbon atom. Finally, p_3 is the number of paths of length 3 (i.e. consisting of 3 adjacent C-C bonds). Thus, for linear n -alkanes C_nH_{2n+2}, $s = n$ and $p_3 = n - 3$ whereas a branched alkane such as myrcane contains 10 non hydrogen atoms and 8 paths of length 3. The molecule further comprises only sp³ atoms, for which r_i is the same as r_c and $a = 0$.

The Kier A3 of this molecule is therefore equal to $\frac{(10-3) \cdot (10-2)^2}{8^2} = \frac{7 \cdot 64}{64} = 7$.

In the case of methyl-1-cyclohexene, each sp² atoms have a covalent radius of 0.59 Å, which is different from the covalent radius of the sp³ atoms (0.68 Å). Hence, for each sp² atom, $(r_i/r_c - 1) = ((0.59/0.68) - 1) = -0.13$ and a , for the whole molecule, is -0.26. As there are 7

heavy atoms (n) in the molecule, $s = 7 + (-0.26) = 6.74$. The Kier A3 of this molecule is finally calculated using the formula for odd numbers of heavy atoms, yielding a value of $(6.74-1) \times (6.74-3)^2 / 8^2 = (5.74 \times 3.74 \times 3.74 / 64) = 1.25$. Kier A3 is a so-called topological descriptor, measuring the extent of branching in the molecule: the lower is the Kier A3, the more branched is the molecule. Furthermore, Kier A3 is sensitive to the location of the branching within the molecule. The Kier A3 value is larger when branching is located at the extremities of the molecule or in the absence of any branching, and decreases when branching is located near the center of the molecule. Finally, Kier A3 can discriminate between sp^2 and sp^3 carbon atoms.

The Average Negative Softness belongs to the class of so-called inductive descriptors and is related to the polarizability (or softness) of the electron cloud. The physical interpretation of this descriptor is by far less trivial than that of Kier A3 [51-54]. The inductive softness computes the effective size and compactness of molecules and is related to the volume of the electronic cloud around each partially negative atom. The Average Negative Softness can be considered as a three-dimensional structural descriptor. As, the electron cloud of sp^3 atoms being more voluminous than that of sp^2 atoms, the Average Negative Softness of, e.g., cyclohexene (6.21) is lower than that of cyclohexane (7.28). Hence, this descriptor is able to discriminate between carbon atoms with different saturations. Note that the term "softness" appears counter-intuitive and in our sense quite unfortunate here, as the value of this descriptor increases with decreasing electron delocalization. The value of this variable increases with increasing number of saturated (sp^3) carbon atoms in the molecules. It generally decreases with increasing electron delocalization, i.e. with increasing molecular polarizability. In fact, the greater is this value; the larger is the effective size of the molecule, based on the extension of the electron cloud of the carbon atoms in hydrocarbons, and the higher is the saturation of these carbon atoms. Using this descriptor, the model takes correctly into account the important role of carbon saturation with respect to T^* .

The values of *Kier A3* and *Average_Neg Softness* are reported in Table II-7 and visualized on Figure II-11.

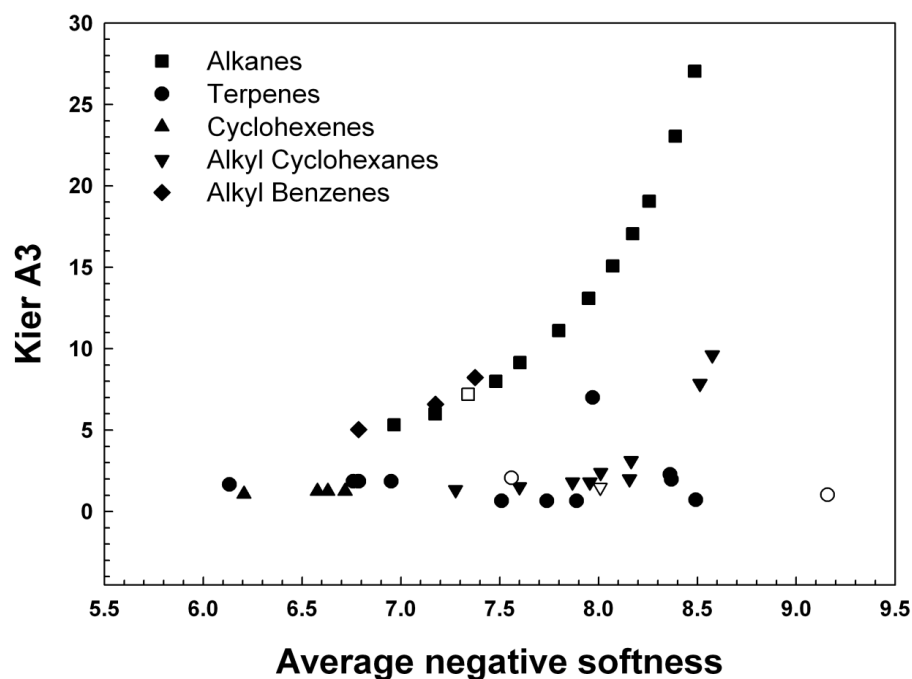


Figure II—11 Contributions of QSPR descriptors of T^* for the modeled hydrocarbons

Two groups of substances with different *KierA3* to *Average_Neg_Softness* ratio emerge from the data set. The first group encompasses the alkanes of the training set. The molecules in this group have a high aliphatic character and a molecular size which increases as the number of carbon atoms increases. This supports the view that the alkane's family is a strong basis to classify unknown oils. A lower aliphatic character and a broader variation of molecular sizes characterize the second group.

The remarkable simplicity of the proposed model suggests that T^* of a given ternary SOW system is precisely controlled by two independent contributions: (i) a purely topological contribution, related to the extent of branching in the molecule and (ii) a three-dimensional contribution, related to the size of the molecule, as measured by the spatial extension of the electron cloud of the partially negative atoms in the molecule. Both descriptors are structural descriptors, whereas the latter is additionally capable of differentiating between carbon atoms with different degree of saturation.

The fit between measured and predicted T^* for C_6E_4 shown on Figure II-12 is very good if we consider that the standard error on T^* is equal to 2 °C in the case of C_6E_4 . The predicted values are within the confidence domain of the model.

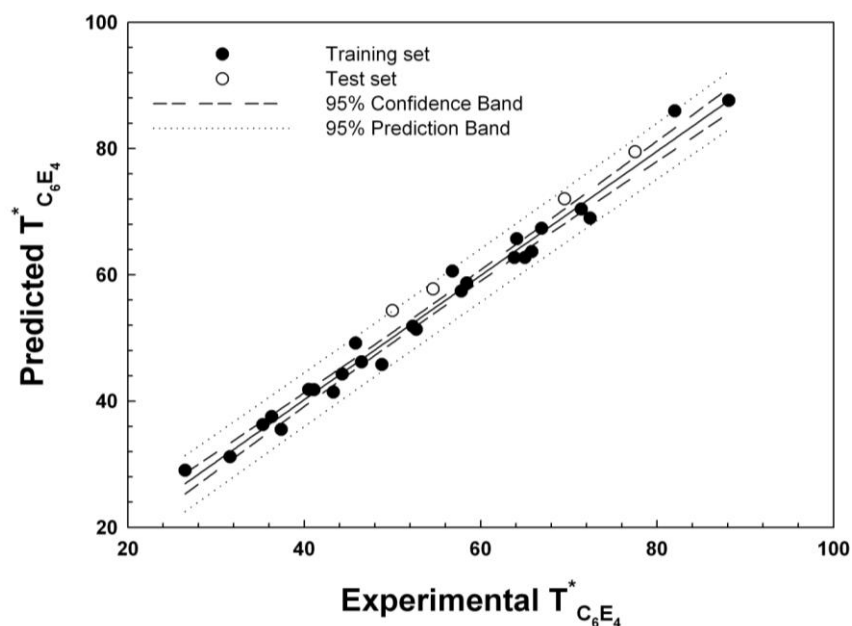


Figure II—12 Parity plot between the experimental and predicted T^* for polar hydrocarbon oils using the training set. The solid lines represent the linear regression, the dashed lines represent the 95% confidence band, and the dotted lines represent the 95% prediction band.

T^* can also be predicted for C_8E_4 and $C_{10}E_4$ using the same descriptors (Figure II-13). The quality of the models slightly decreases but is still largely satisfactory. In the case of $C_{10}E_4$, the two outliers are the long chain alkylcyclohexanes, *i.e.* decyl- and dodecyl- cyclohexane. The alkanes are perfectly modeled up to chain of 28 carbons.

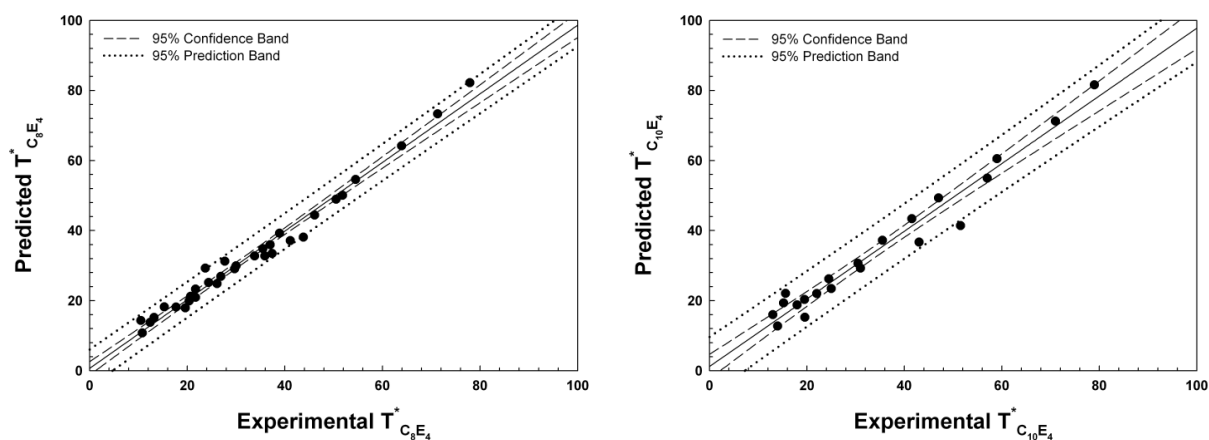


Figure II—13 Parity plot between the experimental and predicted T^* of polar hydrocarbon oils with C_8E_4 (a) and $C_{10}E_4$ (b) using the training plus the validity sets. The solid lines represent the linear regression, the dashed lines represent the 95% confidence band, and the dotted lines represent the 95% prediction band.

Finally, considering the linear relationship between T^* and the EACN of the present oils, it is then possible to deduce the EACN from the two theoretical descriptors, *i.e.* the average negative softness and the Kier A3 (equation 9). From the values of $EACN_{average}$ (see Table II-7), a multi linear regression was performed with the two descriptors leading to equation (9). This relation can be applied to polar hydrocarbon oils having an EACN between + 2 and + 28. An average standard deviation of 0.6 EACN unit is obtained if we consider the three C_iE_j .

$$EACN_{calc} = 2.88 \times \text{Average negative softness} + 0.88 \times \text{KierA3} - 19.84 \quad (9)$$

The absolute character of the EACN scale makes this data a very useful tool for the physical-chemist and for the formulator, especially to predict the phase behavior of microemulsions based on terpene oils. It is also helpful to predict the type and the stability of emulsions prepared by mixing terpene oil with a given C_iE_j at a selected temperature since those characteristics of emulsions are closely related to the phase behavior of the corresponding microemulsion [77].

2.3.3. QSPR prediction for C^* for C_6E_4 surfactant

As C^* data were also collected during our experiments, a QSPR model was built for C^* , likewise T^* , but this time only with C_6E_4 data. The correlation between the experimental values of C^* and the values obtained from fitting equation (10) is shown on Figure II-14. Here again, a simple model can be built, with only three descriptors:

$$C^* = \alpha \cdot \log P (o/w) + \beta \cdot \text{KierA3} - \gamma \cdot \text{SMR_VSA3} + \delta \quad (10)$$

with $\alpha = 5.46 \pm 1$; $\beta = 2.42 \pm 0.6$; $\gamma = 0.74 \pm 0.3$ and $\delta = 10.31 \pm 4$

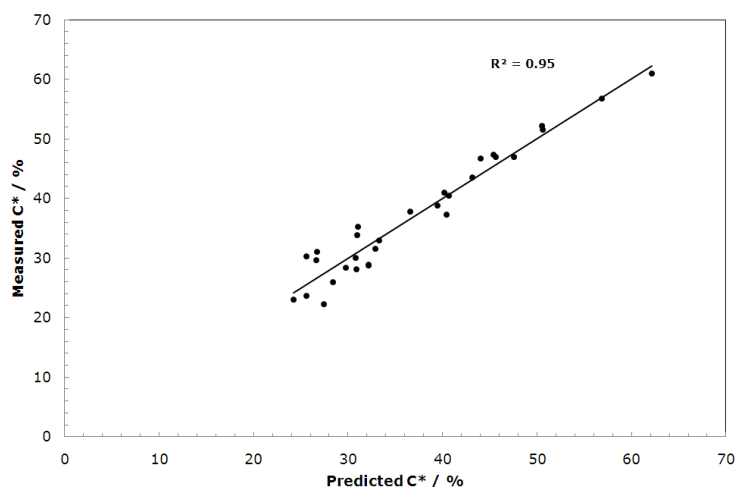


Figure II–14 Linear relationship between measured C^* values for system C_6E_4 /oil/water system and C^* predicted by the model.

The $\log P$ (o/w) descriptor is obtained in MOE environment by one of the numerous methods available to calculate the octanol / water partition coefficient, *Kier A3* has been defined above and *SMR_VSA3* is related to the presence of methyl groups attached to unsaturated secondary carbon, to the presence of terminal vinyl groups and/or to aromaticity. *SMR_VSA3* is proportional to the number of such methyl groups, i.e. it is equal to about 3.2 for 1-methyl-1-cyclohexene (I), α -pinene, β -pinene and δ -3-carene, 6.4 for alpha terpinene, caryophyllene (II), gamma terpinene and limonene, and 10 for para-cymene and terpinolene (III), while this descriptor is zero for all other molecules. The correction brought by this contribution to the model is small but significant.

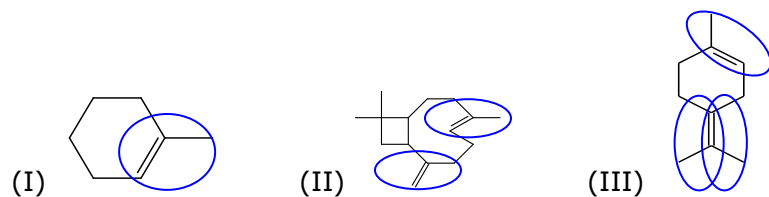


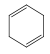
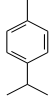
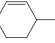
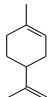
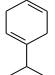
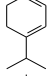
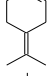

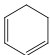
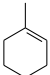
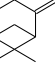
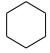
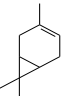
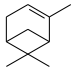
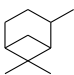
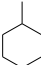
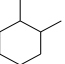
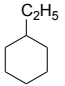
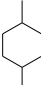
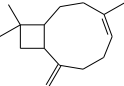
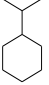
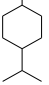
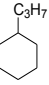
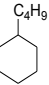
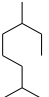


Table II-10 Values of the descriptors QSPR to fit equation (10) for the C* of modelled hydrocarbons including their corresponding chemical structures and the value for T* and C* for the C₆E₄/oil/water system

Oils	Formula	logP(o/w) ^a	KierA3	SMR_VSA3	C ₆ E ₄	
					T* (%)	C* (%)
Cyclohexene		2.67	1.06	0	26.50	22.20
2,5-Norbornadiene		2.40	0.34	0	15.40	23.00
1,4-cyclohexadiene		2.43	0.83	0	11.10	23.70
p-cymene		4.03	1.65	10.78	31.60	25.90
3-Methyl-1-cyclohexene		3.21	1.25	0	35.30	28.20
Limonene		3.60	1.85	6.37	44.30	28.40
γ-Terpinene		4.04	1.85	6.37	43.30	28.70
α-Terpinene		4.04	1.85	6.37	41.10	28.90
Terpinolene		3.46	1.85	9.56	40.50	29.70
4-Methyl-1-cyclohexene		3.20	1.25	0	36.30	30.00
1,3-cyclohexadiene		2.43	0.83	0	16.20	30.30
1-Methyl-1-cyclohexene		2.88	1.25	3.19	37.40	31.00
β-Pinene		4.28	0.65	3.19	45.80	31.50
Cyclohexane		3.62	1.33	0	46.50	32.90

δ -3-carene		3.93	0.65	3.19	48.80	33.90
α -Pinene		3.94	0.65	3.19	52.70	35.30
Pinane		5.19	0.72	0	56.80	37.30
Methylcyclohexane		4.14	1.50	0	52.30	37.80
1,2-dimethylcyclohexane		4.67	1.49	0	54.60	38.80
Ethylcyclohexane		4.76	1.80	0	57.80	40.40
1,4-dimethylcyclohexane		4.67	1.80	0	58.40	41.00
Caryophyllene		6.00	1.97	6.37	64.10	43.50
Isopropylcyclohexane		5.29	2.00	0	63.80	46.70
p-menthane		5.82	2.29	0	66.90	46.90
Hexane	B ₆	4.11	5.33	0	65.80	47.00
Propylcyclohexane		5.37	2.38	0	65.00	47.40
Heptane	B ₇	4.72	6.00	0	71.40	51.60
Butylcyclohexane		5.98	3.11	0	72.40	52.20
Octane	B ₈	5.34	7.20	0	78.20	56.70
Myrcane		6.39	7.00	0	88.10	60.90

Nonane	B ₉	5.95	8.00	0	82.00	60.90
--------	----------------	------	------	---	-------	-------

^a logP(o/w) corresponds to the calculated octanol/water partition coefficient

The occurrence of the logarithm of the octanol / water partition coefficient as descriptor in the expression is not fortuitous, since this variable remains among the best measure of molecular lipophilicity available. Alternative modelling trials have been done without this variable led to poorer models. The calculated *logP* can be obtained by various methods, which have recently been reviewed extensively by Mannhold et al. [81], whereby group contribution methods based on molecular substructures are the most widely recognized. One advantage is that *logP* includes H-bond interactions and electronic effects (π -bonds, aromaticity, etc.) together with other topological information. On the other hand, the *logP* scale offers strong similarities with empirical scales such as the HLB or the HLD of surfactants, as both classes of variables measure affinity ratios between both oil and water.

Additionally to *logP* and *SMR_VSA3*, the magnitude of the Kier A3 descriptor enlightens the contribution of aliphatic extension of the molecule vs. branching. As for T*, two groups emerge in the *Kier 3* vs. *logP* plot (Figure II-15).

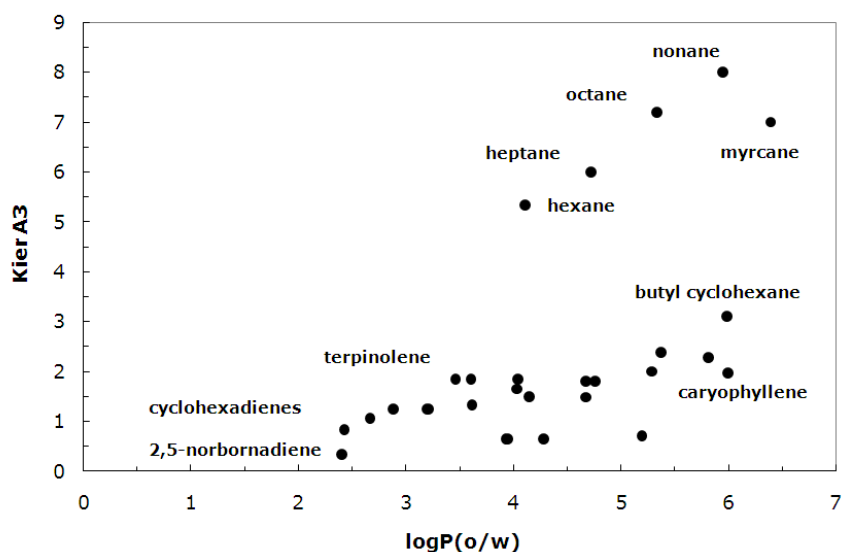


Figure II—15 Contributions of QSPR descriptors of C* for the modelled hydrocarbons

Comparing the impact of *SMR_VSA3* on model reliability (Figure II-16) shows that deviations of the position of methyl groups adjacent to an unsaturated carbon atom or terminal vinyl groups with respect to the main axis of symmetry of the molecule either

increase the calculated C^* value (e.g. β -pinene) or decrease it (e.g. terpinolene). It can be suggested, that the contribution of this particular double bond on molecular polarity plays a significant, but still unexplained role in determining the position of C^* in the phase diagram.

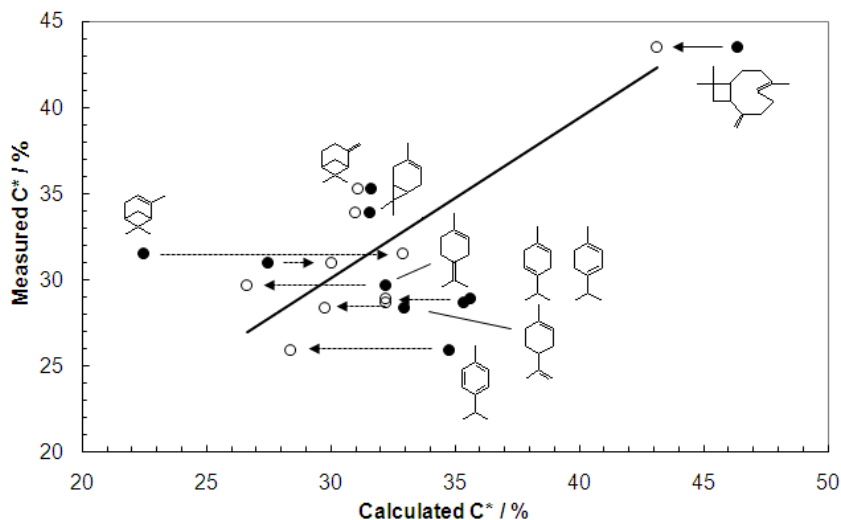


Figure II—16 Comparison between 3-variable model (with *SMR_VSA3*, empty circles) and 2-variable model (without *SMR_VSA3*, dark circles). The arrows show the impact of non-zero *SMR_VSA3* on calculated C^* .

A decrease of C^* is associated with an increase of the surfactant efficiency, i.e. the number of surfactant molecule necessary to co-solubilize an equal amount of oil and water decreases. From the above results, it appears that this effect is induced by three factors: (i) the surface of the oil molecule exposed to water (reflected by the *Kier A3* variable), (ii) electrostatic effects related to electron double bonds and (iii) to the presence and position of specific unsaturated synthons of general formulas $[\text{CH}_3\text{-C=}]$ and $[\text{CH}_2\text{=C-}]$. Emulsifying oils having favourable combinations of the above factors lower C^* at a remarkable extent.

Finally, as it was the case for T^* , Equation (10) predicts low C^* with a reasonable accuracy, independently of the fact that in this domain, the linearity between T^* and C^* is lost. Our assumption is that the existence of a well-defined oil/water interface is not a prerequisite for the existence of the X-point of the fish diagram of microemulsions. In other words, the application ranges of the models built up here should extend to the case of solvo-surfactants (i.e. non ionic short chain amphiphiles) and even to solutions, i.e. in domains where the three-phase body vanishes. This assumption is consistent with the microscopic interpretation of the QSPR descriptors, as none of the latter speculates the existence of an interface in the system.

2.4. Conclusion

The Fish-tail temperatures T^* of SOW systems based on tetraethylene glycol monoethyl (C₆E₄), monoethyl (C₈E₄) or monodecyl (C₁₀E₄) ethers, and a series of hydrocarbon oils including *n*-alkanes, used as references, and substituted cyclohexanes, cyclohexenes, aromatics and terpenes have been determined and their evolution has been rationalized by considering the effective packing parameter \bar{P} of the surfactants in its whole physicochemical environment. It is shown that an increase of the oil penetration into the surfactant palisade should be compensated for a decrease of the fish-tail temperature T^* . A robust linear model based only on two descriptors reflecting topological features related to molecular branching and polarizability of the oils has been established for an accurate prediction of T^* . Another linear model for the prediction of the optimal concentration C^* for C₆E₄/terpenes/water based on three descriptors is also proposed. The value C^* appears to be driven by the surface of the oil molecule exposed to water (reflected by the *Kier A3* variable), the electrostatic effects related to electron double bonds and to the presence and position of specific unsaturated synthons of general formulas [CH₃-C=] and [CH₂=C-] in the oil. Emulsifying oils having favourable combinations of the above factors lower C^* at a significant extent. This QSPR approach also provides a useful tool for the prediction of the Equivalent Alkane Carbon Number (EACN) of polar hydrocarbon oils ranging from -3 to +35 as linear relationships link the T^* of C_{*i*}E₄ (*i* = 6, 8, 10) both between them and with the EACNs [46]. This finding constitutes a very useful tool in the prediction of the type and behavior of microemulsions and emulsions prepared from terpene oils and C_{*i*}E_{*j*} surfactants.

3. Experimental

3.1. Chemicals

Tetraethylene glycol (E₄, 99%), sodium hydroxide (NaOH, 98%), 1-bromoalkanes (C₁₀Br 98%, C₈Br 97%, C₆Br 98%) and tetradecane (>99%) were purchased from Fluka (France). Methanol, petroleum ether, cyclohexane, toluene, *n*-alkanes (from C₆ to C₉) (97%) were obtained from SCRC (China). *n*-decane, *n*-dodecane and *n*-hexadecane were purchased from Acros (>99%), Alkylcyclohexanes, cyclohexene and methylcyclohexenes were purchased from TCI (Japan). All fragrance molecules were provided by Givaudan Shanghai (>98%). Myrcane has been prepared from tetrahydrocitral by Wolf-Kishner reaction and modified according to Huang Min Lon [32] then distilled under vacuum. All components were used as received. Purity was assessed by GC analysis. Milli-Q water (18.2 MΩ cm) was used.

3.2. Synthesis of tetraethylene glycol monoalkyl ethers C₁₀E₄, C₈E₄ and C₆E₄

Tetraethylene glycol monoalkyl ethers C_iE₄ were synthesized according to a known procedure [21] and [29] and scaled up to obtain large amounts of surfactants. Tetraethylene glycol (E₄) 1124 g (5.8 mol) was added to 46 g of NaOH 50% aqueous solution (0.58 mol) under stirring. The resulting yellow mixture was warmed up to 100 °C. The bromoalkane (0.58 mol) was then added dropwise and the system was stirred at 100 °C during 24 h. After cooling, the mixture was charged with 1200 mL of water and extracted with 3 times with 600 mL of toluene. After drying, the organic phase was evaporated and charged with 300 mL of water and 900 mL of methanol and then extracted 3 times with 1200 mL of petroleum ether. The aqueous phase was evaporated partially to remove methanol, charged with 300 mL of water and extracted 3 times with 600 mL of a mixture of cyclohexane/isopropanol (50/1, v/v). The resulting solution was distilled under vacuum. The isolated yield was about 85% (150 g) with a purity >99%. ¹H and ¹³C NMR analyses were carried on a 300 MHz spectrometer (Bruker). Gas chromatography analyses were performed on an Agilent 6890N equipped with FID and the following conditions were used: capillary column HP-5; column temperature programmed linearly from 80 to 300 °C at 15 °C min⁻¹; injector temperature at 250 °C; detector temperature at 300 °C; carrier gas helium at a flow rate of 4.6 mL min⁻¹; splitless.

3.3. Determination of “fish-tail” temperatures (T*) of the C_iE₄/oil/water systems

The “fish-tail” temperatures T* were determined by investigating the phase behavior of the C_iE₄/oil/water systems at a constant water-to-oil weight ratio (WOR = 1) as a function of temperature (ordinate) and surfactant mass percentage (abscissa). The “fish-tail” point located at the intersection of the four Winsor (Winsor I, II, III and IV) regions, corresponds to the minimal surfactant concentration required to obtain a one-phase microemulsion (Winsor IV)[27,46]. Water, oil and surfactant were introduced in a thin glass tube (Ø = 2 mm) the headspace of which was filled with Argon and then frozen at -78 °C with a dry ice/acetone mixture. The tubes were sealed by flame to avoid any loss of oil or water during the experiment. Samples were gently shaken and placed in a water bath, maintained at a constant temperature T ± 0.1 °C, until the equilibrium was reached. The fish diagrams were constructed by visual inspection of the Winsor phases. The “fish-tail” temperature T* values were obtained with an accuracy better than 1 °C.

3.4. Determination of the Gibbs diagram of the C₆E₄/α-pinene/water system

The three-phase triangle (WIII region) as well as the adjacent two-phase WI and WII regions has been determined according to a two-step procedure. Firstly, the three points of the apexes of the WIII triangle have been determined at the T* temperature (i.e. at 52.7 °C) by titration of the 3 coexisting phases.¹⁷ Gas chromatography (GC) analyses were used to determine the phase composition on an Agilent 6890N apparatus, equipped with a HP-1 cross-linked methyl silicone gum column (60 m x 0.32 mm x 0.25 μm), with N₂ as gas vector and with a FID detector. Secondly, the boundaries between the biphasic regions (WI and WII) and the monophasic region (WIV) have been determined by visual inspection of the Winsor the systems at equilibrium.

3.5. Data and calculation methods

The chemical structure of the oils shown in Table II-7, converted in MDL mol format [48] were used as the 2D structure inputs in a Molecular Operating Environment's (MOE) spreadsheet[49]. In a first step, molecular mechanics MFF94x force field was used to calculate the low-energy 3D structures of each compound. These 3D structures have been optimized using PM3 Hamiltonian of MOPAC [50] implemented in MOE. In a second step, a split of the polar hydrocarbon oils into a training (26 candidates) and test (4 candidates) sets has been performed and multiple Quantitative Structure Property Relationship (QSPR) modeling was run using the descriptors provided by MOE, as well as Inductive [51-54] and RECON [55] descriptors, and the uninformative variables (i.e. having a standard deviation less than 0.05) were eliminated. The QSPR model was built by applying Genetic Function Approximation (GFA) script shipped with MOE[56].

Multiple QSPR models were preferred over standard regression analysis because they are generated by statistical analysis and rely on comparable or superior equations. The multiple models were created by evolving random initial equations using a *genetic algorithm*. In the present case, only linear equations were used, as this approach leads to more robust models, which allows moderate extrapolations as well.

The different QSPRs were scored using *Friedman's* Lack of Fit (*LOF*) rating [57-58]:

$$LOF = \frac{LSE}{\left(1 - \frac{C + d \times P}{N}\right)} \quad (11)$$

where C is the number of basic functions (other than constant term) in the model, d is the smoothing parameter (usually equal to 1), P is the total number of function terms, N is the number of samples in the training set, and LSE is the least-squares error:

$$LSE = \frac{1}{N} \sum_{n=1}^N \left(\frac{y_n - \hat{y}_n}{y_n} \right)^2 \quad (12)$$

where y_i and \hat{y}_i refer to the measured and estimated values of the property for the molecule i , respectively. Unlike the more commonly used LSE or R^2 the lack of fit (*LOF*) rating is not systematically reduced by adding more terms to the regression equation, and therefore resists over-fitting better than the LSE or R^2 do.

4. References of chapter II

1. Friberg, S. E., Fragrance compounds and amphiphilic association structures. *Adv. Colloid Interface Sci.* **1998**, 75 (3), p181-214
2. Saito, Y., Katougi, Y., Hashizaki, K., Taguchi, H., Ogawa, N., Solubilization of (+)- α -pinene by cyclodextrin/surfactant mixed systems. *J. Dispersion Sci. Technol.* **2001**, 22 (2-3), p191-195
3. Katougi, Y., Saito, Y., Hashizaki, K., Taguchi, H., Ogawa, N., Comparison of the solubilizing ability of cyclodextrins and surfactants for (+)- α -pinene. *J. dispersion sci. technol.* **2001**, 22 (2-3), p185-190
4. Labows, J. N., Brahms, J. C., Cagan, R. H., Solubilization of fragrances by surfactants. *Surfactants in Cosmetics* **1997**, 68, p605-619
5. Lyndon David Parry, **1999** Patent GB 2 333 302
6. Carlotti, M. E., Gallarate, M., Morel, S., Ugazio, E., Micellar solutions and microemulsions of odorous molecules. *J. Cosmetic Sci.* **1999**, 50 (5), p281-295
7. Tokuoka, Y., Uchiyama, H., Abe, M., Ogino, K., Solubilization of synthetic perfumes by nonionic surfactants. *J. Colloid Interface Sci.* **1992**, 152 (2), p402-409
8. Kayali, I., Qamhieh, K., Lindman, B., Effect of type of fragrance compounds on their location in hexagonal liquid crystal. *J. dispersion sci. technol.* **2006**, 27 (8), p1151-1155
9. Uddin, M. H., Kanei, N., Kunieda, H., Solubilization and emulsification of perfume in discontinuous cubic phase. *Langmuir* **2000**, 16 (17), p6891-6897
10. Kayali, I., Khan, A., Lindman, B., Solubilization and location of phenethylalcohol, benzaldehyde, and limonene in lamellar liquid crystal formed with block copolymer and water. *J. Colloid Interface Sci.* **2006**, 297 (2), p792-796
11. Fanun, M., Al-Diyn, W. S., Structural transitions in the system water/mixed nonionic surfactants/R (+)-limonene studied by electrical conductivity and self-diffusion-NMR. *J. dispersion sci. technol.* **2007**, 28 (1), p165-174
12. Fanun, M., Propylene glycol and ethoxylated surfactant effects on the phase behavior of water/sucrose stearate/oil system. *J. dispersion sci. technol.* **2007**, 28 (8), p1244-1253
13. Yaghmur, A., Aserin, A., Antalek, B., Garti, N., Microstructure considerations of new five-component Winsor IV food-grade microemulsions studied by pulsed gradient spin-echo NMR, conductivity, and viscosity. *Langmuir* **2003**, 19 (4), p1063-1068

14. Yaghmur, A., Aserin, A., Garti, N., Phase behavior of microemulsions based on food-grade nonionic surfactants: Effect of polyols and short-chain alcohols. *Colloids Surf., A* **2002**, 209 (1), p71-81
15. Acharya, A., Sanyal, S. K., Moulik, S. P., Physicochemical investigations on microemulsification of eucalyptol and water in presence of polyoxyethylene (4) lauryl ether (Brij-30) and ethanol. *Int. J. Pharm.* **2001**, 229 (1-2), p213-226
16. Hamdan, S., Ahmad, F. B. H., Laili, C. R., Fauziah, H., *Orient J. Chem.* **1995**, 11 (3), p220-225
17. Friberg, S. E., Vona, S., *Soap, Cosmetics, Chem. Spec.* **1994**, 70, p36-41
18. Kanei, N., Tamura, Y., Kunieda, H., Effect of types of perfume compounds on the hydrophile-lipophile balance temperature. *J. Colloid Interface Sci.* **1999**, 218 (1), p13-22
19. J.L. Salager, R. Anton, J.M. Anderez, J.M. Aubry, Microemulsion formulation with HLD (hydrophilic-lipophilic deviation) method. *Techniques de l'Ingénieur, Génie des Procédés J2157*, **2001**, p1-20
20. Salager, J. L., Marquez, N., Graciaa, A., Lachaise, J., Partitioning of ethoxylated octylphenol surfactants in microemulsion-oil-water systems: influence of temperature and relation between partitioning coefficient and physicochemical formulation. *Langmuir* **2000**, 16 (13), p5534-5539
21. Queste, S., Salager, J. L., Strey, R., Aubry, J. M., The EACN scale for oil classification revisited thanks to fish diagrams. *J. Colloid Interface Sci.* **2007**, 312 (1), p98-107
22. Winsor, P. A., Binary and multicomponent solutions of amphiphilic compounds. Solubilization and the formation, structure, and theoretical significance of liquid crystalline solutions. *Chem. Rev.* **1968**, 68 (1), p1-40
23. Bourrel, M., Schechter, R. S., *Microemulsions and Related Systems* **1988**, 483
24. Salager, J. L., Loaiza-Maldonado, I., Minana-Perez, M., Silva, F., Surfactant-oil-water systems near the affinity inversion - 1. Relationship between equilibrium phase behavior and emulsion type and stability. *J. dispersion sci. technol.* **1982**, 3 (3), p279-292
25. Bourrel, M., Salager, J. L., Schechter, R. S., Wade, W. H., A correlation for phase behavior of nonionic surfactants. *J. Colloid Interface Sci.* **1980**, 75 (2), p451-461

26. Nardello, V., Chailloux, N., Poprawski, J., Salager, J. L., Aubry, J. M., HLD concept as a tool for the characterization of cosmetic hydrocarbon oils. *Polym. Int.* **2003**, 52 (4), p602-609.
27. Kahlweit, M., Strey, R., Haase, D., Firman, P., Properties of the three-phase bodies in H₂O-oil-nonionic amphiphile mixtures. *Langmuir* **1988**, 4 (4), p785-789
28. Poprawski, J., Catté, M., Marquez, L., Marti, M. J., Salager, J. L., Aubry, J. M., Application of hydrophilic-lipophilic deviation formulation concept to microemulsions containing pine oil and nonionic surfactant. *Polym. Int.* **2003**, 52 (4), p629-632
29. Gibson, T., Phase-transfer synthesis of monoalkyl ethers of oligoethylene glycols. *J. Org. Chem.* **1980**, 45 (6), p1095-1098
30. Schubert, K. V., Strey, R., Kahlweit, M., A new purification technique for alkyl polyglycol ethers and miscibility gaps for water-C₁E_j. *J. Colloid Interface Sci.* **1991**, 141 (1), p21-29
31. Burauer, S., Sachert, T., Sottmann, T., Strey, R., On microemulsion phase behavior and the monomeric solubility of surfactant. *Phys. Chem. Chem. Phys.* **1999**, 1 (18), p4299-4306
32. Huang, M., A simple modification of the Wolff-Kishner reduction *J. Am. Chem. Soc.* **1946**, 68, p2487-2488
33. Burauer, S., Sottmann, T., Strey, R., Nonionic microemulsions with cyclic oils: Oil penetration, efficiency and monomeric solubility. *Tenside, Surfactants, Deterg.* **2000**, 37 (1), 8-16
34. Bancroft, W. D., The Theory of Emulsification. *J. Phys. Chem.* **1913**, 17, p501-20
35. Shinoda, K., Arai, H., The correlation between phase inversion temperature in emulsion and cloud point in solution of nonionic emulsifier. *J. Phys. Chem.* **1964**, 68 (12), p3485-90
36. Schuster, D., Encyclopedia of Emulsion Technology, Volume Three: Basic Theory, Measurement, Applications. Marcel Dekker: **1988**, vol. 3
37. Griffin, W. C., Classification of surface active agents by HLB. *J. Soc. Cosmet. Chem.* **1949**, 1, p311-326

38. Salager, J. L., Bourrel, M., Schechter, R. S., Wade, W. H., Mixing rules for optimum phase-behavior formulations of surfactant/oil/water systems. *Soc. Pet. Eng. J.* **1979**, 19 (5), p271-8
39. Binks, B. P., Relationship between microemulsion phase behavior and macroemulsion type in systems containing nonionic surfactant. *Langmuir* **1993**, 9 (1), p25-8
40. Wade, W. H., Morgan, J. C., Jacobson, J. K., Schechter, R. S., Low interfacial tensions involving mixtures of surfactants. *Soc. Pet. Eng. J.* **1977**, 17 (2), p122-8
41. Cash, L., Cayias, J. L., Fournier, G., MacAllister, D., Schares, T., Schechter, R. S., Wade, W. H., The application of low interfacial tension scaling rules to binary hydrocarbon mixtures. *J. Colloid Interface Sci.* **1977**, 59 (1), p39-44
42. Engelskirchen, S., Elsner, N., Sottmann, T., Strey, R., Triacylglycerol microemulsions stabilized by alkyl ethoxylate surfactants-A basic study, Phase behavior, interfacial tension and microstructure. *J. Colloid Interface Sci.* **2007**, 312 (1), p114-121
43. Kunieda, H., Shinoda, K., Evaluation of the hydrophile-lipophile balance (HLB) of nonionic surfactants. I. Multisurfactant systems. *J. Colloid Interface Sci.* **1985**, 107 (1), p107-21
44. Wormuth, K. R., Kaler, E. W., Microemulsifying polar oils. *J. Phys. Chem.* **1989**, 93 (12), 4855-61
45. Arenas, E., Baran Jr, J. R., Pope, G. A., Wade, W. H., Weerasooriya, V., Aqueous phase microemulsions employing N-methyl-N-D-glucalkanamide surfactants with chlorinated hydrocarbons. *Langmuir* **1996**, 12 (2), p588-590
46. Bouton, F., Durand, M., Nardello-Rataj, V., Serry, M., Aubry, J.-M., Classification of terpene oils using the fish diagrams and the Equivalent Alkane Carbon (EACN) scale. *Colloids Surf., A* **2009**, 338 (1-3), p142-147
47. Pizzino, A., Molinier, V., Catte, M., Salager, J.-L., Aubry, J. M., Bidimensional analysis of the phase behavior of a well-defined Surfactant (C₁₀E₄)/Oil (n-octane)/Water – Temperature system. *J. Phys. Chem.* **2009**, 113(50), p16142-16150
48. Inc, M. I. S. San Leandro, CA. USA
49. Inc, C. C. G. *Molecular Operating Environment (MOE)*, version 2007.09, Montreal, Canada, **2007**

50. MOPAC 7 is a public domain program developed and maintained by J. J. P. Stewart and distributed by the Quantum Chemistry Program Exchange, Bloomington, Indiana, USA
51. Pearson, R. G., Hard and soft acids and bases. *J. Am. Chem. Soc.* **1963**, 85 (22), p3533-9
52. Cherkasov, A., Inductive electronegativity scale. Iterative calculation of inductive partial charges. *J Chem Inf Comput Sci* **2003**, 43 (6), p2039-47
53. Cherkasov, A., Shi, Z., Fallahi, M., Hammond, G. L., Successful in Silico Discovery of Novel Nonsteroidal Ligands for Human Sex Hormone Binding Globulin. *J. Med. Chem.* **2005**, 48 (9), p3203-3213
54. Cherkasov, A., 'Inductive' descriptors: 10 successful years in QSAR. *Curr. Comput.-Aided Drug Des.* **2005**, 1 (1), p21-42
55. Lavine, B., K., Davidson, C., E., Breneman, C., Katt, W., Electronic van der Waals surface property descriptors and genetic algorithms for developing structure-activity correlations in olfactory databases. *J Chem Inf Comput Sci* **2003**, 43 (6), p1890-905
56. Inc., R. S. Genetic Algorithm for QSAR (GA.svl) for MOE, **2001-2005**
57. Friedman, J. *Technical Report 102*, Laboratory for Computational Statistics, Department of Statistics, Stanford University: Stanford **1988** (revised **1990**)
58. Rogers, D., Hopfinger, A. J., Application of Genetic Function Approximation to Quantitative Structure-Activity Relationships and Quantitative Structure-Property Relationships. *J Chem Inf Comput Sci* **1994**, 34 (4), p854-66
59. Kahlweit, M., Strey, R., Phase Behavior of ternary systems of the type H₂O-Oil-Nonionic Amphiphile. *Angewandte Chemie - International Edition in English* **1985**, 24 (8), p654-668
60. Lim, K. H., Reckley, J. S., Smith, D. H., Liquid-liquid phase equilibrium in binary mixtures of the nonionic amphiphile 2-(2-hexyloxyethoxy)ethanol and water. *J. Colloid Interface Sci.* **1993**, 161 (2), p465-70
61. Israelachvili, J. N., Mitchell, D. J., Ninham, B. W., Theory of self-assembly of hydrocarbon amphiphiles into micelles and bilayers. *J. Chem. Soc., Faraday Transactions 2: Molecular and Chemical Physics* **1976**, 72, p1525-1568

62. Burauer, S., Sottmann, T., Strey, R., Nonionic microemulsions with cyclic oils: Oil penetration, efficiency and monomeric solubility. *Tenside, Surfactants, Deterg.* **2000**, 37 (1), p8-16
63. Requena, J., Billett, D. F., Haydon, D. A., Van der Waals forces in oil-water systems from the study of thin lipid films. I. Measurement of the contact angle and the estimation of the van der Waals free energy of thinning of a film. *Proc. R. Soc. London, Ser. A* **1975**, 347 (1649), p141-59
64. Chen, S. J., Evans, D. F., Ninham, B. W., Mitchell, D. J., Blum, F. D., Pickup, S., Curvature as a determinant of microstructure and microemulsions. *J. Phys. Chem.* **1986**, 90 (5), p842-7
65. Inoue, T., Interaction of Surfactants with phospholipid vesicles. In *Surfactant science series: Vesicles*, Rosoff, M., Ed. Dekker: **1996**, Vol. 62
66. Tchakalova, V., Testard, F., Wong, K., Parker, A., Benczedi, D., Zemb, T., Solubilization and interfacial curvature in microemulsions I. Interfacial expansion and co-extraction of oil. *Colloids Surf., A* **2008**, 331 (1-2), p31-39
67. Testard, F., Zemb, T., Excess of Solubilization and Curvature in Nonionic Microemulsions. *J. Colloid Interface Sci.* **1999**, 219 (1), p11-19
68. Huibers, P. D. T., Shah, D. O., Katritzky, A. R., Predicting surfactant cloud point from molecular structure. *J. Colloid Interface Sci.* **1997**, 193 (1), p132-136
69. Huibers, P. D. T., Lobanov, V. S., Katritzky, A. R., Shah, D. O., Karelson, M., Prediction of Critical Micelle Concentration Using a Quantitative Structure-Property Relationship Approach. 1. Nonionic Surfactants. *Langmuir* **1996**, 12 (6), p1462-70
70. Huibers, P. D. T., Lobanov, V. S., Katritzky, A. R., Shah, D. O., Karelson, M., Prediction of critical micelle concentration using a quantitative structure-property relationship approach. 2. Anionic surfactants. *J. Colloid Interface Sci.* **1997**, 187 (1), p113-120
71. Anoune, N., Nouriri, M., Berrah, Y., Gauvrit, J.-Y., Lanteri, P., Critical micelle concentrations of different classes of surfactants: a quantitative structure property relationship study. *J. Surfactants Deterg.* **2002**, 5 (1), p45-53
72. Wang, Z., Li, G., Zhang, X., Wang, R., Lou, A., A quantitative structure-property relationship study for the prediction of critical micelle concentration of nonionic surfactants. *Colloids Surf., A* **2002**, 197 (1-3), p37-45

73. Kier, L. B., Hall, L. H., The nature of structure-activity relationships and their relation to molecular connectivity. *Eur. J. Med. Chem. - Chim. Ther.* **1977**, 12 (4), 307-12
74. Hall, L. H., Kier, L. B., The molecular connectivity chi indexes and kappa shape indexes in structure-property modeling. *Rev. Comput. Chem.* **1991**, 2, p367-422
75. Kahlweit, M., Strey, R., Busse, G., Microemulsions: A qualitative thermodynamic approach. *J. Phys. Chem.* **1990**, 94 (10), p3881-3894
76. Schubert, K. V., Strey, R., Kline, S. R., Kaler, E. W., Small angle neutron scattering near Lifshitz lines: Transition from weakly structured mixtures to microemulsions. *J. Chem. Phys.* **1994**, 101 (6), p5343-5355
77. Salager, J. L., Principles of Emulsion Formulation Engineering. In *Adsorption and Aggregation of Surfactants in Solution*, Mittal, K. L., Shah, D. O., Eds. Marcel Dekker New York: **2003**
78. Bouton, F., Durand, M., Nardello-Rataj, V., Borosy, A.P., Quellet, C., Aubry J.M., A QSPR Model for the Prediction of the "Fish-Tail" Temperature of C₁₂E₄/Water/Polar Hydrocarbon Oil Systems *Langmuir*, **2010**, 26 (11), p7962-7970
79. Garate, J.M., Aggregation of alcohols ethoxylates in n-heptane *J. Surfact. Deterg.*, **2009**, 12, p231-236
80. Kunieda, H., Friberg, S. E., Critical Phenomena in a surfactant/water/oils System. Basic Study on the Correlation between Solubilization, Microemulsion, and Ultralow Interfacial Tensions *Bull. Chem. Soc. Jpn.* **1981**, 54, p1010
81. Mannhold, R., Poda, G.I., Ostermann, C., Tetko, I.V., Calculation of molecular lipophilicity: State-of-the-art and comparison of log *P* methods on more than 96,000 compounds. *J. Pharm. Sci.*, **2008**, 98 (3), p861-893

Chapter III

III. Influence of terpenoids on emulsions and microemulsions

Chapter II is mainly dedicated to the study of microemulsions with polar saturated hydrocarbons, olefins or aromatics as the oily phase. In this chapter III, further complex systems are exposed with several connections. Firstly, systems at equilibrium, i.e.: Winsor systems, with an oily phase containing terpenoids having a polar function (alcohols, phenol, nitrile, ketones, aldehydes or esters) are investigated. The presence of polar functions increases the monomeric solubility of polyethoxylated fatty alcohol surfactants in oil and makes possible the appearance of a cosurfactant behavior when the oil is amphiphilic (alcohols, phenols). On perfumery creation level, the terpenoids are more interesting than terpenes because they give access to a range of more pleasant and diversified olfactive notes. Secondly, systems at non-equilibrium such as emulsions formulated from various oils: terpenes, alkanes, silicones, terpenoid alcohols and other terpenoids are investigated. The presence of polar oils can have significant consequences not only on the phase inversion temperature but also on the emulsion stability because of an acceleration of Ostwald ripening effect. We segmented this chapter in three paragraphs preceded by an introduction and follow by an experimental part. Paragraph III.2 is focused on the impact of terpene alcohols on the position of the "X" point defined by (T^* , C^*) of the fish diagrams. Phase diagrams of tetraethylene glycol monoalkyl ether (C_8E_4 and $C_{10}E_4$), three model oils: dodecane, eicosane and octamethylcyclotetrasiloxane (D4) at constant water-to-oil ratio, are built. The influence of increment concentration of geraniol and pelargol is investigated and compared to a linear alcohol: *n*-octanol in the silicone-based microemulsion case. The choice of geraniol and pelargol as fragrance molecule models is justified because they are massively used in fragrance creations, besides that they are all primary alcohols, they possess a remarkable isomeric skeleton illustrated in Figure III-1, geraniol is unsaturated isomer of pelargol, itself is the branched isomer of *n*-octanol. Their structures allow the impact of unsaturation and methylation on the PIT value.

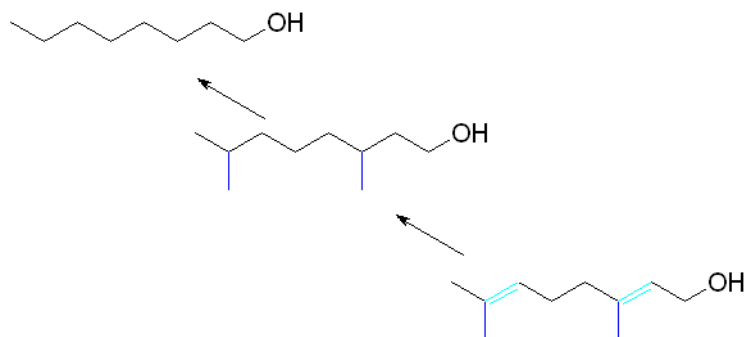
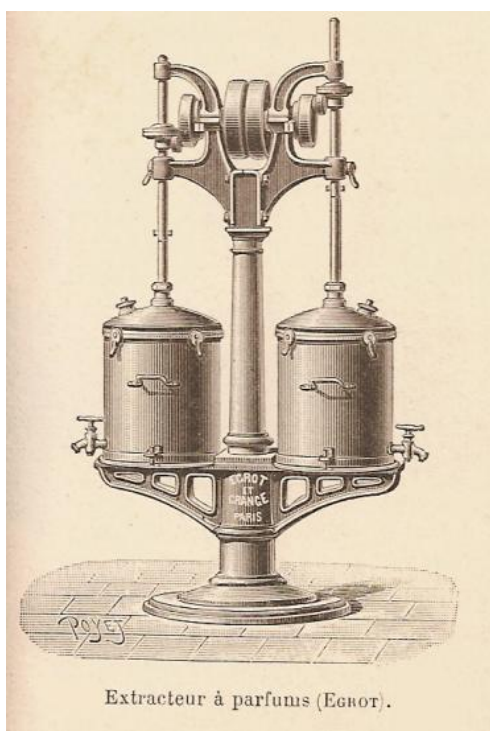


Figure III—1 Chemical structure of *n*-octanol (top), pelargol (middle) and geraniol (bottom)

In the paragraph III.3, the study of emulsions is developed with a similar approach. Firstly pure C_8E_4 is used to quantify the impact of pelargol on the Phase Inversion Temperature (PIT) of C_8E_4 / dodecane / water emulsion system and then, compared with results of section 1, a correlation between T^* and PIT is shown. Secondly, the influence on the PIT of an emulsion Brij30 / octane / water of various terpenoids and functionalized fragrant molecules as a function of their concentrations is reported and discussed. The HLD equation used to rationalize the effect of fragrances on PIT by comparing the a.A parameter with a series of aliphatic alcohols (C_1 to C_{16}). The effect of the hydrophobic chain structure and nature of the polar function on cosurfactant properties are discussed. In the paragraph III.4, the stability of Brij30 / octane / water emulsion is studied and a cosmetic emulsion is prepared and served as a model to evaluate the influence of fragrant terpene alcohols on its stability.



1. Introduction

The cumulated quantity of terpenoids used as fragrance ingredients is estimated at 50000 tons per year representing about 400 million Euros. Only a few of them such geraniol, linalool, citronellol and their esters exceed 5000 tons per year [1]. The latter molecules are crucial to a large development of floral accords and represent often more than 30% of the components of basic fragrances. In addition, these molecules cannot be considered as simple oils as in chapter II in the case of terpenes because they have a strong effect on the phase behavior of surfactant / oil / water systems. For example, the EACN of α - and γ -terpineol is estimated at -16.8 [2]. Kahlweit et al. clarified the role of alcohols in microemulsions. They described alcohols as weak amphiphiles while added to a binary water / oil mixture; as a result, the alcohols were treated as "co-solvents" that partition between the aqueous domain and the amphiphilic film [3]. Lately Penders and Strey [4] reported that the alcohol has two major effects: one is to change the effective hydrophilicity of the amphiphilic mixture (C_iE_j + alcohol) and the second one increases the efficiency (or solubilization capacity) of ternary C_iE_j / oil / water system, while at the same time the three-phase region of the microemulsion system is distorted compared to that of the same system without the alcohol [4]. The effect of alcohol at the interface depends on its carbon chain length and Garciaa et al. have shown that long chain alcohols, specifically octanol and higher alcohols, are able to increase the solubilization in surfactant / oil / water systems according to the so-called "lipophilic linker" mechanism [5]. Stubenrauch demonstrated that geraniol could efficiently be used as a *tuning variable* to formulate some temperature-insensitive surfactant microemulsions based on alkylpolyglucoside replacing C_iE_j [6]. In our own experiments, geraniol and pelargol are chosen as typical floral fragrances to illustrate the influence of terpene alcohols on alkane-based and silicone-based microemulsions and emulsions. Octamethylcyclotetrasiloxane (D4) possesses the same EACN value than eicosane, thus a comparison can be done between these oils. In addition, the linear alcohol, octanol (C_8OH) is also studied and compared with 3,7-dimethyloctan-1-ol (pelargol) and 3,7-dimethyl-2,6-octadien-1-ol that are respectively branched and unsaturated branched octanols.

2. Influence of terpene alcohols on the “X” point (T^* , C^*) of C_iE_4 / oil / water systems

2.1. Results

2.1.1. Alkane-based microemulsions

The phase behavior of microemulsion C_8E_4 / dodecane / water and $C_{10}E_4$ / eicosane / water systems was characterized by performing temperature-concentration sections at constant oil / water mass fraction of 0.5. As well, the influence of terpene alcohols on the resulting “fish” temperature and the optimal concentration is also studied. The choice of dodecane and eicosane is justified on the one hand, by the restriction imposed on the temperature range accessible by C_iE_j surfactant, and on the other hand, by the possibility of studying a significant range of fish temperature reduction generated by the alcohol.

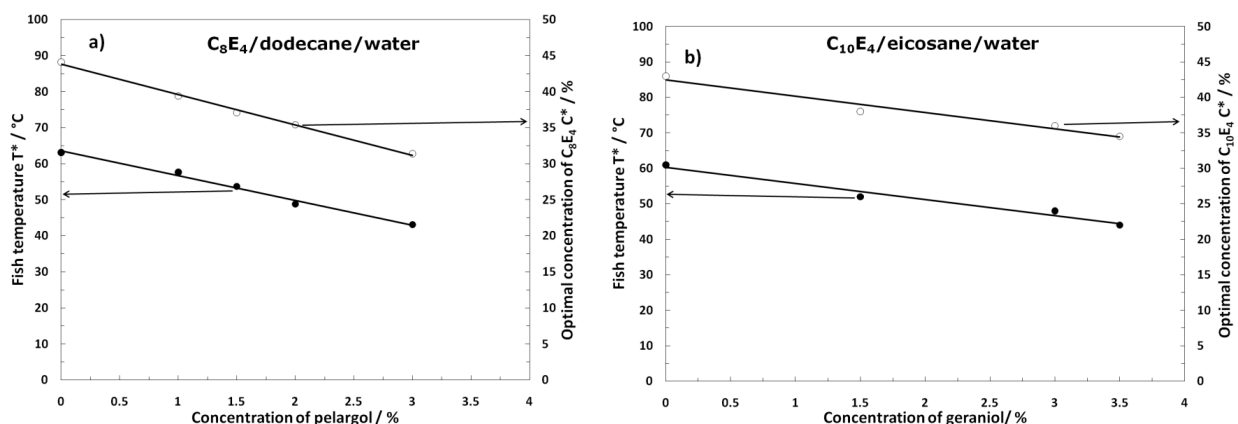


Figure III–2 - Effect of terpene alcohols on the fish temperature T^* (●) and on the optimal concentration C^* (○) for C_8E_4 / dodecane / water / pelargol and $C_{10}E_4$ / eicosane / water / geraniol systems respectively as a function of terpene alcohol concentration – WOR = 1.

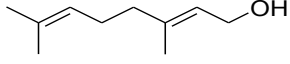
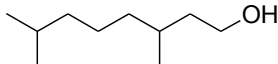
Figure III-2 shows the influence of pelargol (Figure III-2 a) and geraniol (Figure III-2 b) concentrations (horizontal axis), on the “X” point, localized between the body and the tail of the fish diagram, respectively for C_8E_4 / dodecane / water and $C_{10}E_4$ / eicosane / water systems. The fish temperature T^* (left vertical axis) and the optimal concentration of surfactant C_iE_4 , C^* (right vertical axis) linearly varies in the studied interval of terpenoid alcohol concentration. Trend lines have been drawn on both systems for visual guidance. The influence of geraniol on $C_{10}E_4$ / eicosane / water system looks similar to the influence of pelargol on C_8E_4 / dodecane / water system. Both terpene alcohols shift the “X” point to lower values. Only 3% of geraniol decreases the value of the fish temperature for eicosane-based microemulsion by 17 °C and reduces the concentration to achieve a Winsor IV by 7%.

Similarly, for C_8E_4 / dodecane / water microemulsion, at 3% of pelargol, the optimal temperature T^* is lowered by 20 °C as well as C^* by around 13%. These behaviors are explained by the capacity of the alcohols to be solubilized in the oil phase as well as at the interface. It seems that pelargol has a stronger influence on the C_8E_4 / dodecane / water microemulsions than geraniol on the $C_{10}E_4$ / eicosane / water microemulsions as shown in Figure III-2, the slope of the trend line for fish temperature, as a function of pelargol concentration is lower than the one with geraniol.

Obviously, terpene alcohols like medium chain *n*-alkanols play a double role in the quaternary C_iE_4 / alkane / water system as "co-surfactant" and as "co-solvent". As co-surfactants, pelargol and geraniol are preferentially localized in the amphiphilic film, making the co-surfactant mixture (C_8E_4 + pelargol or $C_{10}E_4$ + geraniol) more hydrophobic. In the role of "co-solvent", pelargol and geraniol influence the relative proportions of C_iE_4 in the amphiphilic film due to the higher monomeric solubility of the terpenoid alcohols in *n*-alkane. As a result, the addition of terpene alcohols to the ternary C_iE_4 / alkane / water microemulsion causes the monophasic region to be shifted to lower temperatures. Also on increasing the terpene alcohol concentration, the efficiency of the amphiphilic mixture (C_iE_4 + terpenoids alcohol) increases. This causes an enhancement of solubilization capacity, which is seen from a decrease in the concentration of amphiphile to achieve a Winsor IV. The solubilization of water and *n*-alkane is larger for the surfactant mixture C_iE_4 / terpene alcohol, meaning that there is a strong synergistic effect of the C_iE_4 / terpene alcohol combination. Taking the monomeric solubilities of the amphiphiles into account, the surfactant mixture behaves like a single surfactant of longer chain length. Table III-1 also summarizes the effect of terpene alcohols on the values of "X" points for C_iE_4 / alkane / water as a function of the terpene alcohol concentration.

Figure III-3 summarizes the evolution of the "X" point for C₁₀E₄ / eicosane / water / geraniol and C₈E₄ / dodecane / water / pelargol systems at WOR = 1.

Table III-1 - Effect of terpene alcohols on the "X" points (T*, C*) for C₁₀E₄ / eicosane / water / geraniol and C₈E₄ / dodecane / water / pelargol systems respectively as a function of terpene alcohol concentration.

	C ₁₀ E ₄ /eicosane/water		C ₈ E ₄ /Dodecane/water	
	Geraniol		Pelargol	
Alcohol (%)				
	T* (°C)	C* (%)	T* (°C)	C* (%)
0	61	43	63.1	44.1
1	-	-	57.6	39.4
1.5	52	38	53.7	37.1
2	-	-	48.8	35.4
3	48	36	43.1	31.4
3.5	44	34.5	-	-

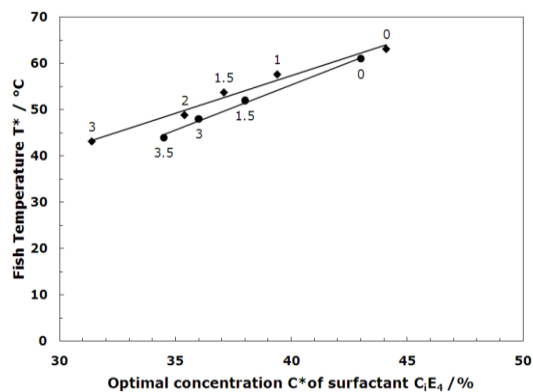


Figure III-3 - Evolution of the "X" points for C₁₀E₄ / eicosane / water / geraniol (●) and C₈E₄ / dodecane / water / pelargol (◆) systems at WOR = 1 - The percentage of alcohol is indicated on the top of the point for pelargol and on the bottom of point for geraniol.

2.1.2. Silicone-Based microemulsions

In this section, octamethylcyclotetrasiloxane (D4) is used as the oil in C₁₀E₄ / D4 / water microemulsion system to study the influence of geraniol on phase behavior. The fish temperature T* and the optimal concentration C* are measured and compared to the same system replacing geraniol by octanol.

Figure III-4 shows the influence of octanol (Figure III-4 a) and geraniol (Figure III-4 b) concentration (horizontal axis) on the "X" point of $C_{10}E_4$ / D4 / water microemulsion system. The fish temperature T^* (left vertical axis) and the optimal concentration of surfactant $C_{10}E_4, C^*$ (right vertical axis) vary also linearly in the same range of alcohol concentration.

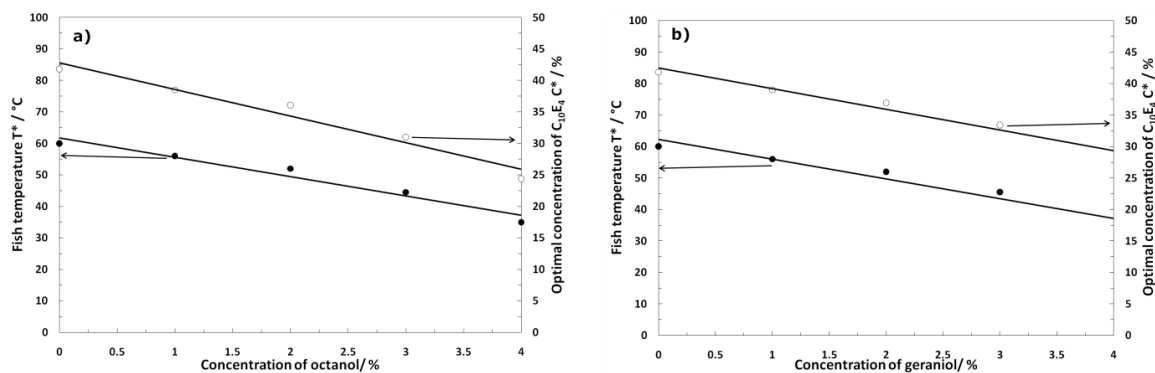
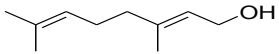
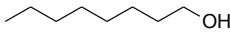


Figure III-4 - Effect of octanol (a) and geraniol (b) on the fish temperature T^* and the optimal concentration C^* for $C_{10}E_4$ / octamethylcyclotetrasiloxane (D4) / water / alcohol systems as a function of alcohol concentration.

The choice of eicosane as oil in $C_{10}E_4$ / eicosane / water system is not due to fortuity. As reported in the literature, Queste et al. determines $T^*_{\text{eicosane}} \approx 59$ °C [7] and Silas et al. found $T^*_{D4} \approx 60$ °C [8] and, in other words $ACN_{\text{eicosane}} \approx EACN_{D4}$. Consequently, despite their different chemical nature, D4 can be compared to eicosane. The value of the "X" point for $C_{10}E_4$ / D4 / water has been reported for the first time in 2001 by Silas [8] and our study leads to similar values with a T^* equal to 60 °C and a C^* equal to 41.8% as reported in Table III-2. This table also reports the effect of geraniol and octanol on the values of the "X" points for $C_{10}E_4$ / D4 / water as a function of the alcohol concentration. In Figure III-4, the addition of octanol and geraniol considerably increases the surfactant efficiency of $C_{10}E_4$ / D4 / water microemulsion while the fish temperature decreases with the same monotony. At 3% of alcohol, the fish temperature of $C_{10}E_4$ / D4 / water microemulsion is close to 45 °C with 25% of temperature decrease whereas the optimal concentration is reduced by almost 20%. It is noticeable that the influence of geraniol is more important by 40% on the silicone-based microemulsion than on the eicosane system, certainly due to the poor solubility of the terpene alcohols in silicone oil and a better transfer at the interface. In the same time, the comparison of the influence of octanol and geraniol on the $C_{10}E_4$ / D4 / water microemulsion reveals that the slope of the trend for 3,7-dimethyl-2,6-octadien-1-ol has the same influence on the fish temperature of the system than octanol itself. However, the difference is coming from the optimal concentration in $C_{10}E_4$, which is slightly smaller for geraniol than for octanol.

Table III-2 - Effect of terpenoid alcohols on the "X" point (T*, C*) for C₁₀E₄ / eicosane / water / geraniol and C₈E₄ / dodecane / water / pelargol systems respectively as a function of terpene alcohol concentration.

C ₁₀ E ₄ /D4/water system				
Geraniol			Octanol	
				
Alcohol (%)	T* (°C)	C* (%)	T* (°C)	C* (%)
0	60	41.8	60	41.8
1	56	39	56	38.5
2	52	36.9	52	36.1
3	45.5	33.4	44.5	31
4			35	24.4

2.2. Discussion

The rationalization of the influence of the terpene alcohols on the phase behavior of C_iE₄ / oil / water systems could be explained by the Winsor Ratio *R*. It is well known that alcohols with carbon chains longer than 4 allow the formation of reverse micelles at lower concentrations than alcohols with shorter chains. This effect can be clarified by the ratio of cohesive energies [9]. The number *R* is the ratio of the net interaction energy of surfactant with oil to the net interaction energy of surfactant with water, both in the presence of alcohol [10].

$$R = \frac{a_o^s - (a_o^s - a_o^a)X_a}{a_w^s - (a_w^s - a_w^a)X_a} \quad (1)$$

where *X_a* is the mole fraction of alcohol in the interfacial region of a micelle. The interaction energies of surfactant and alcohol with oil are respectively *a_o^s* and *a_o^a*. In addition, *a_w^s* and *a_w^a* are respectively the interaction energies of surfactant and alcohol with water. The *R* ratio measures the affinity of the surfactant to solubilize in oil with respect to its affinity to solubilize in water. For *R* < 1, the surfactant solubilizes in aqueous phase and direct micelles are created, for *R* > 1, the surfactant solubilizes in oil phase and reverse micelles are created [10]. Finally for *R* = 1 the surfactant system is balanced and the optimal formulation is achieved which means for a defined quantity of surfactant the system solubilizes the same quantity of oil and water.

For a given surfactant, a_o^s and a_w^s are fixed; in our case, for $C_{10}E_4$, $a_o^s > a_o^a$ because the number of carbon atoms of the surfactant is higher than that of the alcohols.

At the same time, it is assumed that $a_w^s > a_w^a$ since the coulomb interaction is much stronger than molecular interaction. In that case, the effect of geraniol and octanol on R may be estimated; a_w^a is constant because both alcohols possess a single hydroxyl group, which means that only a_o^a has to be taken into account, also a_o^a increases with the size of the alcohol carbon chain. Thus, a smaller quantity of alcohol is required to ensure the $R > 1$ condition if the hydrocarbon chain of an alcohol has a longer alkyl chain. Bourrel et al. [10] reported that the numerator of the right-hand side of equation 1 enlarges with increasing the alcohol chain length then passes through a maximum before decreasing. The author also showed that for a fixed alcohol concentration, the longer the hydrocarbon chain of alcohol, the smaller the water uptake of reverse micelles. Lang et al. [11] also reported that the effect of increasing alcohol chain length on the water uptake for cationic reverse micelles is comparable to that of increasing surfactant chain length [11-12]. In case of branched alcohols, the minimum concentration of alcohol required for the formation of reverse micelles increases in the following order: 1-heptanol < 4-heptanol < 2,4,3-pentanol. Higher concentrations of the more branched alcohols are required to move the surfactant to the oily phase. Since branching decreases the a_o^a value, a larger amount of a branched alcohol is needed to satisfy the condition for reverse micelle formation $R > 1$. Considering the influence of the concentration of pelargol, geraniol and octanol on the different C_iE_4 / oil / water system, the following classification may be suggested octanol > pelargol > geraniol.

3. Influence of terpenoids on the Phase Inversion Temperature of emulsions

Oil-in-water (O/W) emulsions and, to a lesser extent, microemulsions are widely used as solubilization media for a broad variety of substances which are not or sparingly soluble in water, such as cosmetic oils or fragrances. On the other hand, with the growth of waterborne consumer products worldwide, new quality standards are required, especially in terms of long-term stability of these products under extreme temperature conditions. Understanding and predicting the influence of fragrance on the phase behavior of emulsions is consequently a crucial challenge for the formulator. A common feature to all surfactant / oil / water (SOW) systems is the existence of a phase inversion transition, where the (micro) emulsion phase transforms from oil-in-water into water-in-oil system. This transition can be induced by either changing the temperature (nonionic surfactant case) or

salinity (ionic surfactant case). For non-ionic surfactant solutions in water, this transition is usually referred to as “cloud point” [13].

3.1. Correlation between T^* and the PIT of C8E4 / dodecane / water / pelargol system

The accurate determination of T^* requires the construction of the temperature-surfactant concentration two-dimensional phase diagrams under equilibrium conditions. This method is however time consuming, especially at high surfactant concentrations, where the equilibration times may be extremely long. A possible simplification is to rely on the so-called PIT method [14] where the phase inversion temperature is determined by scanning the temperature upwards and downwards at a defined heating (cooling) rate, and measuring the electrical conductivity of the system. With this method, a more or less sudden change of electrical conductivity marks the onset of the phase transition region and the PIT is defined as the temperature at the inflexion point of the conductivity vs. temperature curve (Figure III-5).

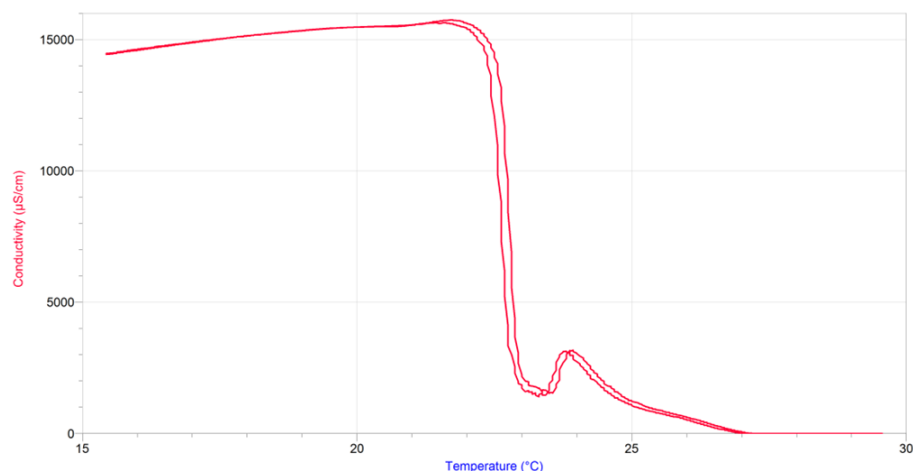


Figure III—5 - Illustration by screen copy of Vernier® software for conductivity vs. temperature of $C_{10}E_4$ / octane / water system at equal volume oil / water and 4% of surfactant

In this perspective, the Brij30, a commercial surfactant characterized by a distribution of the lengths of both alkyl and polyethyleneglycol moieties and the presence of variable amounts of free alcohol has been chosen for PIT study. The choice of such ill-defined surfactant system has been motivated by practical considerations. On one hand, this surfactant is closer to real life systems used in personal care and others industries. On the other hand, it offers a broad experimental operative window for the determination of the PIT. Finally, this system has been thoroughly described in the scientific literature [15-16]

A principal disadvantage of polydispersed commercial surfactant systems is that the fish diagrams in both presence and absence of additives are strongly bended (Figure III-6 b). Therefore, the relationship between the PIT and T^* in this case is not straightforward. On the contrary, for a monodispersed surfactant, the body of the fish is almost symmetrical (Figure III-6 a).

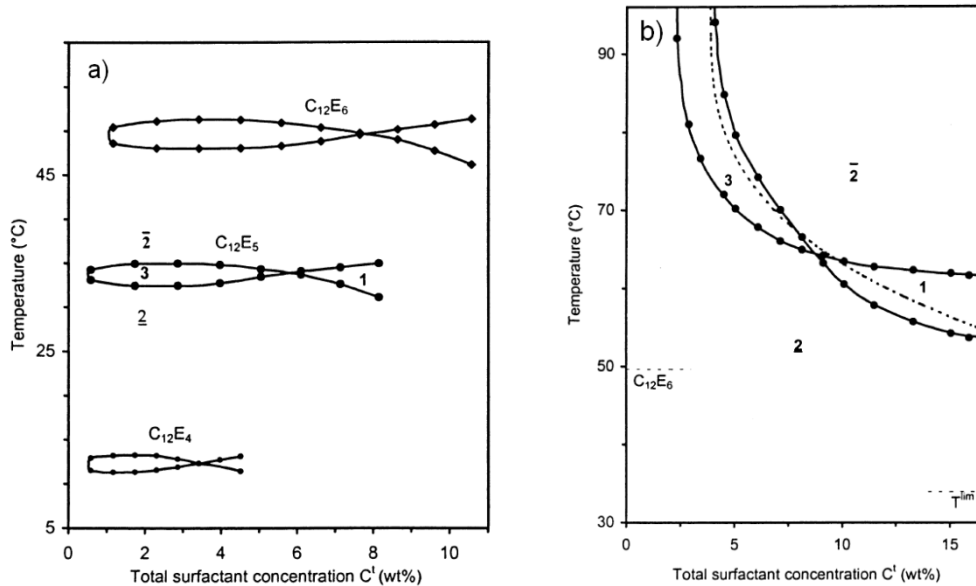


Figure III-6 - Phase behavior of nonionic surfactants / isoctane / water system - Difference between fish diagram of monodispersed (a) and polydispersed (b) surfactants [17].

Ben Ghoulam et al. confirmed that the effect of surfactant partitioning between the excess phases is much stronger at low concentrations, with a substantial accumulation of the most ethoxylated species at the interface. It gives the overall character to the total surfactant system and consequently shifts T_{HLB} to highest temperature values. At high surfactant concentrations, the partitioning effect becomes less marked, and therefore the interface composition tends to behave like the monodispersed surfactant [17].

The determination of the fish diagram for the commercial surfactant Brij30 has been also done with a series of tubes at equal volume of oil and water as shown in Figure III-7. The positions of the different Winsor lead to the determination of the "X point" at $T^* \approx 26.5$ °C and $C^* \approx 5.9\%$. As shown in Figure III-7, the temperature scans for our PIT experiments reported in paragraph 3.2 have been performed at a concentration of Brij30 equal to 6.5% in weight and thus are situated in the Winsor IV region, that is to say just above the critical point of the fish diagram. As stated in Ben Ghoulam's work, this configuration minimizes implicitly the partition of the most ethoxylated species at the interface. In other words, the value of PIT at this concentration can be considered as accurate as T^* .

Under such conditions, only apparent values of a and A parameters in the HLD equation are accessible.

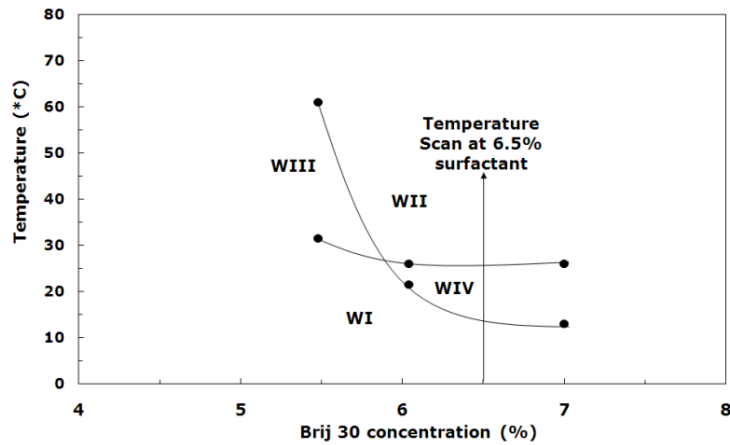


Figure III—7 – Phase behavior of Brij30 / octane / water at equal volume of oil and water

The PIT of the emulsion system is determined from the curve of conductivity as a function of temperature by drawing two straight-lines tangents and parallels. One is located at the highest conductivity value when the conductivity is beginning to decrease and another one at the lowest conductivity value before it goes to zero. Exactly in halfway of these two tangents, a straight-line is drawn and cut the conductivity profile at a defined point. From this defined point, a perpendicular line with the temperature axis is drawn until reach the PIT value. This method is named the tangent parallel method (see experimental part at the end of chapter III for more details). Figure III-8 shows the conductivity of Brij30 / octane / water system for a concentration of 6.5% wt of surfactant as a function of the temperature. The PIT is around 21 °C, which is consistent with the results determinate from the fish diagram shown in Figure III-7.

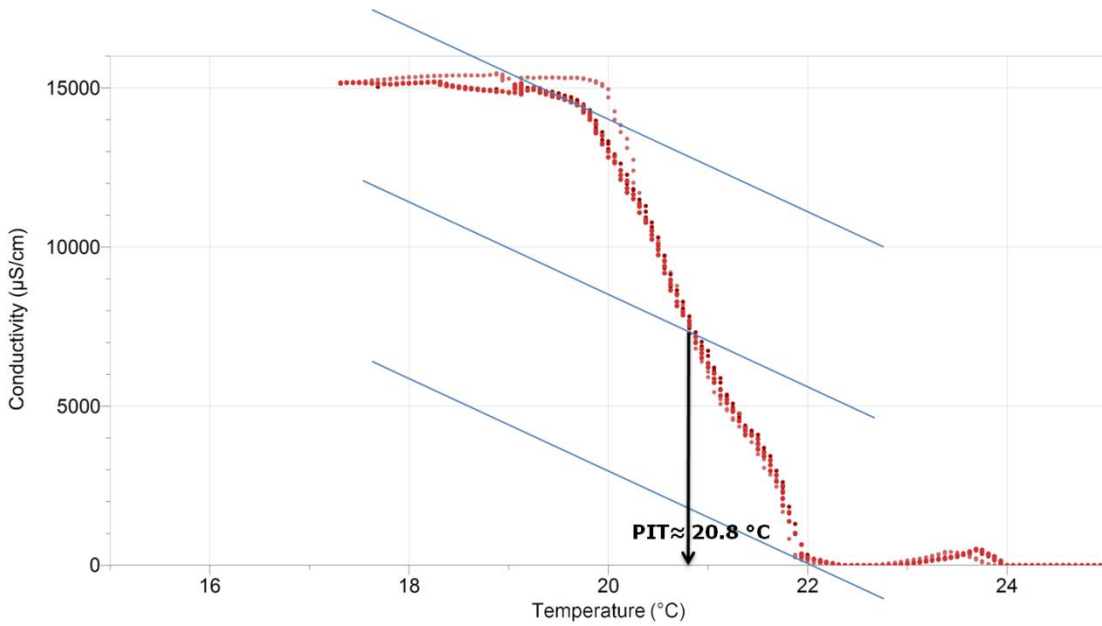


Figure III—8 Conductivity as a function of the temperature of Brij30 / octane / water system at equal volume oil / water and 6.5% of surfactant

The relation between the fish temperature for a C_8E_4 / dodecane / water / pelargol system (ratio oil/water in weight equal to 1) at equilibrium and the PIT of the agitated C_8E_4 / dodecane / water / pelargol emulsion (ratio oil/water in weight equal to 1 and concentration in C_8E_4 fixed to 20%) is shown in Figure III-9 as function of the concentration of pelargol. There is a linear relationship between PIT and T^* in the range from 0 to 2.5% of pelargol. It has to be noticed that this range of alcohol concentration is in line with fragrance creation.

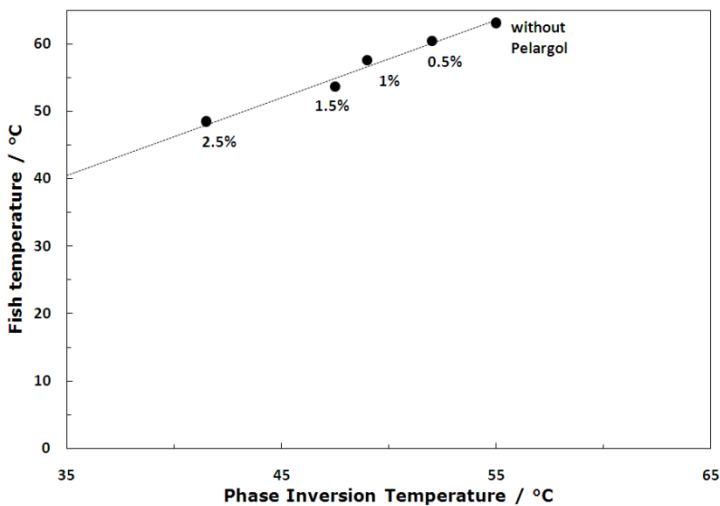
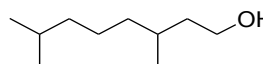


Figure III—9 - Correlation between Fish temperature T^* of C_8E_4 / dodecane / water / pelargol and Phase inversion temperature PIT for the system C_8E_4 / dodecane / water / pelargol at fixed concentration of C_8E_4 equal to 20% as a function of the concentration of pelargol.

Table III-3 summarized the values of T^* for the microemulsion system and PIT of the emulsion system.

Table III-3 - Effect of pelargol on the fish temperatures T^* and PIT (20% C_8E_4) for C_8E_4 / dodecane / water / pelargol systems

C_8E_4/Dodecane/water system		
Pelargol		
		
Alcohol (%)	PIT (°C)	T^* (°C)
0	55	63.1
0.5	52	60.4
1	49	57.6
1.5	47.5	53.7
2.5	41.5	48.5

The influence of the concentration of a well-defined surfactant C_8E_4 on the PIT of C_8E_4 / dodecane / water / pelargol system as a function of pelargol concentration has been checked for two concentrations: 10% and 20% in weight, the data are represented in Figure III-10. The increase of surfactant concentration tends to increase the PIT temperature of the system and nonlinearity is revealed for lower surfactant concentration. A tentative of explanation of this phenomenon can be done by putting in parallel our results with the recent work done by Pizzino [18] in 2008. In fact, Pizzino explains, in the case of $C_{10}E_4$ / octane / water system, at 1% and 3% of surfactant concentration ($C^* = 10.5\%$ in that case), the relation between the phase diagram at equilibrium and the standard inversion line in the corresponding composition-formulation map is directly linked to the “three phase” area (WIII). Also the slope of this line is a function of the surfactant concentration. At low concentration, this line is more curved than at higher concentration. The curvature is linked to the partitioning of the surfactant between oily and water phase even for a monodisperse surfactant [18]. In our case, the value of C^* for C_8E_4 / dodecane / water system is 44.1%. Our experimental concentrations are situated under the C^* value. Thus, the higher PIT value for a concentration of 20% of C_8E_4 surfactant and consequently closer value to T^* is consistent with the results of Pizzino.

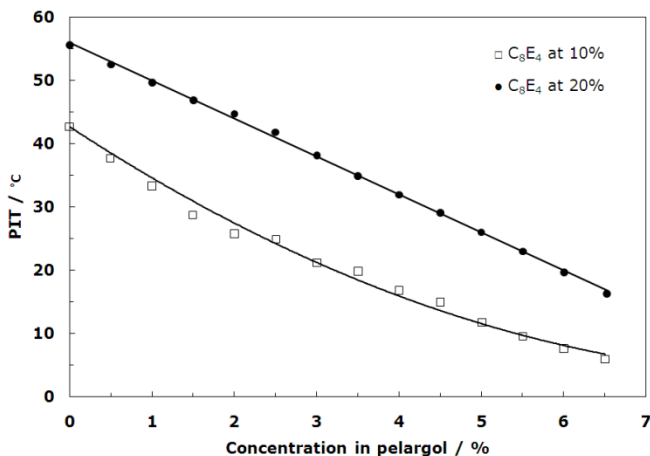


Figure III-10 - Influence of concentration of surfactant on the value of the PIT for C₈E₄ / dodecane / water / pelargol

3.2. Alkane-based emulsions

3.2.1. Influence of *n*-alcohols on the PIT of the Brij30 / octane / water system

For polyethoxylated nonionic surfactant systems, an increase of temperature tends to reduce the hydrophilicity of the polar group, and for that reason, the surfactant becomes less hydrophilic which will cause the emulsion inversion from O / W to W / O morphology at the so-called phase inversion temperature PIT [14]. The Brij30 / octane / water system itself has a phase inversion temperature, which varies from batch to batch. In this study, two batches are used and they have a PIT of 20 °C and 31 °C, respectively. The initial slope of the PIT vs. alcohol concentrations for different *n*-alcohols in Brij30 / octane / water are reported in Table III-4 and for 4 of them, the complete curves are shown in Figure III-11. Water-soluble alcohols such as methanol and ethanol slightly increase the PIT. A significant decrease of PIT is detected with the addition of propanol. Increasing further the chain length of the alcohol from C₄ to C₈ leads to an additional decrease of the PIT. Nonanol and higher alcohols still depress the PIT, but to a lesser extent than octanol which seems to have the largest effect among the aliphatic alcohol series (see also the white circles in Figure III-11, below). These results are in line with the literature [19-21].

Table III-4 - Effect of different alcohols on the PIT of the Brij30 / Octane / Water system = 6.5 / 46.7 / 46.7 w/w. The slopes value $\partial\text{PIT} / \partial[\text{alcohol}]$, expressed in °C / %, of the tangent of the curves shown on Figure III-11, at a concentration equal to zero, are specified in the second row of the table.

Alcohol	C ₁	C ₂	C ₃	C ₄	C ₅	C ₆	C ₇	C ₈	C ₉	C ₁₀	C ₁₂	C ₁₄	C ₁₆
$\partial\text{PIT} / \partial[\text{alcohol}]$ (°C / %)	0.6	0.5	-1.3	-4	-11.9	-15.4	-16.4	-17.3	-16.3	-15.1	-14.3	-13.8	-13.6

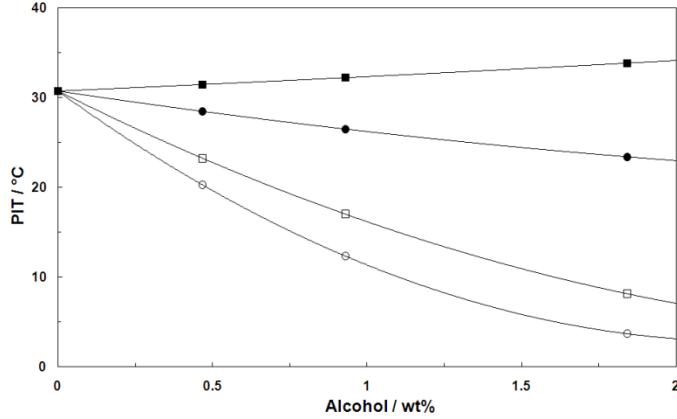


Figure III-11 - Evolution of the PIT (°C) for the system Brij30 / octane / water / alcohol as a function of the Alcohol concentration (wt. %): ethanol (■) butanol (●) hexanol (□) octanol (○) (for the sake of simplicity 4 alcohols only are represented)

The slope $\partial\text{PIT}/\partial[\text{alcohol}]$ represents the ability for aliphatic alcohol to alter phase inversion temperature, a positive slope expresses an increase of PIT whereas a negative one indicates a decrease. According to the HLD theory and assuming a linear relationship between the PIT and the fish temperature T^* , the magnitude of the slope is proportional to the complex term $a.A$ in equation (2). It is well known that linear alcohols participate in the formation of the interfacial film and, consequently, modify both its rigidity and spontaneous curvature [22]. Short chain alcohols C_1 and C_2 slightly increase the hydrophilicity of the interfacial film whereas C_5 alcohols and higher Alcohol Carbon Number [23] will have the opposite effect. This effect is well measured by the $a.A$ function, which has an initial positive slope for the hydrophilic alcohols and negative slope for the lipophilic ones. At low alcohol concentrations, it can be approximately expressed as a linear function of the alcohol concentration with a proportionality coefficient that increases with the Alcohol Carbon Number [24-25].

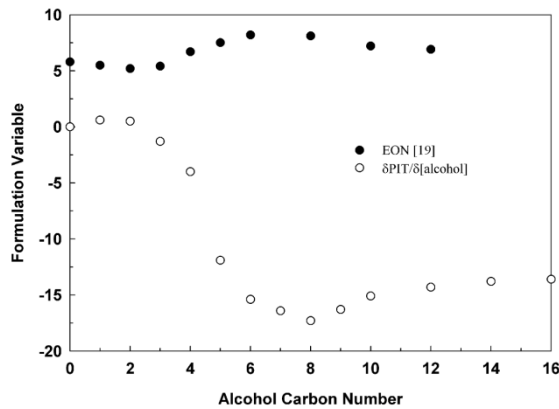


Figure III-12 - Influence of Alcohol Carbon Number on the slope value $\partial\text{PIT} / \partial[\text{alcohol}]$ for the system Brij30 / octane / water and EON value (see text) for the system ethoxylated nonylphenol / octane / water [19].

Bourrel and Salager [19-26] have previously published the influence of linear alcohols on optimum position for phase diagram formulated with ethoxylated nonylphenol, isooctane and water. For each alcohol, the formulation scan is carried out by varying the EON (Ethylene Oxide Number) of the surfactant, so that, at the fish-tail point, the effect of the alcohol type (i.e. the number of carbon atoms) is counterbalanced by the surfactant EON. The location of this point and its change from one case to the next provide information on the formulation change in the abscissa and the solubilization change in the ordinate as seen on Figure III-13. Since the composition of the total system remains constant (oil, water and temperature), the interfacial film composed by surfactant + alcohol is constant, only a change in surfactant EON compensates for the effect of the change in alcohol in the opposite way. Consequently, a shift to a lower or higher EON is observed. If a more lipophilic surfactant is required to bring the system to the optimum, this means that the alcohol contribution is hydrophilic. In contrast, an increase in surfactant + alcohol at the fish-tail point denotes a decrease in solubilization; more surfactant is required to achieve the WIV microemulsion in which all of the oil and water are solubilized. Figure III-13 shows that as the Alcohol Carbon Number increases, the following changes take place in four successive stages, which are denoted by (a) to (d) and identified by arrows in Figure III-13.

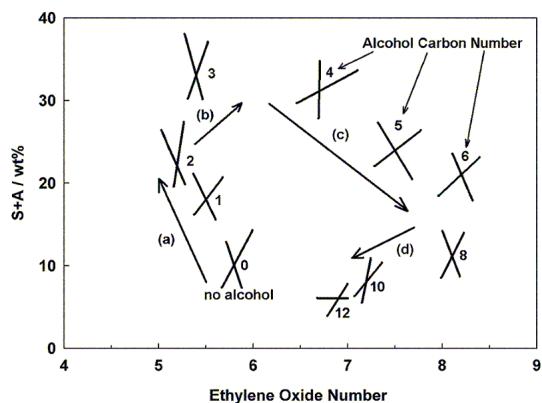


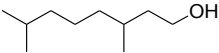
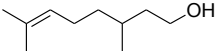
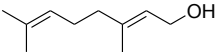
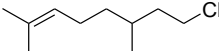
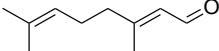
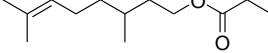
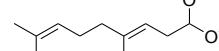
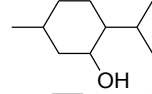
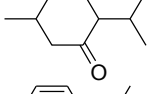
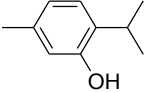
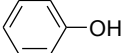
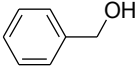
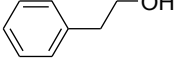
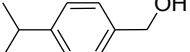
Figure III-13 - "X" point position in the amphiphile concentration/formulation map as a function of the length of the *n*-alcohol co-surfactant. The effect of alcohol is compensated for by changing the degree of ethoxylation (EON, ethylene oxide number) of the nonionic surfactant extracted from [4,26]

As apparent from the data points in Figure III-12, which show a clear correlation between the EON and $\partial\text{PIT} / \partial[\text{alcohol}]$ vs. Alcohol Carbon Number behaviors, similar conclusions can be drawn as for the effect of the hydrophilicity (respectively hydrophobicity) of the alcohols on a.A.

3.2.2. Influence of fragrances on the PIT of the Brij30 / octane / water system

As for aliphatic alcohol, the effect of various functionalized fragrances (entries **1** to **14**) on the PIT of the Brij30 / octane / water system was determined as a function of the fragrance concentration. Fragrance molecules have been chosen for their structural and chemical diversity, as well as their perfumery interest. Chemical structures, values of the slopes at a concentration equal to zero for the studied molecules are reported in Table III-5 and variation of the PIT values as a function of the fragrance concentration are shown in Figures III-14 and III-15.

Table III-5 - Influence of different fragrance molecules on the PIT (°C) of the Brij30 / Octane / Water system = 6.5 / 46.7 / 46.7 w / w. The slope values $\partial\text{PIT} / \partial[\text{fragrance}]$, expressed in °C / %, of the tangent to the curves shown on Figures III-14 and -15, at a concentration equal to zero.

Entries	Fragrance	Chemical Structure	$\partial\text{PIT} / \partial[\text{fragrance}]$ (°C/%)
1	Pelargol		-20.1
2	Citronellol		-19.7
3	Geraniol		-25.4
4	Citronellyl nitrile		-13.1
5	Citral		-2.9
6	Citronellyl propionate		1.2
7	Citral dimethyl Acetal		3.2
8	Menthol		-4.2
9	Menthone		0.3
10	Thymol		-4.2
11	Phenol		-11.6
12	Benzyl alcohol		-13.1
13	Phenylethyl alcohol		-15.2
14	Cuminic alcohol		-6.5

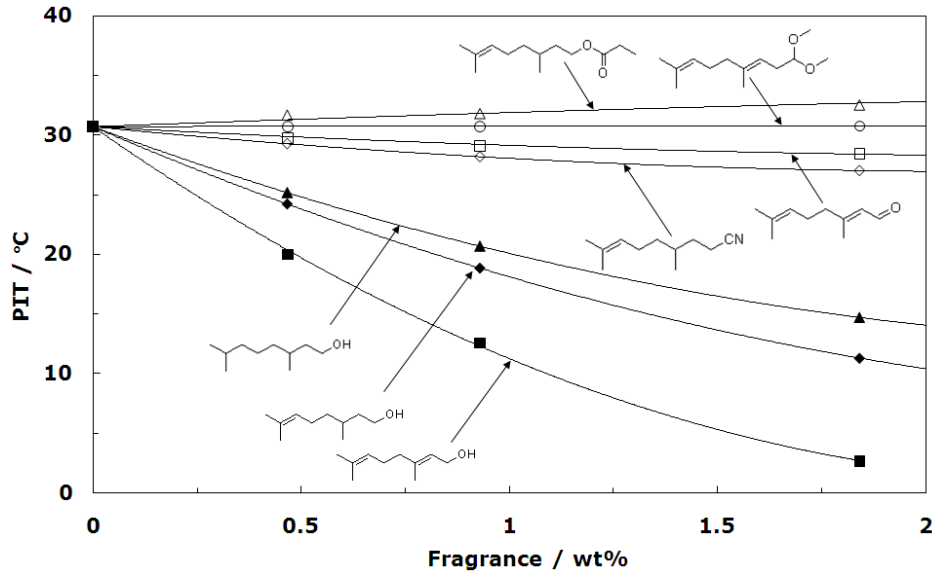


Figure III-14 - Evolution of the PIT (°C) for the Brij30 / octane / water / fragrance systems as a function of fragrance concentration (wt.%) geraniol(■) citronellol(◆) pelargol(▲) citronellyl nitrile(◇) citral(□) citral dimethyl acetal(○) citronellyl propionate(△)

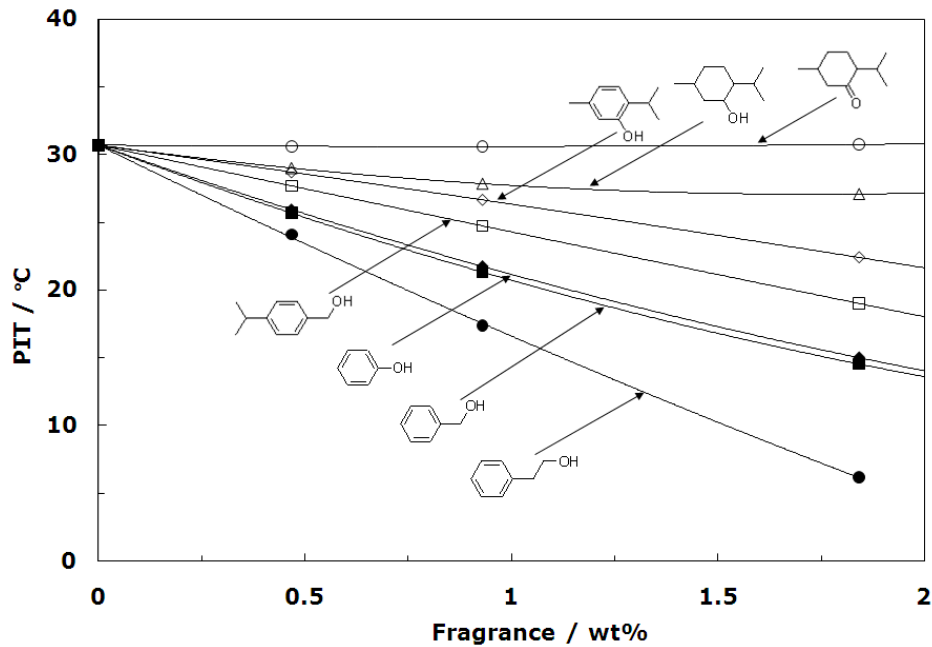


Figure III-15 - Evolution of the PIT (°C) for the Brij30 / octane / water / fragrance systems as a function of fragrance concentration (wt.%) menthone (○) menthol(△) thymol (◇) cuminic alcohol (□) phenol (◆) benzyl alcohol(■) phenylethyl alcohol(●).

Among fragrance compounds, alcohols and phenols appear to have the strongest impact on PIT as illustrated in Figures III-14 and 15. The effect of substituting the hydroxyl function by other polar chemical functions can be inferred from the analysis of the behavior of citronellyl nitrile **4** and citronellyl propionate **6**. The effect of ester function is fully counterbalanced by the aliphatic character of the citronellyl backbone, which results in minimal impact on the PIT for all the fragrance concentrations investigated. The comparison between citronellyl nitrile and citronellol **2** provides some information on the relative contribution of polarity and hydrogen bonding to PIT depression. The highly polar (aprotic) nitrile function has a much lower impact than the less polar (protic) hydroxyl function (for comparison the dipole moment of propionitrile and 1-propanol in the gas phase are 4.02 Debye and 1.68 Debye, respectively) [27]. This confirms the view that hydrogen donor/acceptor capability of the terminal group is the major factor influencing the interaction of the additive with the surfactant at the oil/water interface and, thereby, the value of $a.A$ of the HLD equation. In fact, Salager et al. [32] suggested an empirical correlation known as the hydrophilic-lipophilic deviation (HLD) as a dimensionless form of the thermodynamically derived surfactant affinity difference (SAD) equation to describe microemulsion systems. Similar to the Winsor R-ratio, the HLD value measures the deviation from the optimum formulation, however the parameters are easier to quantify. Negative, zero, or positive HLD values correspond to the formation of Winsor Type I, Type III or Type II microemulsions, respectively. HLD equation for nonionic surfactants is described as follows [32]:

$$\text{HLD} = (\alpha - \text{EON}) + bS - k\text{ACN} + aA + t \Delta T \quad (2)$$

where ACN is the alkane carbon number of the *n*-alkane; EON is the ethylene oxide number of the nonionic surfactant; S and b are respectively salt concentration and a constant characteristic of the type of salt, $a.A$ are two characteristic parameters linked to the nature, type and behavior of alcohols as a function of its concentration; A, α and k are constants for a given type of surfactant, t is a temperature coefficient, ΔT is the temperature deviation from 25 °C.

The aldehyde and acetal function respectively represented by citral **5** (geranial) and citral dimethyl acetal **7** also have a limited effect on the PIT in comparison to the parent geraniol **3**. The marked decrease of the PIT in the series pelargol **1**, citronellol **2** and geraniol at high alcohol concentration can be related to the introduction of double bonds in the backbone of

the molecules, which increase both the polarizability and the rigidity of the molecule, making it more suitable for packing within the surfactant palisade.

The behavior of cyclic alcohols is shown in Figure III-15. The evolution of $a.A$ within this series suggests that steric hindrance of the hydroxyl group plays a significant role. Hence, both menthol **8**, thymol **10** are significantly less active than cuminic alcohol **14**, which is in line with the H-bond building capability of sterically hindered hydroxyl functions [28]. Remarkably, the effect of steric hindrance dominates the effect of aromaticity in this case. The behaviors of phenol **11**, benzyl alcohol **12** and phenyl ethyl alcohol **13** are surprising, however. Phenol and benzyl alcohol are soluble in water and should therefore interact preferably with the polar head groups of the surfactant and show a positive or at least neutral effect on PIT. Furthermore, the depression of the PIT induced by phenyl ethyl alcohol is more pronounced than that observed by Tchakalova et al. using $C_{10}E_5$ as surfactant [29]. Here again, as stressed by these authors, one could expect that phenyl ethyl alcohol interacts with the polar head groups from the surfactant layer and is not embedded in the surfactant palisade. Our data show that, in the contrary, the effect of phenyl ethyl alcohol is as large as that of hexanol, a very efficient co-surfactant $\partial PIT / \partial[\text{hexanol}] = -15.4 \approx \partial PIT / \partial[\text{phenylethyl alcohol}] = -15.2$. On the other hand, we demonstrate that inserting a second and third carbon atom between the hydroxyl group and the aromatic ring has a remarkable effect on $a.A$ since the value of $\partial PIT / \partial[\text{phenol}] = -11.6 > \partial PIT / \partial[\text{benzyl alcohol}] = -13.1 > \partial PIT / \partial[\text{phenylethyl alcohol}] = -15.2$.

Table III-6 summarizes in a qualitative point of view, the experimental result of the influence of a structural backbone or a chemical function modification of a molecule on the PIT variation in the Brij30 / octane / water / fragrance system

Table III-6 - Influence of structural and chemical function change on the PIT variation

Entries	Structural/Function modification	ΔPIT
C₁ to C₈	increasing alcohol carbon chain with a maximum at C ₈	↘
1 => 2 => 3	nb. of saturations in the alcohol carbon chain	↘↘
2 => 4 ; 5 => 7 2 => 6 ; 3 => 5	from primary alcohol to nitrile/acetal/aldehyde/ester	↗
8 => 9	secondary alcohol to ketone	↗
11 => 10	phenol to branched phenol	↗
11 => 12 => 13	distance of hydroxy group from phenyl ring	↘

3.3. Silicone-based emulsions

The influence of three terpenes and two terpene alcohol molecules on the PIT value for emulsions made of Brij30 / silicone / water is studied as a function of the molar fraction of fragrance in silicone. The choice of using molar fraction of fragrance in silicone instead of percentage has been driven by a lower impact of fragrance on the system and the higher molecular weight of silicone oils versus octane. Polydimethylsiloxane (PDMS), hexamethyldisiloxane (HMDS) and decamethylcyclopentasiloxane (D5) as shown in Figure III-16-left are used as oils in these PIT experiments. The choice of one polymeric (C₁₂H₄₂Si₅O₄), one cyclic and one linear siloxane is motivated by, on one hand, the need to evaluate the polymerization and cyclization impact on the PIT values. On the other hand, these three silicones are frequently used to formulate cosmetic emulsions, as they possess an excellent spreading property on hair or skin. HMDS and D5 are also good solvents for many hydrophobic active ingredients including fragrances. Finally, they are common substitutes for ethanol when low Volatile Organic Compound (VOC) products are requested. Fragrances have been selected based on one hand, for terpenes, their structure as shown in Figure III-16 middle and the value of their EACN [30], on the other hand, for two terpene alcohols as shown in Figure-III-16 right, their higher capacity to decrease the PIT of the system Brij30 / octane / water.

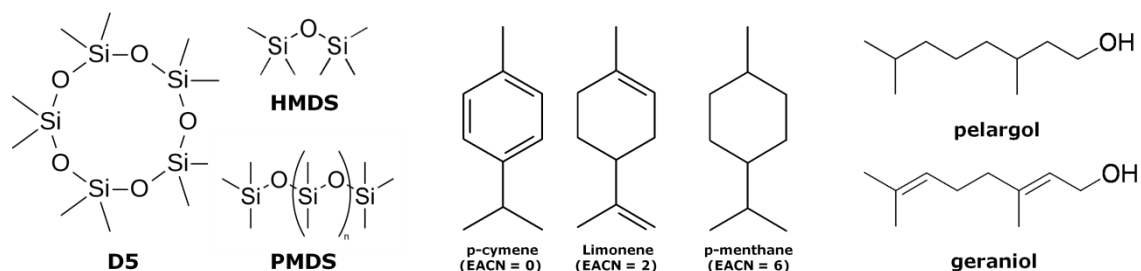


Figure III-16 – Chemical structure of the different oils (D5, HMDS and PDMS), terpenes (p-cymene, limonene, p-menthane) and terpene alcohols used in Brij30 / silicone / water / fragrance systems

In order to evaluate the appropriate quantity of Brij30 needed to perform our PIT experiments with the silicones as oil, the determination of the PIT as a function of Brij30 concentration has been completed and the PIT values are summarized in Figure III-17. HMDS has been selected to carry out this trial taking into account his hypothetical EACN value, which is probably lower than the one of D5. The Brij30 / HMDS / water system PIT value decreases quickly with increasing concentration of surfactant. At 5% surfactant concentration, PIT value of the system is equal to 45.5 °C, and fall down to 20 °C only by increasing surfactant concentration up to 20%. In fact, in order to maintain an accessible range of experimental temperature taking into account the capacity of terpene alcohols to lower the PIT value, as well to limit the quantity of surfactant involved, a 10% concentration of Brij30 is consequently used for the PIT experiments.

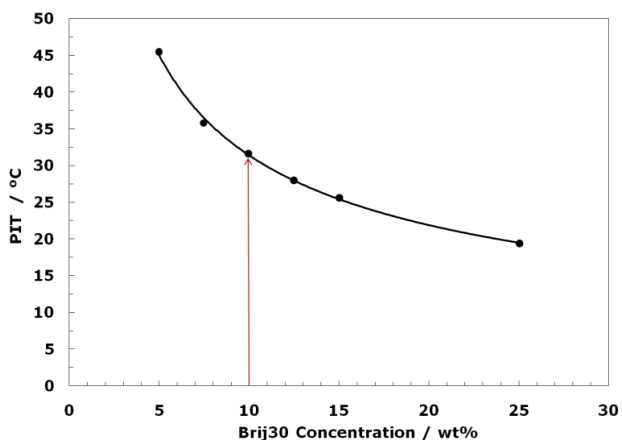


Figure III-17 – Evolution of the PIT for Brij30 / HMDS / water system as a function of the concentration of Brij30

The influence of fragrance molecules on the PIT value for emulsions made of Brij30 / silicone / water with silicone = "HMDS", "D5" and "PDMS" are studied as a function of the molar fraction of fragrance in silicone and their experimental value are reported respectively in Figures III-17, III-18 and III-19.

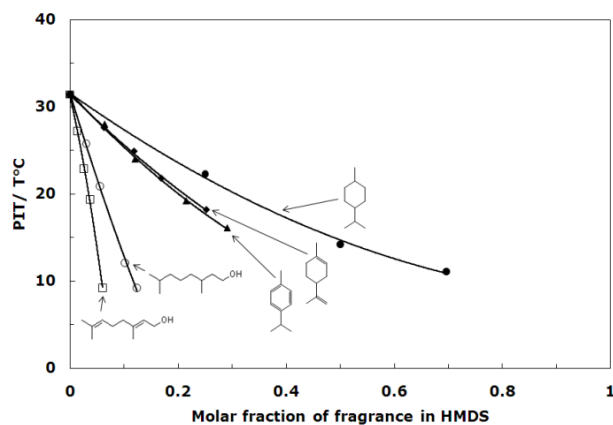


Figure III-18 - Evolution of the PIT (°C) for the Brij30 / HMDS / water / fragrance systems as a function of the molar fraction of fragrance in silicone geraniol (□) pelargol (○) p-cymene (▲) limonene (◆) p-menthane (●).

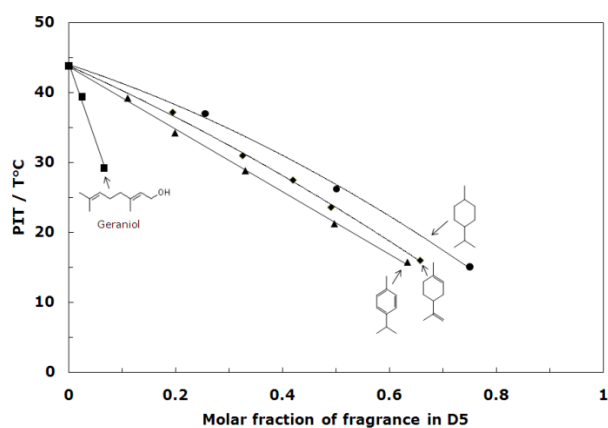


Figure III-19 - Evolution of the PIT (°C) for the Brij30 / D5 / water / fragrance systems as a function of the molar fraction of fragrance in silicone geraniol (■) p-cymene (▲) limonene (◆) p-menthane (●).

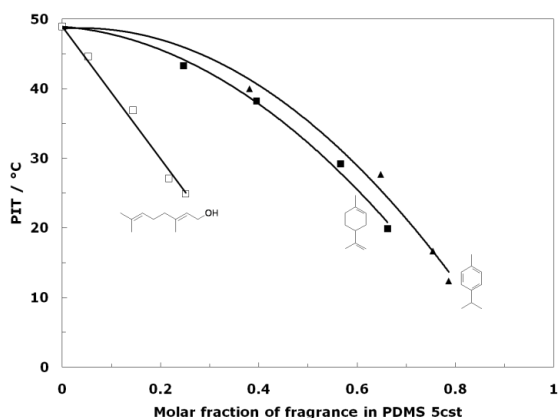


Figure III-20 - Evolution of the PIT (°C) for the Brij30 / PDMS 5cst / water / fragrance systems as a function of the molar fraction of fragrance in silicone geraniol (□) limonene (■) p-cymene (▲).

As shown in Figures III-17, III-18 and III-19, the terpene alcohols bring the highest effect on the PIT for the three systems compared to terpenes. In addition, geraniol has the strongest influence on PIT comparing to pelargol in the case of Brij30 / HMDS / water system and the general appearance of the curves is similar too. This is in line with our previous results for Brij30 / octane / water system. Geraniol has the strongest impact on PIT for emulsion formulated with the silicones that have the lowest molecular weight. For instance, the PIT deviation at fraction molar equal to 0.05 is around 18 °C for HMDS-based system, 7 °C for D5-based system and 3 °C for PDMS-based system.

Terpenes have a lower impact on PIT as illustrated in Figures III-17, III-18 and III-19. Molar fraction of terpenes required, to reach the same lowering of the "PIT" that for terpenes alcohols, have to be multiplied at least by a factor of 5. For a low molecular weight HMDS-based system, p-menthane and limonene have almost the same effect, remarkably the influence of terpenes on the system follow the progression of terpenes EACN. The impact rank is as follow: p-cymene > limonene > p-menthane. It is interesting to observe again the role of silicone molecular weight for this classification. For a large molecule like PDMS, the influence on PIT seems to be softened, and for a lower molecular weight like HMDS, EACN values of fragrance have a stronger effect. One interpretation of this phenomenon is that terpene fragrances can almost completely segregate at the interface and replace the silicone oil thus reduce the apparent EACN value of the oily phase and consequently decrease the PIT value of the system. This observation is interesting for the cosmetic formulator as silicone oils are often used as a carrier for hydrophobic active ingredients, thus fragrance terpenes may be used to create room temperature emulsion or simply to dilute high molecular weight PDMS and facilitate their emulsification. It is worth to be noticed that for Brij30 / HMDS / water system at molar fraction of p-menthane equal to 0.7, the system is very viscous which means that the system organizes in liquid crystal probably rod-like micelles.

4. Emulsion stability

The use of fragrance in personal care products has two main objectives: makes them more attractive for the consumers while giving a more pleasant character to the products. The preparation of formulated products and particularly emulsion such as lotion and cream frequently remains a challenge for the formulator. Their formulas are often established empirically and their stability issues are often minimized by a great deal of trials. Besides, the formulator commonly considers the fragrance as an additive introduced at the last stage of the product development, on top of a ready-to-use formula. A better understanding of the stabilization / destabilization phenomena is consequently crucial for the personal care industry and it becomes progressively important to rationalize the influence of perfume on the stability of emulsions.

On the other hand, the studies carried out on emulsion breaking in the industry are based on a series of empirical trials, which consist by imposing to the products several temperature cycles: oven 40 °C / 50 °C followed by room or fridge temperature (4 °C). The tests are also carried out under the light of artificial xenon lamp for a few hours to simulate a sun exposure. After that, some observations are then done only on the organoleptic aspect of the product (odor, visual characteristic, consistency) some pH measurement are done too, but are in general never quantified. This process is efficient although time consuming. New techniques based on suitable apparatus make it possible to follow more precisely the ageing of emulsions, where the human eye reaches its limit, and do not distinguish enough the sedimentation phenomena. In addition, our goal is to explore here the possibility of a rigorous follow-up of the stability of the emulsions, then its application to the study of the influence of fragrance raw materials on it.

4.1. Composition-formulation maps

In this study, the Brij 30 / octane / water system is used as an example of industrial emulsion. The fragrance studied is geraniol, since this molecule affects the most the emulsions, with a considerable decrease of the PIT, as the addition of less than 2% of perfume in emulsion lead to a fall of almost 30 °C of the PIT. In order to study the effects of addition of perfume on the stability of this emulsion, several systems have to be formulated, each incorporating a rather small quantity of fragrance since the composition aims to approach an industrial formulation, which seldom exceed 2% of fragrance for the same composition in terms of water, oil and surfactant.

The main phenomenon for emulsions destabilization is the coalescence of the droplets, which can lead to two different results: creaming or sedimentation. The two phenomena are separately studied with different formulations. At the beginning of the destabilization, the kinetics of droplet coalescence can be identified in the middle of the sample after that, the kinetics of creaming or sedimentation of the sample can be studied at the top or the bottom of the sample. In order to characterize precisely our system, the traditional descriptors are used as the PIT described by Shinoda [14] and the composition-formulation map described by Salager [31].

The PIT for the system Brij30 / octane / water (O/W ratio equal to 1 in volume, surfactant concentration 6.5%) have been determined following the same method as section 3, however the quality of the surfactant batch used for this experiment was different, thus the PIT value is found at 37.4 °C. As previously observed, the impact of 1.5% of geraniol in weight let the PIT value reduced to 12.5 °C, which means that despite the batch difference, the influence on PIT is consistent with the results found in section 3, as the value of the PIT starts from 30.7 °C without geraniol to go 5.3 °C with 1.5% of geraniol.

Salager et al.[31] present a bi-dimensional map, shown in Figure III-21 that is divided into six regions by the optimal formulation (HLD = 0) line and the inversion line. For positive HLD value, phase behavior at equilibrium is type WII and according to Bancroft's rule a W / O emulsion is expected. This is true in regions B⁺ and A⁺, however, in the region C⁺ an "abnormal" O / W emulsion is produced because the volume of oil is too small to make it the continuous phase. The "Abnormal" C⁺ emulsions are often w / O / W type, which is a way in which Bancroft's rule is partially satisfied. For negative values of HLD, the SOW phase behavior is type WI. A⁻ and C⁻ are O / W emulsion regions and B⁻ is an "abnormal" W / O emulsion region, the B⁻ regions are often o / W / O type.

Emulsion stability is closely related to the region boundaries; normal A⁺, B⁺ (W / O emulsions) and A⁻, C⁻ (O / W emulsions) regions are found to be quite stable, with increasing stability (at constant HLD) approaching the A⁺ / C⁺ or A⁻ / B⁻ limit, i.e. with increasing disperse phase fraction. Stability decreases from both sides as the A⁺ / A⁻ boundary is approached, i.e. near the three phase region. It is found that abnormal (B⁻, C⁺) emulsions break readily [31].

The viscosity of emulsions in the A⁺, A⁻ regions far from HLD = 0 can be high with respect to their external phase. However, close to HLD = 0 the emulsion viscosity can be extremely low, probably because of the low interfacial tension, which allows easy deformation of the

droplets near the A^+ / A^- boundary. Abnormal emulsions have low internal phase ratio and exhibit viscosities similar to their external phase. However, real systems can show large deviations in the schematic composition-formulation map.

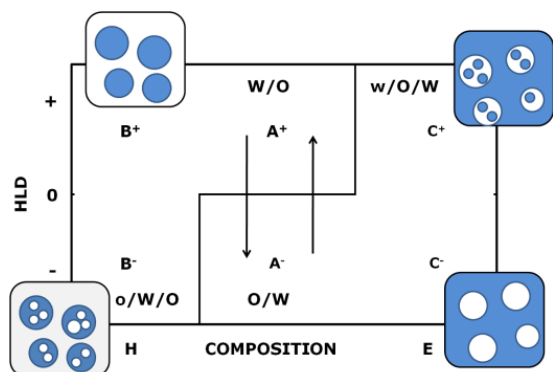
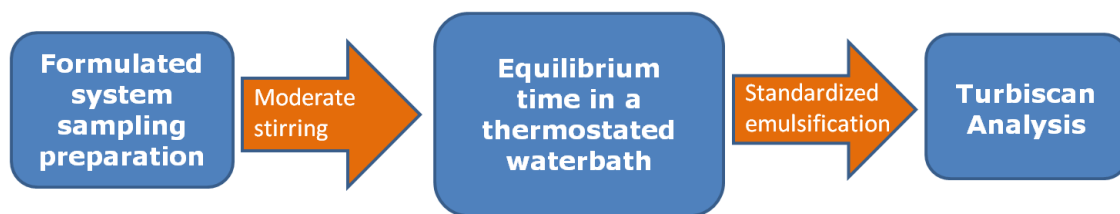


Figure III–21 –Bi-dimensional map composition-formulation adapted from [31-32]

Schematic composition-formulation map for Brij30 / octane / water system

In order to ensure the experiments reproducibility, a standardized emulsification procedure (see Scheme III-1) is established and applied for each trial. The temperature of the formulated systems is controlled by immersion in a thermostated water bath and an equilibrium time before being agitated is applied. Ultraturrax is used to stir the sample at constant speed during a definite time. Scheme III-1 summarized the emulsification process in a schematic version.



Scheme III-1 - Schematic description of emulsion sample preparation

Each tube is prepared following this protocol either for Turbiscan[®] measurements as results shown later or for conductivity measurements at different WOR from 0.1 to 0.9 to build the composition-formulation map as shown in Table III-7. For a W / O system, the electrical conductivity is zero otherwise the system is O / W and a conductivity signal is detected and measured. Each measurement is reported in Table III-7.

This process provides the phase inversion limit and allows drawing the standard inversion line as shown in Figure III-22. Vertical branches of the inversion line have not been determined in these cases.

Table III-7- Value of the conductivity as a function of temperature for Brij30 / octane / water system

WOR T [°C]	0,1	0,2	0,3	0,4	0,5	0,6	0,7	0,8	0,9
59,4	0	0	0	0	0	0	0	0	0
58,8	0,015	0	0	0	0	0	0	0	0
56,8	0,04	0	0	0	0	0	0	0	0
53,7	0,08	0	0	0	0	0	0	0	0
52,3	0	0,085	0	0	0	0	0	0	0
50,4	0	0,105	0	0	0	0	0	0	0
48,9	0	0,185	0	0	0	0	0	0	0
44,7	0	0,21	0,18	0	0	0	0	0	0
41,9	0	0,205	0,29	0,125	0	0	0	0	0
37,9	0	0	0,245	0,325	0	0	0	0	0
36,9	0	0	0,235	0,365	0,101	0	0	0	0
35	0	0	0,245	0,335	0,05	0	0	0	0
32,1	0	0	0,215	0,3	0,39	0	0	0	0
29,8	0	0	0,205	0,25	0,35	0,085	0	0	0
25,4	0	0	0,2	0,25	0,345	0,45	0	0	0
23,1	0	0	0,195	0,235	0,335	0,410	0	0	0
22,1	0	0	0,195	0,225	0,330	0,405	0,095	0	0
20,3	0,085	0,155	0,190	0,230	0,240	0,315	0,335	0	0
17,4	0,080	0,135	0,180	0,225	0,245	0,210	0,430	0	0
14,4	0,070	0,115	0,135	0,205	0,300	0,355	0,460	0,365	0

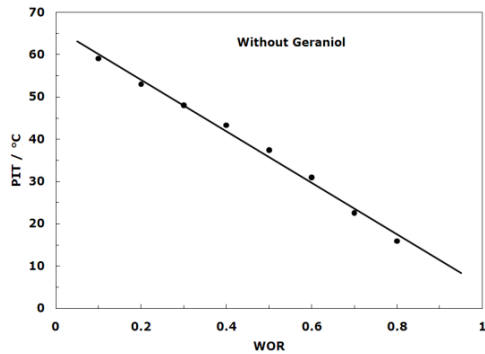


Figure III-22 - Standard inversion line for Brij30 / octane / water system

These measurements highlight the specific behavior of the Brij30, which presents a line of standard inversion strongly bended, involving a difference of PIT for more than 40 °C between a WOR of 0.1 and 0.9. These results are confirmed in the literature [15,17] and may be rationalized by the partitioning effect of the oligomeric polyethoxylated alcohol. Indeed, when the WOR is low the large volume of the excess oil phase solubilizes the less hydrophilic oligomers and therefore the interfacial film is enriched in the more hydrophilic oligomers, which exhibit a higher PIT.

Schematic composition-formulation map for Brij30 / octane / water / geraniol system

In order to better characterize a system, which contains a terpenoid fragrance, the following composition-formulation map is built with the addition of 1.5% of geraniol and summarized in Table III-8, also the determination of the standard inversion line is shown Figure III-23 for Brij30 / octane / water / geraniol system. Only three measurements of PIT have been completed which correspond to WOR = 0.1, 0.2 and 0.3 also it has to be noticed that the PIT value for WOR > 0.6 are lower than 0 °C and therefore they are not experimentally reachable. Table III-8 summarized the value of conductivity as a function of WOR and temperature of Brij30 / octane / water system containing a concentration of 1.5% in geraniol.

Table III-8- Value of the conductivity as function of temperature for Brij30 / octane / water / geraniol system

WOR \ T (°C)	0,1	0,2	0,3	0,4	0,5	0,6	0,7	0,8	0,9
30,4	0,035	0,145	0	0	0	0	0	0	0
27,1	0,040	0,150	0,020	0	0	0	0	0	0
24,2	0,030	0,180	0,015	0	0	0	0	0	0
21,9	0,045	0,0125	0,015	0	0	0	0	0	0
20,3	0,02	0,11	0,035	0,025	0	0	0	0	0
17,8	0,005	0,11	0,175	0,015	0	0	0	0	0
14,6	0,02	0,105	0,18	0,185	0	0	0	0	0
10,5	0,045	0,08	0,15	0,2	0,02	0	0	0	0
6,1	0,045	0,1	0,135	0,195	0,215	0	0	0	0

Figure III-23 shows the standard inversion line in the composition-formulation map of Brij30 / octane / water system containing a concentration of 1.5% geraniol

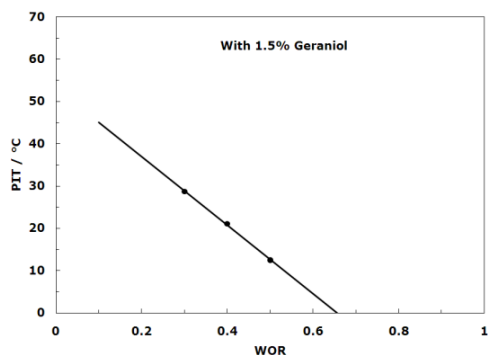


Figure III–23 - Standard inversion line for Brij30 / octane / water / geraniol system

The standard inversion line in the composition-formulation map of Brij30 / octane / water system containing a concentration of 1.5% geraniol is lower than the one for the system without terpenoids, which is explained by the effect of the geraniol on the PIT.

At WOR equal to 0.5, the PIT has approximately shifted of 25 °C, also the standard inversion line seems to have a lower slope than the Brij30 / octane / water system. This means that the effect of geraniol will be much more dominant for formulations containing a high proportion of water (higher WOR). The approximation carried out by linear regression shows that, for a WOR of 0.1, the difference of PIT value with and without geraniol is around 15 °C against about 30 °C for a WOR of 0,9. This information is valuable for the formulators developing emulsion with high water content, the influence of geraniol and by extension others terpenoids alcohols will probably influence a lot the stability of their formulations.

4.2. Effect of geraniol on the creaming of the Brij30 / octane / water emulsion

The main phenomena, which drive the instability of the emulsions, are as follows, classified by importance:

- The *Ostwald ripening* involves the diffusion of dispersed phase material from the smaller droplets towards larger ones due to the chemical potential of the material being higher for a smaller radius of curvature. This phenomenon leads to a change in the size particle distribution of the system.
- The *flocculation* (Figure III-24 c) pushes the particles to gather in clusters, and can be precursor of sedimentation. This phenomenon is due to the existence of weak attractions between the droplets, which separate once they “met” under the effect of the Brownian movement.
- The *sedimentation* (Figure III-24 b) or *creaming* (Figure III-24 a), which is due to gravity actually depends on the difference in density between continuous phase and internal phase. The competition between Brownian movement and gravity (which pushes the heaviest particles than the continuous phase to the bottom and lightest upwards) leads to a loss of homogeneity of the emulsion.
- The *coalescence* (Figure III-24 d) occurs whilst the thin film of continuous phase between two closely approaching droplets breaks; the Laplace pressure differences then cause the droplets to recombine rapidly into a bigger droplet. The phenomenon is an irreversible process (while a weak agitation is enough to disperse the droplets in the case of the preceding phenomena). The process is repeated then, finally restoring the initial biphasic system [33].

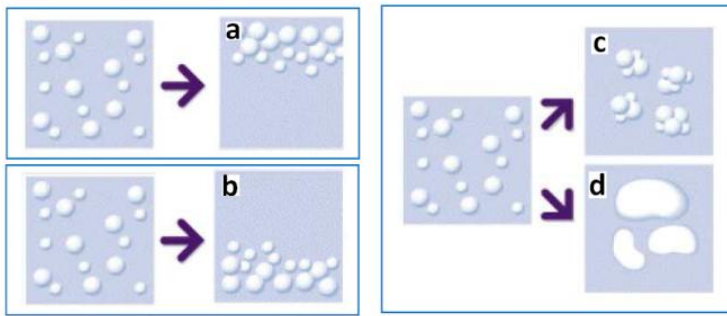


Figure III–24 - Different instability phenomenon in emulsions – Creaming (a), Sedimentation (b), flocculation (c) and coalescence (d)

CREAMING

The kinetic of creaming or sedimentation can be measured by transmission of light through the sample. For this measurement, the Turbiscan® system “inspects” the sample tube from the top to the bottom looking at the clearest part of the emulsion. The system allows the definition of a threshold value above which it will be considered that the phase becomes satisfactorily “clear”. In our case, this threshold is defined at 5%. Turbiscan® system indicates as a function of time, the proportion of height (in mm) of the sample, which has a transmission higher than the 5% threshold. The resulting curves are shown below in Figure III-25. Two time descriptors can be then calculated from the experimental curve and they are abbreviated and defined as follow:

- $T_{(1/2)}$: the “half life” of the system corresponds to the time required for the system to reach 50% of the total phase separation height.
- $T_{(lag)}$: the “lag time” corresponds to the time delay experienced in the system to detect the beginning of the phase separation phenomenon at the defined threshold.

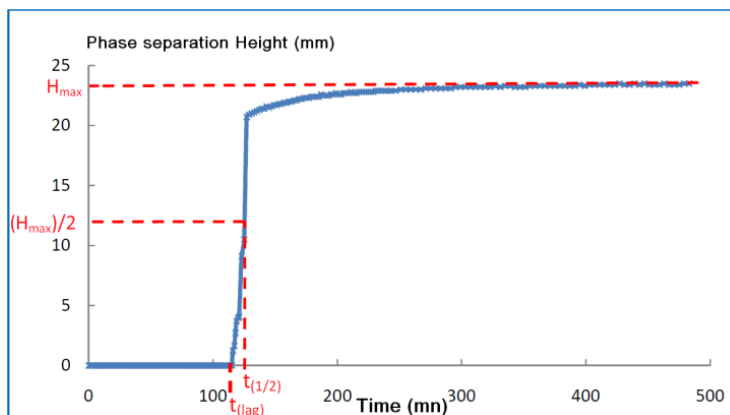


Figure III–25 - Curve of the phase separation height as function of time – determination of the Half life $t_{(1/2)}$ and lag time $t_{(lag)}$ descriptors

Only the half life descriptor $t_{(1/2)}$ will be used in the rest of this work as it seems to be better in terms of precision and repeatability than the lag time. $t_{(1/2)}$ and $t_{(lag)}$ also appears to have the same progression for a defined temperature as shown in Figure III-26.

Figure III-26 shows the evolution of the two descriptors generated by turbiscan: the half life and the lag time as function geraniol concentration and at two different experimental temperatures: 40 °C and 50 °C.

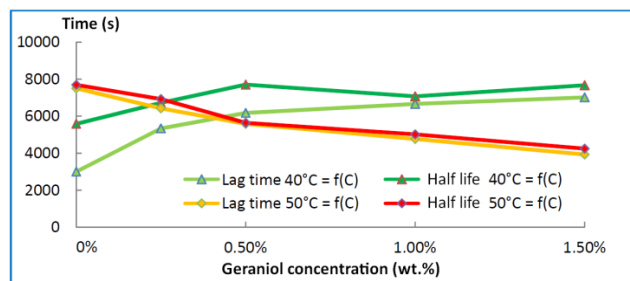


Figure III—26 - Evolution of the half life and lag time descriptors as function geraniol concentration at 40 °C and 50 °C

As previously discussed, the formulation industries often make battery of tests including at different temperatures to assess the stability of their formulated product. Thus, the evaluation of the influence of temperature on the half life descriptor for our studied system is highly desirable. Sample preparation, temperature equilibrium and emulsification process follow the protocol described in scheme III-1 for measurement in Turbiscan®. In the same time, this work has been repeated with different concentrations of geraniol to evaluate the impact of the terpenoid alcohol on the stability of the system.

The evolution of $t_{(1/2)}$ for different concentrations of geraniol as a function of temperature is reported in Figure III-27.

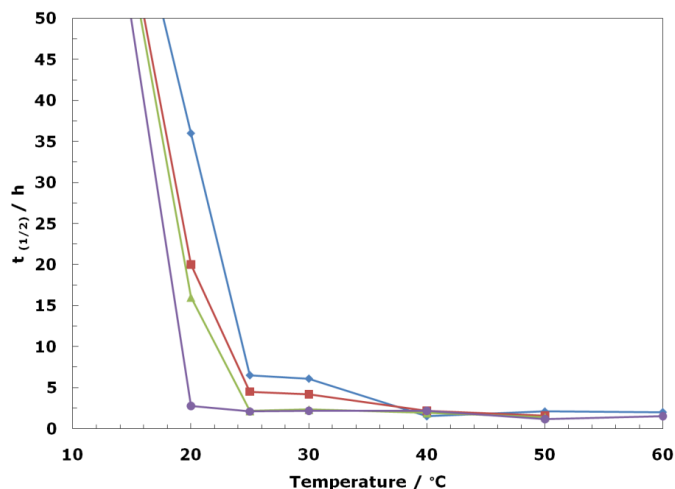


Figure III—27 - Evolution of $t_{(1/2)}$ as function of temperature in °C for Brij30 / octane / water system and as function of the geraniol concentration in % - at 0 % (◆), at 0.5% (■), at 1.0% (▲) and at 1.50% (●)

As illustrated in Figure III-27, the half life curves for Brij30 / octane / water system at different concentration of geraniol as a function of temperature possesses similar profile, on the other hand only the temperature for which the system begins to regain stability is shifted to lower temperature. Also all profiles show divergence with our expectation. In fact, a well instability was expected nearby the PIT of the system (37.4 °C) coming with an increase of stability in higher and lower temperature of PIT. Instead, the system is just stable a few days at lower temperature than PIT and the half-life descriptor decreases continuously as temperature increases until it reaches the PIT then increase again. The higher the concentration of geraniol, the lower is the temperature for which the system begins to be instable. Consequently, emulsions formulated with terpenoid alcohols like geraniol are more susceptible to be destabilized at a temperature next to room temperature.

5. Influence of terpenoid alcohols on the PIT of a cosmetic emulsion

Previously, the influence of fragrances and several terpenoid alcohols on PIT for systems that contained a commercial surfactant (Brij30) and defined oil (alkane or silicone) have been performed. In the present study, the components of our systems are made of exclusively industrial ingredients. A surfactant supplier provides a typical emulsion formula as described on Table III-9, which served as a cosmetic base to evaluate the impact, of four fragrant terpenoid alcohol isomers of *n*-decanol as summarized in Figure III-28, on its phase inversion temperature as seen on Figure III-29.

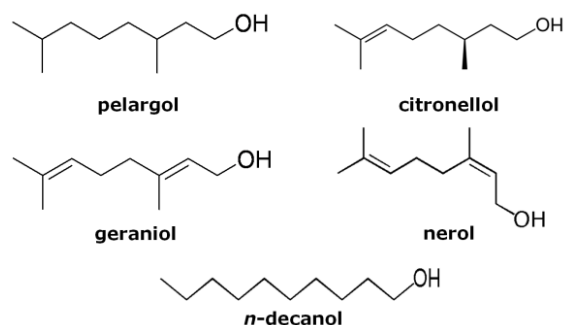


Figure III–28 Terpenoid alcohol isomers of the *n*-decanol tested with commercial emulsion.

Table III-9 shows the studied emulsion formula, it includes the commercial names, the International Nomenclature of Cosmetic Ingredients (INCI) names, the corresponding percentage in the formula and the main function of each ingredient.

Table III-9 Studied Formula used as a typical cosmetic emulsion

Ingredients Name	INCI Name	% (wt.)	Main Function
Lanette O	Cetyl Stearyl Alcohol	3	Emulsion stabilizer
Emulgin B1	Cetareth-12	4	Surfactant
Paraffin oil + fragrance	Paraffin oil + Fragrance	20	Oily Phase
NaCl 10 ⁻² M aqueous solution	Sodium Chloride + water	73	Water Phase

The accuracy and reproducibility for the experiment value are guaranteed by carrying three cycles of phase inversions. After the PIT measurements, the droplets size of the emulsion at 25 °C is determined with the help of laser particle-measurement instrument. Some pictures under the microscope are taken too. Then, the emulsion is kept and each week the droplet size is measured to study the stability of the emulsion.

Figure III-29 shows the evolution of the PIT as a function of alcohol concentration. Again, the PIT tends to decrease when the percentage of alcohol increases. Indeed, as observed earlier, for a given alcohol concentration, the nature of alcohol and thus its capacity to be involved in the interface impacts differently the resulting PIT value.

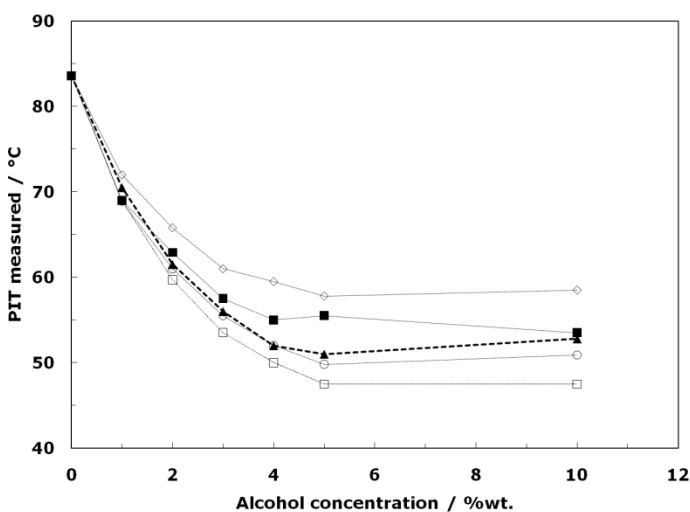


Figure III—29 Evolution of the PIT (°C) for the commercial emulsion system as a function of alcohol concentration (wt.%) pelargol (◇), citronellol (■), n-decanol (▲), nerol (○), geraniol (□)

As mentioned by Graciaa et al., the medium-long chain alcohols in SOW system behaved as “lipophilic linkers.” [20-21, 34]. However, this behavior can be influenced by the formulation factors and the composition hence depends largely on the studied system [34]. The oily phase involved in our emulsion is composed by liquid paraffin, a mixture of typically C_{14}/C_{16} alkanes while the carbon number of alcohols is 10, therefore affinity between oil and alcohol is not weak. As a result, our terpenoid alcohols play two possible roles at the same time with this configuration: the role of “lipophilic linker” and the role of polar oil. The balance between these two roles will change depending on the chemical structure.

On one hand, Pelargol, citronellol, nerol and geraniol possess the appropriate structure to interact with oil at the interface; on the other hand, the different ramification and unsaturation will certainly limit their penetration in the surfactant palisade at the interface taking into account the relatively large surfactant molecules involved in our system ($C_{16}/C_{18}E_{12}$). It can be then supposed that the terpene alcohols will have a higher tendency to behave as polar oil than as a “lipophilic linker”. Since most of these alcohols remain in the oily phase and behaves like polar oil. The more polar oil is added, the higher the polarity of the oily phase is. PIT consequently decreases. The different impacts on the PIT values can be then explained by the difference of polarity between the added alcohols.

Nerol is the cis- and geraniol is the trans-isomer of the same molecule. Gas Chromatography analysis shows that our sample of nerol is composed of 60% of the cis-isomer and 40% of the trans-isomer (geraniol), however we can still observe the isomeric influence on the PIT. This also means that the trans-isomer has a stronger influence on PIT than its cis-isomer probably due to a higher steric hindrance at the interface. In the case *n*-decanol, the role of "lipophilic linker" is probably more significant. It is easier for a linear molecule to penetrate the surfactant palisade and thus, increase the interaction between the hydrophobic part of surfactant and oil. This assumption may explain why the addition of *n*-decanol decreases the PIT faster than expected. From 4% in alcohol, the PIT remains almost constant and if the concentration of alcohol continues to increase, the initial system is destabilized. At this point, the oily phase solubilizes a great amount of surfactant and the remaining surfactant available to form the interfacial film is no more sufficient to stabilize an emulsion. During the heating process, at 10% geraniol concentration, the conductivity line cannot completely reach zero even after reach the inversion from O/W at W/O as shown in Figure III-30. The conductivity signal is more or less deformed but PIT is still measurable.

Figure III-30 shows the profile of conductivity for the studied cosmetic emulsion as a function of temperature, the emulsion contains 10% of geraniol.

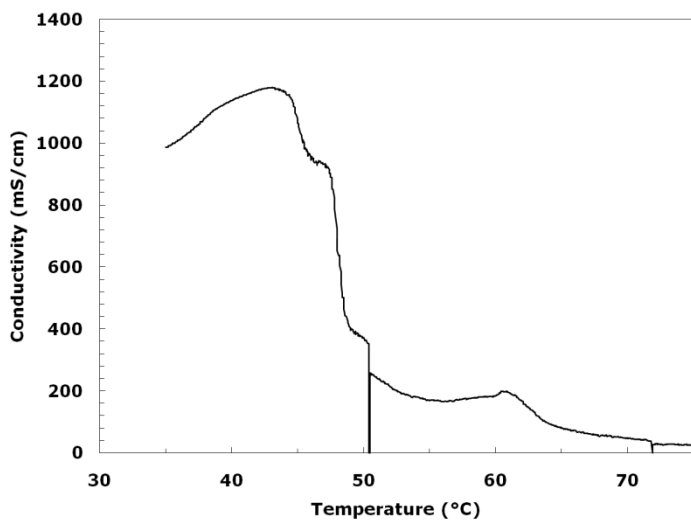


Figure III—30 -Profile of conductivity in mS/cm as a function of temperature in °C for cosmetic emulsion containing 10% of geraniol

For a concentration of alcohol higher than 15%, the conductivity signal is extremely distorted and the PIT cannot be found any longer. The emulsion breaks, as the concentration in surfactant is too low to form an emulsion. At an alcohol concentration of 2% the droplet size of the emulsion does not change significantly anymore but the stability is influenced by alcohol. The droplet size in emulsions containing terpene alcohols increases as time increase while that of the base without alcohol tends to remain constant. Again, the emulsion containing 2% of *n*-decanol takes a very thick texture like cream after one-day production and keeps this consistency until the end of this study (5 weeks.) This phenomenon reinforces our earlier assumption suggested on the role of the *n*-decanol.

Table III-10 shows the evolution of emulsion particle size as a function of time during 5 weeks at room temperature.

Table III-10 Droplet size (in μm) as function of time (in week)

Emulsion	Average Diameter (μm)					
	<i>Initial</i>	<i>week 1</i>	<i>week 2</i>	<i>week 3</i>	<i>week 4</i>	<i>week 5</i>
without alcohol	0.30	0.30	0.31	-	0.33	0.33
+ 10% Pelargol	0.27	-	-	-	-	-
+ 10% Citronellol	0.26	0.27	0.41	3.71	-	-
+ 10% <i>n</i> -decanol	0.26	too viscous	-	-	-	-
+ 10% Nerol	0.29	-	-	31.65	-	NA
+ 10% Geraniol	0.25	0.55	5.37	35.50	40.75	-

Increasing the concentration of Nerol does not change significantly the particle size of emulsion. However, it changes the particle distribution profile. The higher the concentration of nerol is the more polydisperse the emulsion is, leading to increased instability. Above 15% of nerol, the particle size increases suddenly. At this concentration, the emulsion crosses the threshold of a new domain. Table III-11 shows the particle size of the commercial emulsion as a function of nerol concentration in emulsion.

Table III-11 – Droplet size for commercial emulsion as a function of the nerol concentration in emulsion

Percentage of Nerol in emulsion	Average diameter(μm)
1	0.27
2	0.29
3	0.35
5	0.31
10	0.73
15	1.11

6. Conclusion

The influence of two isomeric terpene alcohols have been studied on alkane and silicone based microemulsions systems. The pelargol and geraniol effectively decrease the position of the X point (T^* , C^*) in the fish diagram; they clearly exhibit co-surfactant properties by increasing the effective affinity of the surfactant for the oily phase and consequently decrease the fish temperature of the system. These terpene alcohols are somehow as effective as octanol. Regarding emulsion systems at non-equilibrium formulated with alkane or silicone oil, the presence of polar oils such as phenylalcohol and geraniol have significant effect not only on the PIT, in the system but also on the stability by acceleration of the sedimentation process. In the composition-formulation map, the standard inversion line for a Brij30 / octane / water system is significantly shifted to lower temperature in the presence of 1.5% geraniol. At WOR = 0.5, the PIT suffers a decrease of 25 °C, in the same time the standard inversion line have a lower slope than system which does not contain the terpene alcohol. That means that the effect of the geraniol will be much more significant for a formulation containing a high proportion of water. Finally, the result of a similar investigation on a commercial emulsion, characterized by a typical higher WOR and formulated with polydisperse surfactant and oily phase, confirmed the co-surfactant properties of terpene alcohols. Despite the fact that a high quantity of alcohol is requested ($\approx 4\%$ seldom met in cosmetic industry) to lower the PIT (initial system without fragrance ≈ 80 °C) in such magnitude that allows to reach the highest temperature (50 °C) met in industrial emulsion stability test.

7. Experimental

7.1. Chemicals

Brij[®]30 were sampled by Sassol China and pure tetraethyleneglycol mono-octyl ether C₈E₄ (cloud point at 7.1% in water = 40.85 °C) was synthesized and purified on laboratory scale using a method previously described in [6]. Propanol (C₃OH, > 98%), isopropanol (IsoC₃OH, > 98%), butanol (C₄OH, > 98%), pentanol (C₅OH, > 98%), hexanol (C₆OH, > 96%), octanol (C₈OH, > 98%), decanol (C₁₀OH, > 98%) and dodecanol (C₁₂OH, > 98%) were purchased from SCRC (China). Dodecane (> 99%) was purchased from Acros (USA) and octane (> 97%) was from SCRC (China). All fragrance molecules were provided by Givaudan Shanghai. Lanette O is a commercial combination of C₁₆OH and C₁₈OH; Emulgin B1 is a commercial combination of ethoxylated C₁₆OH and C₁₈OH with an ethoxylate degree of 12 units, both ingredients are supplied by Cognis. Liquid paraffin is supplied by Cooper. All components were used as received. Purity was assessed by GC analysis. Milli-Q water (18.2 MΩ cm) was used.

7.2 Determination of fish temperatures (T*) and optimal concentrations (C*) of the C_iE₄ / oil / water systems

The “fish-tail” temperatures T* and the optimal concentration C* were determined by investigating the phase behavior of the C_iE₄ / oil / water systems at a constant water-to-oil weight ratio (WOR = 1) as a function of temperature (ordinate) and surfactant mass percentage (abscissa). The “fish-tail” point located at the intersection of the four Winsor (Winsor I, II, III and IV) regions corresponds to the minimal surfactant concentration required to obtain a one-phase microemulsion (Winsor IV) [31]. Water, oil and surfactant were introduced in a thin glass tube (Ø = 2 mm) the headspace of which was filled with Argon and then frozen at -78 °C with a dry ice / acetone mixture. The tubes were sealed by flame to avoid any loss of oil or water during the experiment. Samples were gently shaken and placed in a water bath, maintained at a constant temperature T ± 0.1 °C, until the equilibrium was reached. The fish diagrams were constructed by visual inspection of the Winsor phases. The “fish-tail” temperature T* values were obtained with an accuracy better than 1 °C.

7.3. PIT measurement for surfactant / oil / water systems

10 ml of sodium chloride aqueous solution (0.01M), 10 ml of alkane or silicone oil, 6.5% in weight of Brij[®]30 in case of alkane oil (10/20 % in weight in the case of silicone oil) were introduced into a dual chamber glassware (with PTFE stopper) connected to a circulator water bath as shown in Figure III-31. The water bath, connected to a computer, was controlled by software, which generates ramps of temperature with a speed of $1\text{ }^{\circ}\text{C}\cdot\text{mn}^{-1}$. To ensure homogeneous stirring, PTFE 3-blade agitator (with propeller) was dipping into the emulsion at a constant speed of 700 rpm. The conductivity of the resulting emulsions was measured as function of temperature using a conductimeter (Vernier CON-BTA model) and dipping cell (with a Pt / Platinized electrode) with a cell constant of 1 cm^{-1} . The temperature of the emulsion was real time monitored by a temperature sensor, which is kept into the emulsion. A small hole was done on top of the stopper in order to introduce the fragrances. The concentration of surfactant as well as the volume ratio of oil to aqueous solution remains constant throughout the experiment.

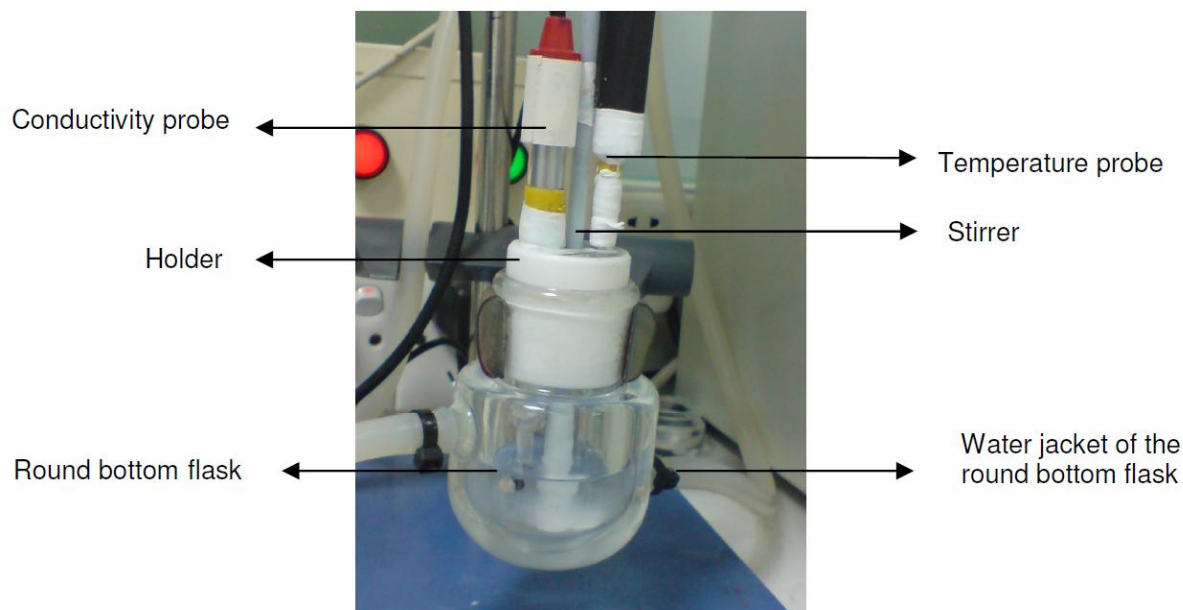


Figure III–31 - Set up of phase inversion temperature experiment

The change from o/w to w/o or vice versa is monitored using a conductivity sensor and the temperature of the solution can be varied by the water bath, which is connected to the round bottom flask that contains the solution. The change in temperature is always set at $1\text{ }^{\circ}\text{C}$ per minute. To ensure a homogenous solution, the solution was subjected to a stirrer, which is set at 700 rpm. The PIT is determined from the graph of conductivity against

temperature using the parallel tangents of the curve. The temperature at which the phase inversion occurs is where the mean of the parallel tangent lines cut the curve as shown in Figure III-3.

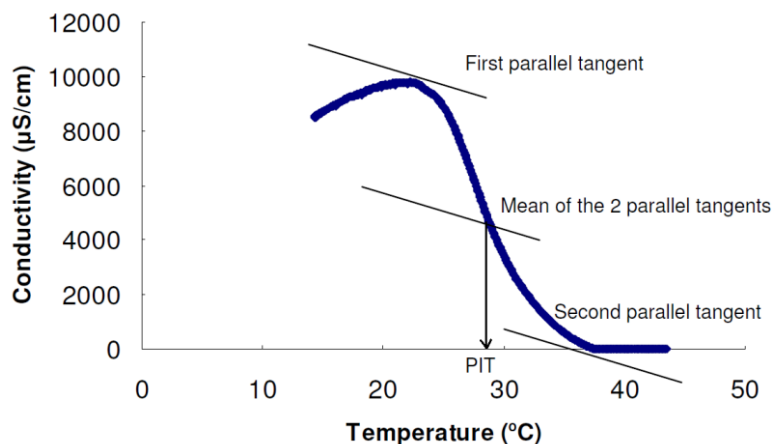


Figure III–32 – Schematic representation of the determination of the PIT by the tangent method

7.4. Preparation of the commercial emulsion

Cognis, the surfactant supplier for this work, proposed the composition of the studied emulsion summarized in Table III-9. According to Cognis, the surfactant proportion in this formula corresponds to the minimal quantity necessary to obtain a typical cosmetic emulsion produced in the industry. In order to prepare the samples, the formulation is separated into two parts. Part 1 made of Lanette O + Emulgin B1 + paraffin thick + the studied terpene alcohols and Part 2 made of the aqueous Sodium Chloride solution are heated at 60 °C in a separate vessel. When part 1 is molten and homogeneous, slowly add part 2 in part 1 under slow agitation (50 rpm). Then, increase the agitator speed to 700 rpm and finally cool down to room temperature.

This formulation possesses a PIT is towards 80 °C. The region of PIT emulsion is performed twice in order to get the future experimental condition as shown in Table III-12. The experiments are carried out around the PIT +/- 20 °C. The conductivity of the system was measured during the experiment with the mentioned in section 7.3 apparatus. The studied variables are the temperature and the proportion between liquid paraffin and the added alcohol in the oily phase. The mass relationship between the aqueous and oily phase is fixed at 73/20.

Table III-12 resumes the value of the PIT for two consecutive experiments. This has been done to check the reproducibility of the measurements.

Table III-12 –PIT values measured for the described commercial emulsion for two repetitions

Studied system	Measured PIT (°C)	
	Exp 1	Exp 2
Emulsion without alcohol	83.6	84.5
Pelargol at 10%	65.8	65.5
Citronellol at 10%	62.9	62
<i>n</i> -decanol at 10%	61.5	60.5
Geraniol at 10%	59.7	59.5

8. References of chapter III

1. Charles Sell. Terpenoids, Kirk Othmer Ed. Encyclopedia of Chemical Technology, 5th edition, John Wiley&Sons, **2007**, Vol.24 p468
2. Poprawski, J.; Catté, M.; Marquez, L.; Marti, M. J.; Salager, J. L.; Aubry, J. M., Application of hydrophilic-lipophilic deviation formulation concept to microemulsions containing pine oil and nonionic surfactant. *Polym. Int.* **2003**, 52 (4), p629-632
3. Kahlweit, M., Strey, R., Busse, G., Effect of alcohols on the phase behavior of microemulsions, *J. Phys. Chem.* **1991**, 95, p5344-5352
4. Penders, M. H. G. M., Strey, R., Phase Behavior of the Quaternary System H₂O / n-Octane / C₈E₅ / n-Octanol: Role of the Alcohol in Microemulsions *J. Phys. Chem.* **1995**, 99, p10313-10318
5. Graciaa, A., Lachaise, J., Cucuphat, C., Bourrel, M., Salager, J.L., Improving solubilization in microemulsions with additives. 2. Long chain alcohols as lipophilic linkers. *Langmuir*, **1993**, 9 (12), p3371-3374
6. Stubenrauch, C., Paepflow, B., Findenegg, G.H., Microemulsions Supported by Octyl Monoglucoside and Geraniol. 1. The Role of the Alcohol in the interfacial Layer. *Langmuir* **1997**, 13, p3652-3658
7. Queste, S.; Salager, J. L.; Strey, R.; Aubry, J. M., The EACN scale for oil classification revisited thanks to fish diagrams. *J. Colloid Interface Sci.* **2007**, 312 (1), p98-107
8. Silas J.A, Kaler, E.W., Hill, R.M., Effect of Didodecyldimethylammonium Bromide on the Phase Behavior of Nonionic Surfactant-Silicone Oil Microemulsions *Langmuir*, **2001**, 17 (15), p4534-4539
9. P.A., Winsor Solvents properties of amphiphilic compounds, butterworth, London, **1954**
10. Bourrel. M., et Al. Surfactant Science Series, vol 30, Marcel Dekker, NY, **1988**
11. Lang. J., et Al. *J. Phys. Chem.* **1991**, 95, p9533-9541
12. Jada. A., et Al. *J. Phys. Chem* **1990**, 94, p387-395
13. Mario Corti, M., Minero, C., Degiorgio, V., Cloud point transition in nonionic micellar solutions, *J. Phys. Chem.*, **1984**, 88 (2), p309-317
14. Shinoda, K., Saito, H., The Stability of O / W Type Emulsions as Functions of Temperature and the HLB of Emulsifiers: The Emulsification by PIT- method *J. Colloid Interface Sci.*, **1969**, 30, p258-263

15. Forgiarini, A. Esquena, J. Gonziez, C., Solans, C., Formation of Nano-emulsions by Low-Energy Emulsification Methods at Constant Temperature *Langmuir*, **2001**, 17 (7), p2076–2083
16. Pizzino, A., Catté, M. Van Hecke, E., Salager, J.-L., Aubry, J.-M., On-line light backscattering tracking of the transitional phase inversion of emulsions, *Colloids Surf. A* **2009**, 338, (1-3), p148-154
17. Ben Ghoulam, B., Moatadid, N., Graciaa, A., Lachaise, J., Quantitative Effect of Nonionic Surfactant Partitioning on the Hydrophile–Lipophile Balance Temperature *Langmuir*, **2004**, 20 (7), p2584–2589
18. Pizzino, A., Inversion de phase des emulsions : Relation avec le comportement a l'équilibre et Détection par Rétrodiffusion de Lumière, (Thèse de doctorat, Université des Sciences et Technologies de Lille), **2008**, Chap. 3, p83-112
19. Bourrel, M., Gard, P., Verzaro, F., Biais, J., Collection Colloques et Seminaires, Institut Francais du Petrole, *Interact. Solide-Liq. Milieux Poreux*, **1985**, 42, p303-319
20. Graciaa, A., Lachaise, J., Cucuphat, C., Bourrel, M., Salager, J.L. Improving Solubilisation in Microemulsions with Additives. 1. The lipophilic linker role *Langmuir*, **1993**, 9, p669-672
21. Graciaa, A., Lachaise, J., Cucuphat, C., Bourrel, M., Salager, J.L. Improving Solubilisation in Microemulsions with Additives. 2. Long Chain Alcohols as lipophilic linkers *Langmuir* **1993**, 9, pp3371-3374
22. Farago, B., Richter, D., Huang, J.S., Safran, S.A., Milner, S.T., Shape and size fluctuations of microemulsion droplets: The role of cosurfactant *Phys. Rev. Lett.*, **1990**, 65, p3348
23. Baviere, M., Schechter, R.S. , Wade, W.H., *J. Colloid Interface Sci*, **1981**,81, pp266-279
24. Salager, J.L., In: G. Broze, Editor, Handbook of Detergents: Part A: Properties, Marcel Dekker, New York, **1999**, p253
25. M.Bourrel, M., Salager, J.L., Schechter, R.S., Wade, W.H., *J. Colloid Interface Sci.* **1980**, 75, p451-461
26. Salager, J.L., Anton, R.E., Sabatini, D.A., Harwell, J.H., Acosta E.J., Tolosa, L.I., *J. Surfactants Deterg.*, **2005**, 8, p3-21

27. Yaws, C.L.; Thermophysical properties of chemicals and hydrocarbons, published by William Andrew Inc, **2008**, chapter 19, p672-680
28. Pimentel, G. C., McClellan, A.L., The Hydrogen Bond, Freeman, San Francisco, 1960
29. Tchakalova, V., Testard, F., Wong, K., Parker, A., Benczédi, D., Zemb, T., Solubilization and interfacial curvature in microemulsions: II. Surfactant efficiency and PIT, *Colloids Surf. A* **2009**, 331, (1-2), p42-47
30. Bouton, F., Durand, M., Nardello-Rataj, V., Serry, M., Aubry, J.-M., Classification of terpene oils using the fish diagrams and the Equivalent Alkane Carbon (EACN) scale. *Colloids Surf. A* **2009**, 338, (1-3), p142-147
31. Salager, J.L., Minana-Perez, M., Perez-Sanchez, M., Ramirez-Gouveia, M., Rojas, C.I. Surfactant-oil-water systems near the affinity inversion. Part III: the two kinds of emulsion inversion, *J. Disp. Sci. Technol.*, **1983**, 4, p313-329
32. Salager, J.-L., Anton, R., Anderez, J.M., Aubry, J.M., *Techniques de l'Ingénieur, Génie des Procédés J2157*, **2001**, p1-20
33. Walstra, P., Chap1 pp3-59 Encyclopedia of Emulsion Technology vol.4, ed. :Paul Becher, **1996**, Marcel Dekker Inc., New York
34. Graciaa, A., Lachaise, J., Cucuphat, C., Bourrel, M., Salager, J.L., Improving Solubilisation in Microemulsions with Additives., Part III. Lipophilic Linker Optimization *J. Surf. and Deterg.*, **1998**, 1, p403-406

General Conclusion

This work was aiming to understand better the influence of fragrant terpenes and terpenoids on the phase behavior of different micro- and macro-emulsions.

At first, we started with the determination of the EACN (Equivalent Alkane Carbon Number) of a large set of well-defined mono- and sesquiterpenes using a series of pure $C_{12}E_4$ surfactants synthesized in the lab and by the mean of the HLD equation. By comparing the EACNs of these oils exhibiting a more or less complex chemical structure, some general tendencies are drawn with regard to the structural effect. Aromatization was shown to have the strongest effect on the decrease of the EACN value, as well as cyclization, unsaturation and finally branching to a lesser extent. A higher degree of penetration of terpenes into the surfactant palisade increases surfactant efficiency. Therefore, a lower amount of surfactant is required to generate a single-phase microemulsion based on terpenes in comparison with *n*-alkanes. EACN constitutes a key parameter for practical applications since it can help the formulator to select the appropriate surfactants for given oil in order to obtain microemulsions or emulsions with the desired properties and with the minimum amount of surfactant.

Secondly, the Fish-tail temperatures T^* of SOW systems based on the same $C_{12}E_4$ surfactants, and a series of hydrocarbon oils including *n*-alkanes, used as references, and substituted cyclohexanes, cyclohexenes, aromatics and terpenes have been determined and their evolution has been rationalized by considering the effective packing parameter \bar{P} of the surfactants in its whole physicochemical environment. It is shown (see Figure C-1) that an increase of the oil penetration into the surfactant palisade must be compensated for a decrease of the fish tail temperature T^* .

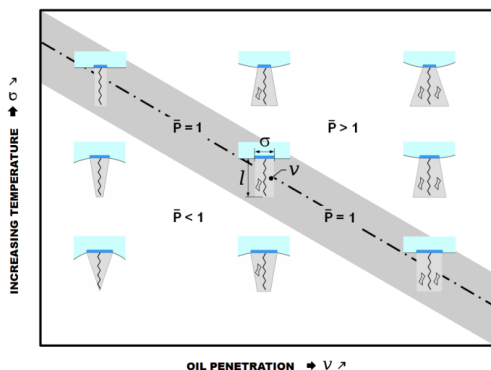


Figure C-1 - Schematic description of the evolution of the effective packing parameter \bar{P} of the surfactant as a function of the temperature and of the oil penetration

A robust linear model based only on two descriptors reflecting topological features related to molecular branching and polarizability of the oils has been established for an accurate prediction of T^* .

$$T_{C_6E_4}^* = a \times \text{Average negative softness} + b \times \text{KierA3} - c$$

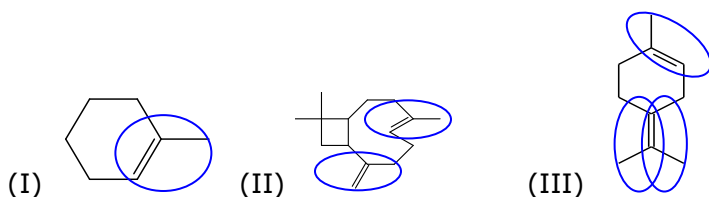
with a , b and c constant depending on C_6E_4 . The Kier A3 descriptor is the third alpha modified Kier and Hall kappa shape index [1,2]. It equals $(s-1)(s-3)^2 / p_3^2$ for odd n , and $(s-3)(s-2)^2 / p_3^2$ for even n , where n denotes the number of non-hydrogen atoms in the molecule $s = n + a$. The value for a is $(r_i/r_c - 1)$ where r_i is the covalent radius of atom i , and r_c is the covalent radius of an (sp^3) carbon atom. p_3 is the number of paths of length 3 (i.e. consisting of 3 adjacent C-C bonds). Kier A3 is a so-called topological descriptor, measuring the extent of branching in the molecule: the lower is the Kier A3, the more branched is the molecule. Furthermore, Kier A3 is sensitive to the location of the branching within the molecule. The Kier A3 value is larger when branching is located at the extremities of the molecule or in the absence of any branching, and decreases when branching is located near the center of the molecule. Finally, Kier A3 can discriminate between sp^2 and sp^3 carbon atoms. The Average Negative Softness belongs to the class of so-called inductive descriptors and is related to the polarizability (or softness) of the electron cloud. The physical interpretation of this descriptor is by far less trivial than that of Kier A3 [3-6]. The inductive softness computes the effective size and compactness of molecules and is related to the volume of the electron cloud around each partially negative atom. The Average Negative Softness can be considered as a three-dimensional structural descriptor. As, the electron cloud of sp^3 atoms being more voluminous than that of sp^2 atoms, the Average Negative Softness of, e.g., cyclohexene (6.21) is lower than that of cyclohexane (7.28). The value of this variable increases with increasing number of saturated (sp^3) carbon atoms in the molecules. It generally decreases with increasing electron delocalization, i.e. with increasing molecular polarizability. In fact, the greater is this value; the larger is the effective size of the molecule, based on the extension of the electron cloud of the carbon atoms in hydrocarbons, and the higher is the saturation of these carbon atoms. Using this descriptor, the model takes correctly into account the important role of carbon saturation with respect to T^* .

Another linear model for the prediction of the optimal concentration C^* for C_6E_4 /terpenes/water based on three descriptors is also proposed and the value of C^* appears to be driven by the surface of the oil molecule exposed to water (reflected by the *Kier A3* variable), the electrostatic effects related to electron double bonds and to the

presence and position of specific unsaturated synthons of general formulas $[CH_3-C=]$ and $[CH_2=C-]$ in the oil.

$$C_{C_6E_4}^* = \alpha \times \log P(o/w) + \beta \times KierA3 - \gamma \times SMR_{VSA3} + \delta$$

with $\alpha = 5.46 \pm 1$; $\beta = 2.42 \pm 0.6$; $\gamma = 0.74 \pm 0.3$ and $\delta = 10.31 \pm 4$. The $\log P$ (o/w) descriptor is obtained in MOE environment by one of the numerous methods available to calculate the octanol / water partition coefficient, $Kier A3$ has been defined above and SMR_{VSA3} is related to the presence of methyl groups attached to unsaturated secondary carbon, to the presence of terminal vinyl groups and/or to aromaticity. SMR_{VSA3} is proportional to the number of such methyl groups, i.e. it is equal to about 3.2 for 1-methyl-1-cyclohexene (I), α -pinene, β -pinene and δ -3-carene, 6.4 for alpha terpinene, caryophyllene (II), gamma terpinene and limonene, and 10 for para-cymene and terpinolene (III), while this descriptor is zero for all other molecules. The correction brought by this contribution to the model is small but significant.



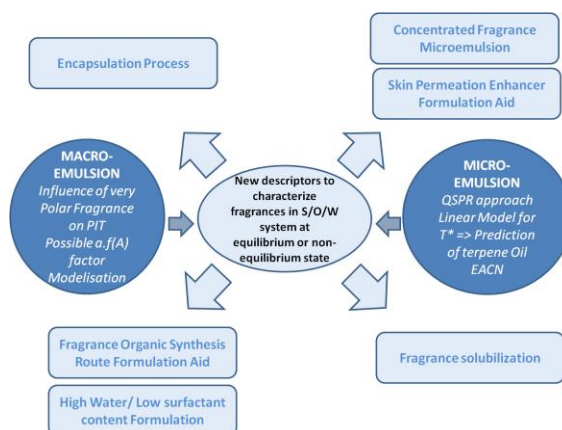
Emulsifying oils having favorable combinations of the above factors lower C^* at a significant extent. This QSPR approach also provides a useful tool for the prediction of the EACN of polar hydrocarbon oils ranging from -3 to +35 as linear relationships link the T^* of C_iE_4 ($i = 6, 8, 10$) both between them and with the EACNs as shown in the first part of this work. This finding constitutes a very useful tool in the prediction of the type and behavior of microemulsions and emulsions prepared from fragrant terpene oils and C_iE_j surfactants.

Thirdly, the influence of two terpene alcohols have been studied on alkane and silicone based microemulsions systems. The pelargol and geraniol effectively decrease the position of the X point (T^* , C^*) of the fish diagram; they clearly exhibited co-surfactant properties by increasing of the effective solubility of surfactant in the oily phase and decreasing the fish temperature of the system.

Finally, for industrial surfactant-based emulsions formulated with paraffin or silicone oil, the presence of polar oils such as phenylalcohol and geraniol have significant effect not only on the PIT but also on the stability of the system by accelerating of creaming process.

In the composition-formulation map, the standard inversion line for a Brij30/octane/water system is significantly shifted to lower temperature in the presence of 1.5% geraniol. At WOR = 0.5, the PIT has shifted 25 °C downwards, moreover the standard inversion line have a lower slope than the one of the system free of terpene alcohol. This means that the effect of the geraniol is much more prominent for water-rich formulations. Finally, a similar study performed on a commercial emulsion with a higher WOR and formulated with polydisperse surfactant and oily phase, confirmed the co-surfactant behavior of terpene alcohols. Despite the fact that a high quantity of alcohol is requested ($\approx 4\%$ seldom met in cosmetic industry) to lower the PIT (initial system without fragrance ≈ 80 °C) down to the highest temperature (50 °C) met in industrial emulsion stability test.

Scheme C-2 summarizes this thesis work and gives some perspectives. Dark blue circles represents our main results in microemulsion with the prediction of the fragrance EACN and in macroemulsion with the prediction of the a.A. A systematic determination of these “descriptors” would be valuable for fragrance manufacturers or their clients to characterize the fragrance behaviors in SOW systems. In one hand, EACN descriptor characterizes the fragrance molecules which may behave like polar oils and on the other hand, the a.A descriptor characterizes the fragrance molecules which may behave like a cosurfactant. It gives to the formulator more possibilities of development such as creating new routes for fragrance synthesis, making concentrated fragrance microemulsions, helping on the encapsulation or water solubilization processes and facilitating the formulation of low surfactant/high water content systems. Finally, these two descriptors would be useful for filing patents in the domain of personal care products, replacing advantageously the current data such as logP partition coefficient or boiling point even the chemometrics descriptors whose the “true physicochemical meaning” is often difficult to apprehend.



Scheme C-2 – Schematic representation of our work and the possible prospects in the different domain of formulations

References of General Conclusion

1. Kier, L. B., Hall, L. H., The nature of structure-activity relationships and their relation to molecular connectivity. *Eur. J. Med. Chem. - Chim. Ther.* **1977**, 12 (4), 307-12
2. Hall, L. H., Kier, L. B., The molecular connectivity chi indexes and kappa shape indexes in structure-property modeling. *Rev. Comput. Chem.* **1991**, 2, p367-422
3. Pearson, R. G., Hard and soft acids and bases. *J. Am. Chem. Soc.* **1963**, 85 (22), p3533-3539
4. Cherkasov, A., Inductive electronegativity scale. Iterative calculation of inductive partial charges. *J. Chem. Inf. Comput. Sci.* **2003**, 43 (6), p2039-47
5. Cherkasov, A., Shi, Z., Fallahi, M., Hammond, G. L., Successful in Silico Discovery of Novel Nonsteroidal Ligands for Human Sex Hormone Binding Globulin. *J. Med. Chem.* **2005**, 48 (9), p3203-3213
6. Cherkasov, A., 'Inductive' descriptors: 10 successful years in QSAR. *Curr. Comput.-Aided Drug. Des.* **2005**, 1 (1), p21-42